Univerzita Karlova v Praze

Fakulta tělesné výchovy a sportu

Studijní program: Biomechanika
Studijní obor: Biomechanika
Školící pracoviště: Fyziologický ústav AVČR

Mgr.Renata Konopková

Mapování optických signálů mozku

Optical Signals of the Brain

Disertační práce

Školitel: MUDr.Jakub Otáhal, PhD

Praha, 2010

Prohlášení:

Prohlašuji, že jsem závěrečnou práci zpracovala samostatně a že jsem uvedla všechny použité informační zdroje. Současně dávám svolení k tomu, aby tato závěrečná práce byla archivována v knihovně Fakulty tělesné výchovy a sportu Univerzity Karlovy v Praze a zde užívána ke studijním účelům. Za předpokladu, že každý, kdo tuto práci použije pro svou přednáškovou nebo publikační aktivitu, se zavazuje, že bude tento zdroj informací řádně citovat.

Souhlasím se zpřístupněním elektronické verze mé práce v Digitálním repozitáři Univerzity Karlovy v Praze (http://repozitar.cuni.cz). Práce je zpřístupněna pouze v rámci Univerzity Karlovy v Praze

Souhlasím – Nesouhlasím*

V Praze, 1.7.2010

Podpis

* **Nehodící se škrtněte**

Acknowledgement:

Ráda bych poděkovala všem lidem, bez jejichž cenných rad a spolupráce by tato disertační práce nevznikla. Ing. Miroslavu Horáčkovi a Ing. Vojtěchu Paskovi, kteří pracovali na vývoji detekčního zařízení optických signalů. Ing. Monice Martinkové a Ing. Evě Krajčovičové, které zpracovaly software VisionBrain a byly mi velkou oporou. V neposlední řadě bych ráda poděkovala člověku nejdůležitějšímu MUDr. Jakubu Otáhalovi, PhD, který mně celé studium vedl a udával směr i know-how rozsáhlému projektu optických signálů.

Tato práce byla řešena v rámci grantu 1QS501210509 AVČR

Abstrakt:

Optické singaly jsou signaly které detekujeme pomoci světla odraženého nebo prochazejicícho biologickými tkáněmi. Detekce takových změn může být použita pro stanovení fyziologických i patofyziologických procesů probíhajících v biologických tkáních (in vitro) nebo i v tkáni živého organismu (in vivo).

Cílem této disertační práce bylo představení detekce optických signálů jako zobrazovací metody a navržení zařízení pro registraci těchto signalů in vivo.

Disertace obsahuje navrhy experimentálního detekčního zařízení a to jak pro zdroj světla, tak pro upevnění optické soustavy na experimentální zvíře.

Vlastní praktická část studie zahrnuje detekci transmitance živých hipokampálních řezu potkana při různých námi nastavených podmínkách na úrovni iontových kanálů, glutamatergní synaptické aktivity, signalu z glie a mitochondriálního signálu.

V neposlední řade se v disertaci věnuji zdroji šumu, který detekujeme a musíme odlišovat od vlastních změn optických vlastností ve tkáni způsobených vlastními fyziologickými procesy. Pro synchronní registraci electricke a optické aktivity byl navržen software VisionBrain.

Klíčová slova: ***vnitřní optické signaly, hipokampus, zobrazovací metody, biomechanika***

Abstract

Intrinsic optical signals are the signals reflecting changes in transmittance or reflectance of the light illumitating the tissue. Registration of such changes can be applied for the detection of physiological condition in the slices of biological tissues (in vitro) or in the whole animal (in vivo).

The aim of this project is to introduce this topic and show different possibilities for the detection of changing optical properties of nervous tissue both in vitro and in vivo.

The detection system of both light source and attachment of the optical fibre to the skull of the animal for in vivo experimets have been designed. The proper experimental part of the study have been done in hippocampal tissue slices and shows the correlation of the tissue activity and the optical signal at level of ion channels, glutamatergic synaptic activity, glial component of the signal and mitochondrial signal.

We are dealing with the source of the noice that we record while detecting rather subtle changes of optical properties. We are indroducing the software VisionBrain for synchronous detection of both electrical and optical changes.

Keywords: ***Intrinsic optical signals, hippocampus, imaging,*** **biomechanics**

1 Introduction

These days many newly developed imaging techniques appeared. Such techniques benefit from the emergence of many functional imaging technologies covering multiple spatial and temporal scales with the aim to map the processes in the CNS, Intrinsic Optical Signals belong to these.

In neuroscience we have learnt a great deal about the elementary processes that govern the function of individual cells of the nervous tissue, but there are also many processes still remaining unrevealed. Recordings of trajectory of light transmitted or reflected from the tissue become very promising tool in the detection of nervous tissue activity and with the new advances of the microscopy new amazing possibilities appeared. Information offered by optical imaging can be further combined with electrophysiological recordings which give us other relevant information.

In the recent years, certain investigation has been undergone in the field of optical signals. We can divide these experiments used both in the animal and human studies (in vivo) and also in the experiments with nervous tissue (in vitro). In vivo the situation is even more complicated because of the presence of the respiratory and cardiac movements, hand in hand with the spontaneous movements of the animal and the flow of the blood present in the tissue results in the signal noises that has to be avoided. In vitro imaging is used especially for the experimental purposes to define some of the events, get rid of the unwanted signals. In vitro experiments also are mainly preliminary experiments followed by in vivo usage.

The optical properties of the tissue and its detection are fairly well established, but there are some discrepancies in terms of definition of the signal. The biggest inconvenience of the signal is the fact we don't record any direct changes, in stead of that we are detecting the consequences of many processes in the tissue occurring during its activation.

Neurovascular coupling is fundamental for modern haemodynamics-based functional brain-imaging techniques in vivo. The techniques such as PET, fMRI and oximetry (Vanzetta and Grinvald, 2005), in contrast to EEG or magneto-encephalography and single and multi-unit electrical recordings, make possible to map the activity of large neuronal populations at very high spatial resolutions. The large disadvantage of such techniques is mostly the high cost and difficult handling.

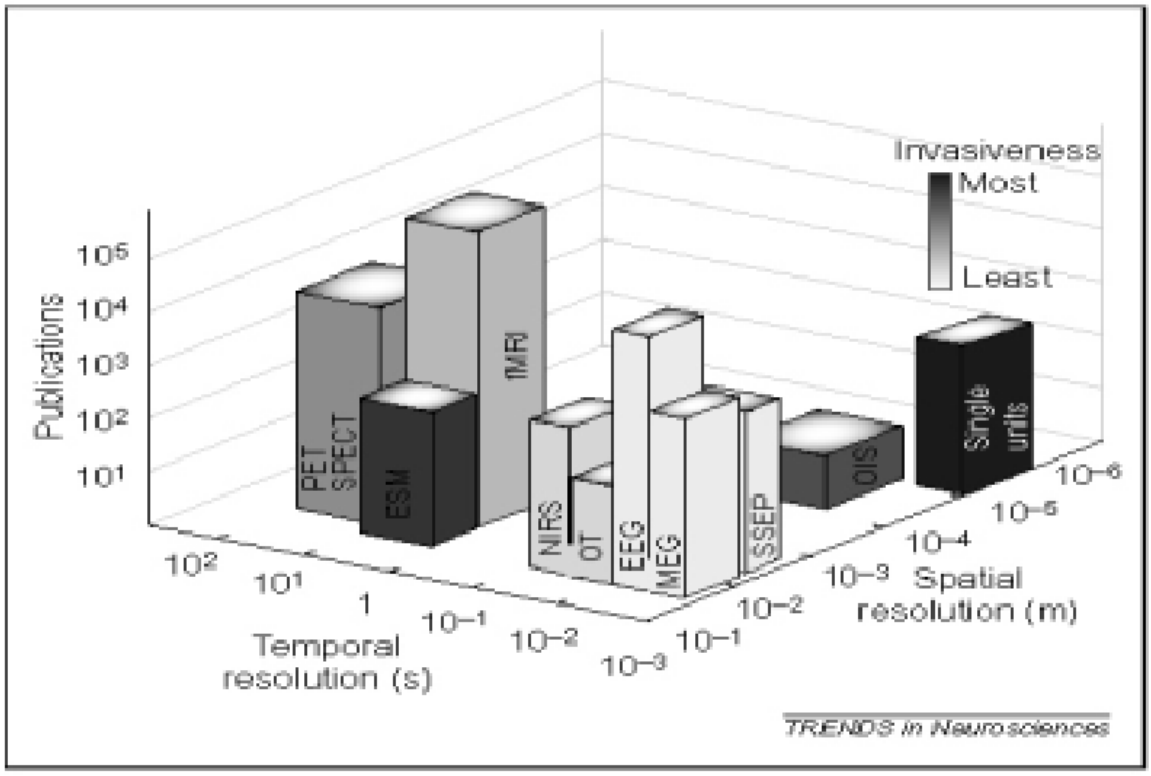

Figure 1 Comparison of the techniques visualizing function of the brain. Every method is compared according to the temporovisual scale. On the figure, we can also see the number of publication made with help of each of them. EEG- electroencephalogram, EMS, electric stimulation, fMRI functional magnetic resonance, MEG, magnetic encefalogram, NIRS, near-infrared refractory spectroscopy, OT , optic tomografy, PET, possitron emisson tomography, SPECT, SSEPs, somatosensoric evoked potentials. (Pouratian et al., 2003)

In this work, I would like to present optical signals, signals detecting changing optical properties, in context of cellular compartments, cellular and overall

biomechanical properties and design the device that would enable the detection of changing optical properties of the nervous tissue in vivo.

In the first part, I would like to introduce the basic processes in the CNS, define the signal at its cellular level. In the experimental part, I am presenting experimental work where we are using pharmacological agents to influence the ionic channels of excitatory mediators, volume changes as well as glial component of the signal and autofluorescence measurements.

In the second experimental part, I have collected and summarized the work that has been done so far at the Department of Developmental Epileptology as a part of the work dealing with the optical signal detection in vivo, where cardial and respiratory movements of the whole CNS should be involved.

1.1 Cellular Organization of the Brain

1.1.1 Neuron and Glial Cells

CNS consist of 10^{11} neurons and at least three times as many glial cells (Hansson and Ronnback, 2004). In general, neuron is an excitable cell (4 μm to 150 μm of pericarion) that is able to process and transmit information. All neurons are electrically excitable, maintaining voltage gradients across their membranes. To maintain these gradients metabolically driven ion pumps and ion channels embedded in the membrane are used. Their purpose is to generate appropriate intra-extracellular concentration ions such as sodium, potassium, chloride, and calcium. Changes in the cross-membrane voltage alter the function of voltage-dependent ion channels. If the voltage changes by a large enough, action potential can be generated and spread further via synapse.

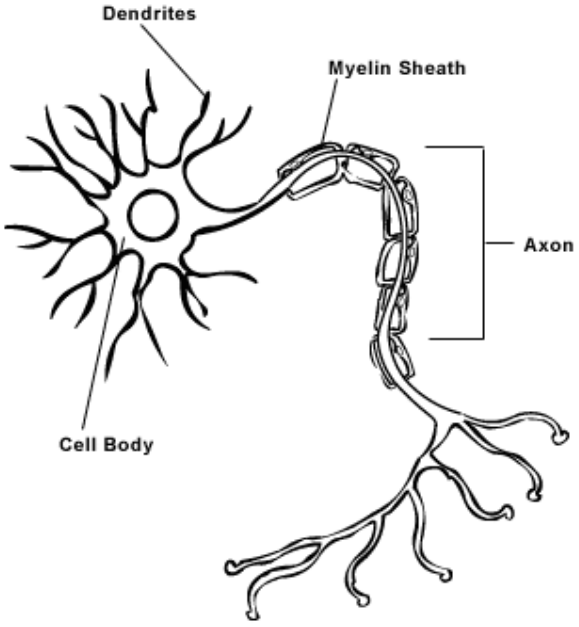

Figure 2 Neron, cell body gives rise to dendrites and axon.
(http://creationwiki.org/File:NEURON2.gif**)**

In a typical neuron we distinguish a cell body, dendrites, and an axon. Dendrites extrude from the cell body, often giving rise to a complex "dendritic tree". An

axon arises from the cell body at a site called the axon hillock and travels often for a greater distance (

Figure **2**). According to neuronal projection, we can divide neurons schematically into groups, where pseudouniporal neurons have dendrite and axon in one process; bipolar with single axon and single dendrite opposite to each other and multipolar neurons with more than two dendrites.

Neurons are highly specialized cells differentiated accoding to the region where they are placed and connections they possess. As a result, there is a great variety of neurons .The soma can vary from 4-100 um in diameter. The length of axon can also extend tens or even thousands of times the diameter of the soma. Fully differentiated neurons are mostly amitotic, although recent research show that some areas of the brain such as subventricular zone can dispose new neurons originating from stem cells (Alvarez-Buylla, 2002).

Neurons compared to the other eukaryotic cells have extremely polarized cellular structures and enlarged cellular volume. Neuron such as every eukaryotic cell contains organelles with membrane delimited compartments playing vital roles. Inside of the cell there is cytoplasm where such processes as glycolysis take place. Cytoskeleton in neuron is a network of filamentous structures forming different shapes such as microfilaments, neurofilaments and microtubules. In neurons, cytoskeleton is essential for moving vesicals and other organelles (axonal transport), this process is energy demanding. Endoplasmatic reticulum and golgi apparatus is essential for the synthesis and processing of proteins and lipids (Sekine, 2009). Lysosome are acid containing vesicles digesting unwanted material in the cell thank to hydrolases. Mitochondria own double membrane and own DNA and generate energy and participate in metabolism, calcium signaling and apoptosis (Duchen, 2004). Nucleus is another membrane bound stucture containing DNA, is necessary for the coded production of specific proteins (

Figure 3).

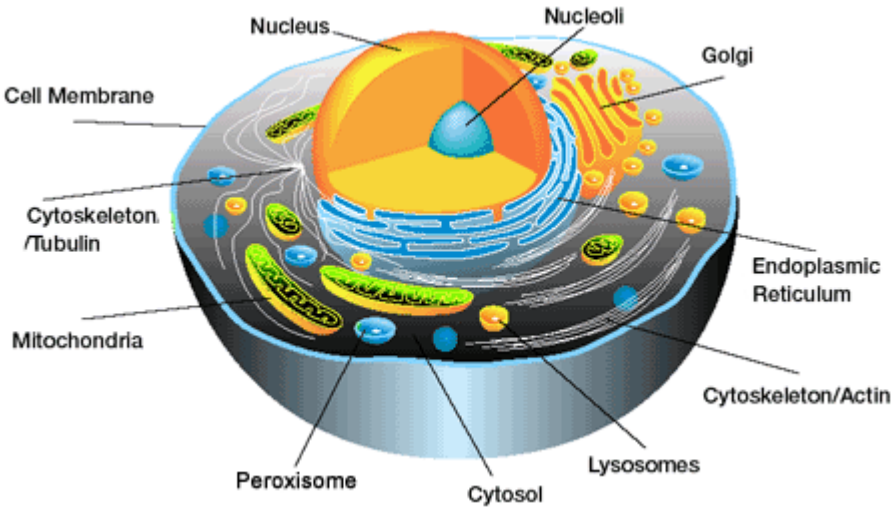

Figure 3 Schema schows cellular organelles.

Glial cells are the other cell types in CNS, they have non-neural character and predominantly supporting, nourishing and healing function in CNS (Frontczak-Baniewicz, 2006; Abbott, 2006). It would be impossible to find one guiding function for glial cell. Furthermore from the 90thies (glial revolution) the findings about the role of glia contribution to function in CNS changed and recently, it has been proposed that glial cells expresses some functional and neurochemical properties that have been previously considered as specific to neurons (Perea, 2009).

When we go into more detail, there are many kinds of glial cells including two big groups : macroglial and microglial cells. The most common type of macroglial cells are astrocytes with the predominant function of regulating ion concentration and thus play an important role in IOS generation and overall changes in optical properties of the nervous tissue. Importantly astrocytes are responsible for the clearance of extracellular potassium, which was proved when this reuptake of K+ was blocked, slowed recovery rate of extracellular K+ which is important for ability of neurons to become able to generate action potential (Buchheim2005, (Kofuji and Newman, 2004). It has been proposed that buffering of K+ by glial cells may also be associated with Cl- fluxes and can even influence the release of transmitter during astrocytic swelling leading to neuronal stress in certain

pathologies (Kimelberg et al., 2006). Astrocytes also anchor the blood supply for neurons and even regulate blood flow regarding energy demands because they produce vasoactive metabolites (LeMaistre, 2009), and form end-feet (Figure 4) (Kimelberg, 2006, Gordon, 2008). Astrocytes can further contribute via ATP release (important intracellular signal) to calcium wave propagation and can modulate neuronal excitability in general (Darby, 2003).

The other macroglial cells are ependymal glia forming cavities within CNS, oligodendrocytes producing myelin. Microglia cells are capable of phagocytosis protecting neurons in CNS and Schwann cell in PNS.

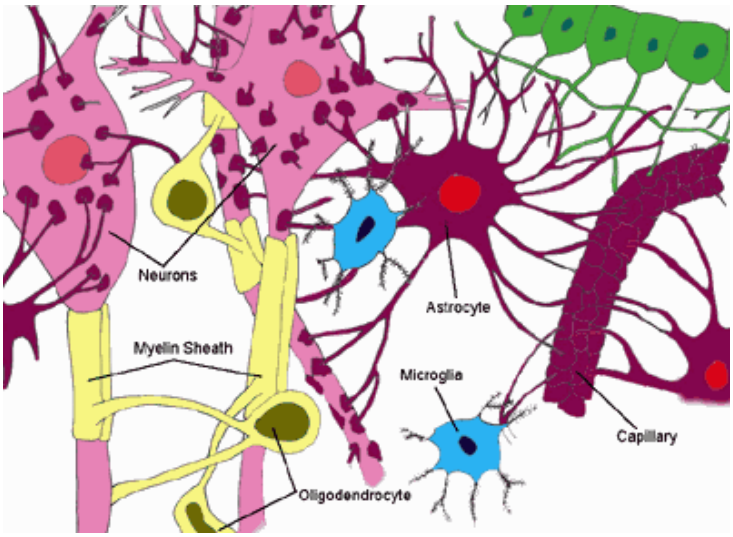

Figure 4
Glial cells. Note that astrocytes forming end-feet, they reach with their processes to both neurons and capillaries. (http://library.thinkquest.org/C0126536/glial.gif)

1.2 Cerebral Cortex

Cerebral cortex can be devided into groups of isocortex (neocortex) with the six layer organization and allocortex with less than six layers (hippocampus, olfactory cortex).

1.2.1 Allocortex, hippocamupus

The hippocampal formation is a useful model for the study of properties of central nervous system (CNS) because of its unique properties which are a well visible layers with strictly laminated inputs, predominantly unidirectional connections and synapses that are highly plastic (Bliss and Lomo, 1973). Acute or cultured slices of hippocampus are above all able to survive for prolonged periods in vitro. Further the historical and recent research interest about this structure is extensive. There has been made a large number of detailed investigations on the properties of hippocampal neurons, mostly the pyramidal cells. (McBain, 2008; Banke and McBain, 2006)

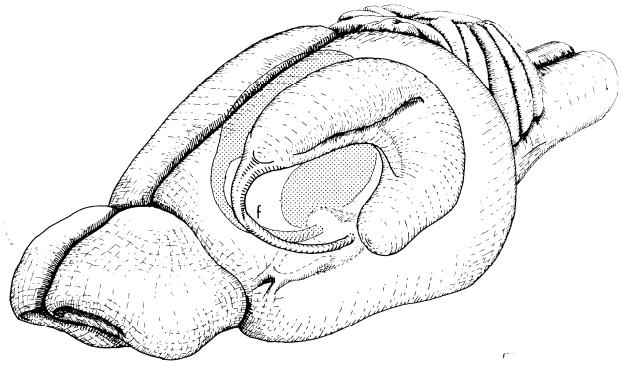

Figure 5 The C-shaped hippocampus is shown in a transparent shell of the rat brain. (Paxinos and Watson, 1998)

The bilateral hippocampal formation appears similar to the curved horns of a ram, hence its early name "Cornu Ammonis" (Ammon's horn), after which its CA1-3 fields of the hippocampus proper are named. Each roughly C-shaped side extends from the septal nuclei dorsally and caudally over the diencephalon, and

then ventrally and rostrally tucks under the temporal lobe. Left is anterior, right is posterior.

General features of hippocampal formation

Hippocampal formation of the rat with its surface area approximately 1.2cm^2 (the surface of the entire isocortex is estimated with 1.5cm^2) is a prominent component of the rat nervous system and attracts the attention of neuroanatomists since the beginning of formal study of the nervous system. Many neurophysiological principles were discovered on hippocampal preparations among these there are for example: the identification of excitatory and inhibitory synapses and their localization, transmitters and receptors, the discovery of long-term potenciation and long-term depression: post-tetanic potentiation, the role of oscillations in neuronal networks and the underlying mechanisms of epileptogenesis.

Hippocampus receives both cortical and subcortical inputs. The information received from cortical sources is regarded to be the major substrate for cognitive functions. Subcortical inputs, predominantly from the medial septal complex, the hypothalamus, and the brain stem, are regarded to be rather modulatory and may reflect the behavioral state of the organism. Hippocampal intrinsic circuitry has been studied and there is one unique feature of the hippocampal intrinsic circuitry, this is the largely unidirectional organization of the projections that interconnect the various hippocampal regions. For this reason, hippocampal formation is used as a model structure of CNS.

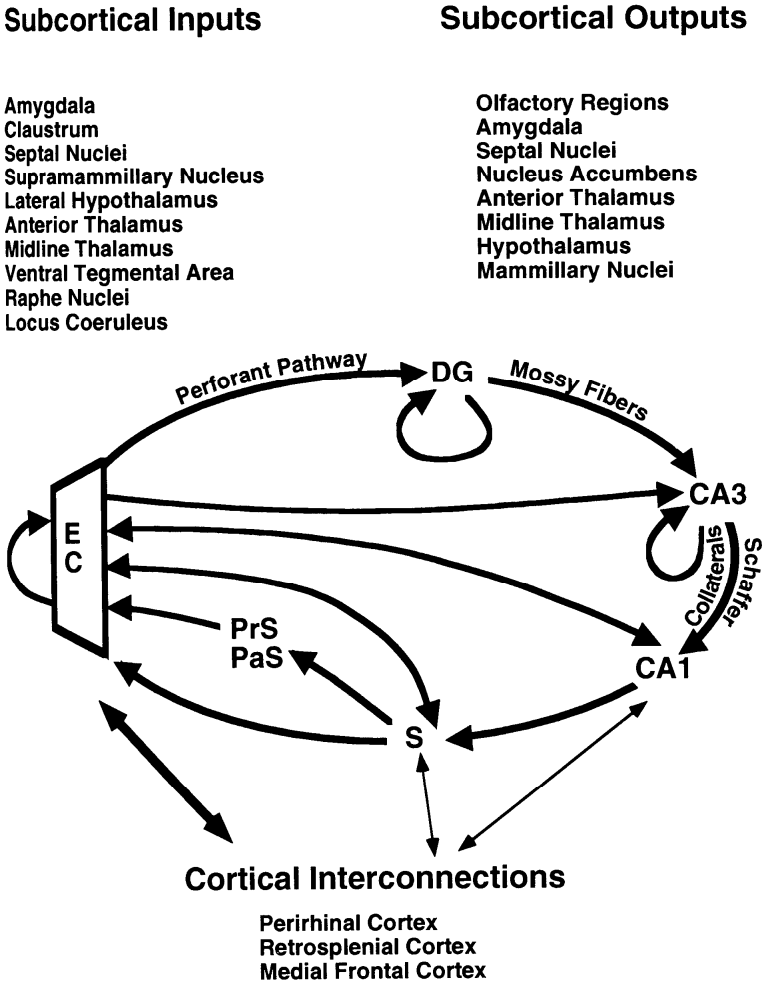

Figure 6 This diagram illustrates the major intrinsic connections of the rat hippocampal formation. Many of the named pathways, mossy fibers, and Schaffer collaterals are unidirectional. Several of the major cortical and subcortical inputs and outputs of the hippocampal formation have been listed. DG – Dantate gyrus, CA1-3 – Cornu ammonis, S – Subiculum, PrS – Presubiculum, PaS – Parasubiculum, EC – entorhinal cortex(Paxinos and Watson, 1998).

Definition of hippocampus

Hippocampus can be also called allocortical it means the three layered regions that have a single principal cell layer with fiber or plexiform layers above and below the principal cell layer. This stands only for the four cytoarchitectonically distinct regions of hippocampus; enthorhinal cortex, dentate gyrus, hippocampus

or hippocampus proper (Cornu Ammonis = Ammons horn = CA), which is subdivided into three fields CA3, CA2, CA1, and subiculum.

Gyrus dentatus (GD)

DG is characterized by sparse and unidirectional projections to CA3 pyramidal cells, mossy fibers (MF). It has been hypothesized that the function of the MF is to enforce a new separated pattern of activity onto CA3 cells, representing memories already stored on CA3 recurrent collateral connections. Interestingly, the neurogenesis was found to occur in the adult DG, with the newly existing cell functionally added into the circuitry contributing to the ongoing activity.(Treves et al., 2008) DG contains three layers, molecular layer (contains dendrites of granule cells, basket and polymorphic cell, axonal arbors) is closest to the hippocampal fissure, the principal cell layer or granule cell layer- which is made up primarily of densely packed columnar stacks of granule cells, the polymorphic cell layer (mossy cells) which is more often called the hilus, on the other side of the granule cell layer, closest to CA3. In the brain the major DG input is from enthorhinal cortex via the so-called perforant path. The entorhinal to dentate gyrus projection is not reciprocated. Subcortical inputs to the dentate gyrus originate from the septal nuclei from the supramamillary region of the posterior hypothalamus, and from several monoaminergic nuclei from the brain stem. Granule cells of gyrus dentatus project via their mossy fibers to the CA3 field of the hippocampus proper.

Hippocampus propper

Lorente de Nó devided the hippocampus proper into three fields CA1, CA2, CA3 that are cytoarchitectonically different. CA3 and CA2 have larger cells. CA3 region recieves mossy fiber input from the dentate gyrus. CA2 is a terminal portion of the CA3 field. The vast majority of neurons in the pyramidal cell layer and the principal cells are pyramidal cells. Intrahippocampal connections of CA3

include highly collateralized axons of pyramidal cells CA3 that distribute fibers within the hippocampus to the same fields in the contralateral hippocampus, and subcortically to the lateral septal nucleus. The projections to CA3 and CA2 are typically called the associational connections, and the CA3 projections to the CA1 field are typically called the Schaffer collaterals. All portions of CA3 and CA2 project to CA1. The CA1 field gives rise to two intrahippocampal projections; to the adjacent subiculum and to the deep layers of the entorhinal cortex.

Connectivity of hippocampus

The cross-section of the hippocampal formation has a laminar profile. Each field (DG, CA1, and CA3) contains a thin plane of projection cell bodies, granule cells in the DG and pyramidal cells in fields CA1-3. The anatomical layout of these principal cell layers and a subset of their intrahippocampal projections form the classical "trisynaptic circuit". Projection cells are aligned with their apical dendrites extending toward the hippocampal fissure, which is also the division between the dentate gyrus and CA1, and the basal dendrites and axons extending toward the outer surface of the hippocampus (

Figure 7).

In the CA fields, the narrow, cell-free layer just deep to the pyramidal cell layer is called stratum oriens, in which most of the basal dendritic tree is located, and deep to this is the fiber-containing alveus. In the CA3 field, but not in CA2 or CA1, there is a narrow layer called the stratum lucidum, containing **the mossy fiber** projections from the dentate gyrus. Just above the pyramidal cell layer in CA2 and CA1, and just above the stratum lucidum in CA3, is the stratum radiatum, in which the CA3 recurrent collaterals and CA3-CA1 **Schaffer collaterals** are located. In addition to the projection cells, each layer of each field also contains a heterogeneous mix of interneurons, the vast majority of which are GABAergic. The interneurons receive inputs from the same regions as

the principal cells in that field, and they also project to and receive inputs from the local principal cells. They are predominantly local circuit neurons, but some are also known to project outside their subfields (Paxinos and Watson, 1998).

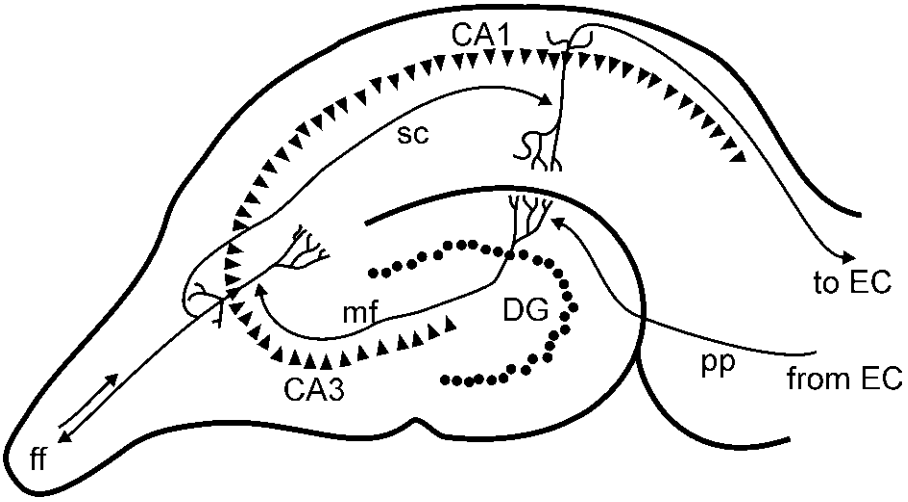

Figure 7 Cross-section of hippocampus. This schema of the coronal cross-section of dorsal hippocampus illustrates the layout of the principal cell layers of DG, CA3, and CA1. It also illustrates the layout of a subset of the intrinsic outputs of these principal cells, known classically as the "trisynaptic circuit" (2): EC to DG (synapse 1), DG to CA3 (synapse 2), and CA3 to CA1 (synapse 3). EC = entorhinal cortex; DG = dentate gyrus; pp = perforant pathway; mf = mossy fibers; sc = Schaffer collaterals; ff = fimbria/fornix.

1.2.2 Neocortex

The neocortex is a part of CNS playing an important role in memory, attention and cognition. It is constituted of six horizontal layers of grey matter each with different composition of neuronal cells and connections to the other neural structures. Neocortex is devided into occipital, temporal, parietal, frontal cortex each with its distinct function. Neocortex has a folded surface in large mammals, two thirds of human cortex in hiden in so called sulci. In rat the surface is without sulcies, rat is considered to be lisencephalic (Neal, 2007).

Laminar pattern

As it has been already mentioned the different cortical layers each contain a characteristic distribution of neuronal cell types and connections with other cortical and subcortical regions. In fact staining cross-sections of the cortex to reveal the position of neuronal cell bodies and the intracortical axon tracts allowed neuroanatomists in the early 20th century to produce a detailed description of the laminar structure of the cortex in different species. After the work of Korbinian Brodmann (1909), the neurons of the cerebral cortex are grouped into six main layers, from outside (pial surface) to inside (white matter): In the molecular layer I, there are a few scattered neurons and consists mainly of extensions of apical dendritic tufts of pyramidal neurons and horizontally-oriented axons and glial cells. The external granular layer II contains predominantly small pyramidal neurons and numerous stellate neurons. The external pyramidal layer III possesses small and medium-size pyramidal neurons, as well as non-pyramidal neurons with vertically-oriented intracortical axons. In the granular layer IV, there are different types of stellate and pyramidal neurons, the main target of thalamocortical afferents. The internal pyramidal layer V, includes large pyramidal neurons some of those can be distinguished as intrinsic bursters (IB). The multiform layer VI, contains few large pyramidal neurons and

many small spindle-like pyramidal and multiform neurons; layer VI sends efferent fibers to the thalamus, establishing a reciprocal interconnection between the cortex and the thalamus. Neocortex is not homegenous in structure. The regions have different thickness, contain different cells and are also organized differently. The neurons of neocortex have different shape and can be devided into two bigger groups which are the pyramidal cells and local interneurons. Pyramidal neurons have triangular shape, making one apical dendrite which origins from the apex of the cell soma, the axon makes medial arbors and reaches up to the first layer. Axon originating in the cell soma goes through the cortex to the white matter (Paxinos and Watson 1998).

Connections of the cerebral cortex

Pyramidal cells are present in all layers except for the layer I with the most frequent presence in the layer II., III. and V.. Axons of the pyramidal cells are the efferents of the cortex and are able to project to bigger distances outside the cortex, the other neuronal cell types influences just the cell in their proximity. Excitatory synapses of pyramidal cells are glutamatergic. The cerebral cortex is connected to various subcortical structures. Most sensory information is routed to the cerebral cortex via the thalamus except for olfactory information that passes throught the olfactory bulb. The vast majority of connections are from one area of the cortex to another rather than to subcortical area. The cortex has three areas sensory, motor, and association areas.

Sensory areas

The information from the senses are the so called sensory areas, the primary sensory areas are received from the thalamus. The mammalian neocortex contains two somatosensory areas SI and SII. Each of this has a distict cytoarchitecture containing a separate representation of the body surface. SII is located lateral to SI. Somatosensory cortex has the six layers typical of

neocortex. The layer IV is rich in granule cells and has a poorly marked boundary between layer II and III. There are further the areas for the representation of the head ParI, and for the forelimbs and hindlimbs Fl and Hl. SI contains granular aggregated in regions in Fl and Hl. Barrels, made up of granule cells, and granular aggregates may be lumped together as granular zones. The cytoarchitecture of SII is comparable to that of SI. However, in SII there are no aggregates of granule cells and layer IV is thinner than in SI.

Motor areas

Located in the both hemispheres of the cortex and are closely related to the control of voluntary movements. The centre of control is contralateral to the side of the movement. The motor areas of the cortex are primary executing voluntary movement and supplementary selecting voluntary movements.

1.3 Neurophysiology

1.3.1 Signal transmission

Neuron is neuronal cell transmitting information via signaling using either chemical or electrical way. To understand these processes we have to go into more detail.

Water

About 80% of the brain is water. All transmembrane ionic shifts e.g. K^+, Na^+, Ca^{2+}, H^+ and membrane transport mechanisms such as neurotransmitter uptake are followed by water movement. Water can move in and out of the cell with simple diffusion that is enabled by lipid bilayer or it can be by facilitated through so called aquaporins.

Aquaporins

Aquaporins (AQPs) are a family of water-selective channels providing main osmotically driven pathway for the water transport through cell membranes. Water homeostasis is important for the activity of neural tissue. Water is also major component of all living organisms, so appropriate regulation of water flow through the cellular membranes is a central requirement for all living organisms. Six aquaporin subtypes are found in rodent brain (AQP1, AQP3, AQP4, AQP5, AQP8, AQP9). AQP1 is present in choroid plexus and participate in SCF forming. AQP4 found in astrocytes, ependymal cells, glia limitans and is believed to play an important role in water homeostasis and might play role in maintaining low level of extracellular K^+ (Tait et al., 2008). (Badaut et al., 2002) AQ4 is considered to be the main pathway in the permeability of BBB for water and increased expression of AQ4 in glial cells has been found in spinal cord after spinal cord injury and sclerotic hippocampus in temporal lobe epilepsy (Nesic et al., 2006; Holthoff et al., 2007;Lee et al., 2004). Permeability of AQ4 can be increased by erythropoietin and contribute to neuronal demage after stroke (Gunnarson et al.,2009).The more exact information concerning selective

inhibition of aquaporins might be benefitial in terms of avoiding of their harmful effects while overly expressed in such pathologies (Gunnarson, 2004). Interestingly in the brain, cotransporters such as EAAT and NKCC has been also found to transport water(Macaulay, 2004).

Cellular organels such as mitochondria acts as an osmometer, changes in mitochondrial volume occur in many other physiological and pathophysiological conditions such as intracellular signaling, ischemic damage or anoxia. Among others mitochondrial swelling is one of the earliest signs of cell injury. Mitochondrial volume changes are modulated by the net movement of solutes such as K^+ and Ca^{2+} ions across the inner mitochondrial membrane. AQP8 is believed to play an important role in diffusion of water into the cell and can contribute to the very rapid entry of solutes and water into the matrix and cause the damage leading even to the apoptotic cell death (Calamita, 2005).

Because of the fact, that the intracellular potassium is considerably higher than for other ions, the osmotic balance is controlled mainly by the potassium fluxes. (Kaasik, 2007) The role of mitochondrial calcium is furthermore of our particular interest these days, intramitochondrial increase in calcium lead to massive swelling and this occurs as a result of the opening of a non-specific pore in the inner membrane of mitochondria. (Halestrap, 2009)

1.4 Ions in the brain

Ionic balance is crucial for the intact neuronal functions. Ionic levels are maintained constant and every little fluctuation affect homeostasis. For proper function of the neuron e.g. signal processing sodium, potassium and chloride ions are of the most importance. In the following chapter I will describe basic roles of these crucial ions.

Na^+

Sodium is major positively charged monovalent ion of the human body. In the nervous tissue is its concentration high extracelulary and low in the neurons. The described concentration gradient is made by unequal charge distribution in versus outside the cell and by permanent action of sodium-potassium pump. For further details on equilibrium see chapter 1.4.1.. Plasma membrane is impermeable for sodium ions and thus for their movements sodium channels are present in the membrane. Sodium channels are integral membrane proteins conducting sodium ions through a cell's plasma membrane. They are classified according to the trigger that opens the channel i.e. either a voltage-change (voltage-gated sodium channels) or binding of a substance (a ligand) to the channel (ligand-gated sodium channels). Voltage gated sodium channels are responsible for the rising phase of action potentials.

K^+

Potassium distribution is the most important determinant of resting membrane potential on the neuronal membrane. Contrary to sodium, the potassium is major intracellular positively charged monovalent ion. Dominant K^+ conductance gives a negative resting membrane potential close to K^+ equilibrium with maintain the negative membrane potential with minimal energy demands. (Amedee, 1997).

Extracellular concentration of K^+ in most parts of the rat brain is about 2.5-3mM, during electrical stimulation it can rise more than three times, interestingly during physiological activity for example in response to sensory stimulation, the changes are smaller, even less than 0.10mM. During seizure activity the level of K^+ can reach the ceiling level to 10-12mM, levels of K^+ can reach even higher value in ischemia or in spreading depression (Kettenmann, 1999). Although moderately elevated extracellular K^+ have relatively little influence on membrane potential ir influences excitability due to alkalization of the tissue. In experiments using ion-sensitive electrodes (constant detection of extracellular K^+

concentration), it has been suggested that IOS, LT respectively, is proportional to K^+ changes.

Cl^-

Chloride is the most important negatively charged ion of the nervous tissue. Distribution of the chloride on plasma membrane is dependent mainly on activities of chloride transoprters NKCC1 and KCC2. In adult, where major chloride transporter is KCC2, chloride anione is actively pumped from the cell and thus producing higher concentration of chloride extracellulary. Therefore when chloride channels in such situation open it produces hyperpolarization of the cell because of incrasing negative charge of cell. However, during maturation NKCC1 (pumps Cl^- into the cell) maintains high intracellular concentration of chloride ion. After opening of chloride channels it causes depolarization of the cell. Activity dependent conducances of chloride are mainly through ligand gated ion channel which is part of the ionotropic GABA A receptor.

1.4.1 Equilibrum potential

Neurons such as all other cells are surrounded by plasma membrane impermeable to ions. Like this, neuron maintains different concentrations of ions between the inside and the outside of the cell. In the mammalian brain, the difference in the concentration of ions is largely different. The interior of the cell of the neuron has a larger concentration of negatively charged proteins (106 mM). The other important ions are K+ (150mM) intracellulary/(5mM) extracellulary, Na+(15mM/150mM), Cl- (9mM/125mM). Ions crossing the membrane are driven by osmotic fluxes and also by electric fields through specialized channels. The point where all the influences are in balance is called equilibrum potential E_m.

If the membrane is in thermodynamic equilibrium, the membrane potential must be equal to Nernst potential. We are using this quotation to estimate the potential of the ion of charge z across the membrane (1).

$$E = \frac{RT}{zF} \ln \frac{[\text{ion outside cell}]}{[\text{ion inside cell}]}.$$

(1)

R is the universal gas constant: R = 8.314 J $K^{-1}mol^{-1}$

T is the absolute temperature

F is the number of coulombs per mole of electrons: F = 9.648 C mol^{-1} (Faraday constant)

z is the number of electrons transferred in the cell reaction

In the cell and its environment more ions are present. To determine this, we can use the Goldman-Hodgkin-Katz equation (2):

$$V_{rest} = \frac{RT}{F} \ln \frac{P_K[K^+]_{out} + P_{Na}[Na^+]_{out} + P_{Cl}[Cl^-]_{in}}{P_K[K^+]_{in} + P_{Na}[Na^+]_{in} + P_{Cl}[Cl^-]_{out}}$$

(2)

P ion is the permeability for that ion (meters per second)

[ion] out is the extracellular concentration of that ion (moles per cubic meter, to match the other SI units)

[ion] in is the intracellular concentration of that ion (moles per cubic meter)

R is the ideal gas constant (joules per kelvin per mole)

T is the temperature (kelvins)

F is Faraday's constant (coulombs per mole)

$$V_{rest} = 58 \log \frac{1(10) + 0.03(460) + 0.1(40)}{1(400) + 0.03(50) + 0.1(540)} = -70mV$$

(3)

Since PK dominates, its resting potential is close to membrane potential. During an action potential the ratio is PK: Pna: PCl =1 : 15 : 0.1 so that (4)

$$V_m = 58 \log \frac{1(10) + 15(460) + 0.1(40)}{1(400) + 15(50) + 0.1(540)} = +44mV \quad \textbf{(4)}$$

Later on we can approximate the GHK equations by a linearized version (5):

$$V_{eq} = \frac{g_{Na} E_{Na} + g_K E_K + g_{Cl} E_{Cl}}{g_{Na} + g_K + g_{Cl}} \quad \textbf{(5)}$$

where the conductances g are proportional to the permeabilities.

In conclusion, membrane potential is the voltage difference between the intracellular and extracellular spaces. On both sides of the membrane there are high concentrations of different ions, sodium (Na^+), potassium (K^+), chloride (Cl^-) and calcium (Ca^{++}) are the most prominent. Na^+ and Cl^- are the main extracellular ions, K^+ is present inside of the cell, Ca^{2+} is primary held as a signaling molecule. In addition inside of the neuron, there are negatively charged proteins (106 Mmol) causing the negative membrane potential even in the resting state.

The membrane potential arises from the interaction of all ion channels and ion pumps present in the membrane, as they maintain different ion concentrations on the intracellular and extracellular side of the membrane.

This is just to note that changes in all ion concentrations during activity can be regarded as a signals passing through extracellular space. These ions are not only those I mentioned before, but also $HCO3^-$, H^+ nad $NH4^+$ which are linked predominantly to different metabolic states.

Movement of ions - General description of ion channels

The only possible way to travel across the lipid bilayer is by passing through specific channels. Ion channels are the integral membrane proteins enabling ions to move between extracellular space and cell interior.

Ion channels have a central pore through which ions can move once it is opened (Hille, 2001). Most channels are specific (selective) for one ion. Interestingly most potassium channels are characterized by 1000:1 selectivity ratio for potassium over sodium, although potassium and sodium ions have the same charge and differ just slightly in their radius. The channel pore is usually small so that ions must pass through it in single-file order. Depending on channel pore can be either opened or closed for ion passage. Beside ion channels there are ion pumps in the phospholipid bilayer, requiring energy (ATP) for transportation, and ion transporters. Transporters are transmembrane molecules binding the transported ion or another particle on one side of the membrane, move it across and release it on the other side.

Primary and secondary active transport

Ion pumps produce the power and the motion of ions within the membrane, as they split ATP to provide the energy required to move ions against electrochemical gradient (primary active transport). Secondary active transport uses energy stored in standing ion gradients, most often that of Na^+. So as Na^+ moves into the cell, it can take another ion or compound.

Ion channels can be also classified by the way they respond to different situations or presence of specific molecule. Ion channels involved in the action potential are mostly voltage sensitive, releasing the ions at certain voltage on the membrane. The so called ligand-gated channels are open and closed chemically depending on ligand molecule which is most commonly the neurotransmitter. The other channels can also react on mechanical forces or in response to such stimuli as light temperature or pressure. As it has been previously mentioned, in

excitable cells, a sufficiently large depolarization can evoke an event called an action potential, in which the membrane potential very rapidly undergoes a large change, often briefly reversing its sign. In neurons, the factors that influence the membrane potential include numerous types of these ion channels.

1.4.2 Action potential

Transient change in the electrical potential on the surface of a excitable cell in response to stimulation leading to the transmission of an short term electrical impulse that travels across the cell membrane is called action potential. This change is generated by the different transporting processes on the membrane consisting of phospholipid bilayer and containing ions pumps and ion channels.

The phases of AP can be divide into the rising phase, the peak phase, the falling phase, the undershoot phase, and finally the refractory period. For AP to be generated, the voltage-sensitive ion channels have to open. This changes the membrane permeability and according Goldman equation (2), the equilibrium potential Em changes and subsequently does the membrane voltage. If the depolarization is sufficient, it causes the opening of votage-sensitive sodium channels and increasing permeability to sodium currents. The sharp rise in Vm corresponds to the rising phase of AP. As the sodium ion channels become open, the rising phase ends at the peak of the AP when the sodium permeability is maximal (the sodium equilibrium voltage $E_{Na} \approx$ +55 mV). At the moment of peak, the sodium channels close and this causes the sink in the membrane voltage, when at the same time potassium channels open, and potassium flow repolarize the membrane and produces the falling phase of the AP. More potassium channels are opened, so the potassium permeability of the membrane is transiently high and it leads to hyperpolazition (afterhyperpolarization)

Membrane that underwent the depolarization recently cannot fire another action potential immediately again, the ion channels have to return to their usual state. The absolute refractory period is the time when no new action potential can be

fired, the relative refractory period is the time when provoking of AP is possible only with help of stronger stimulus.

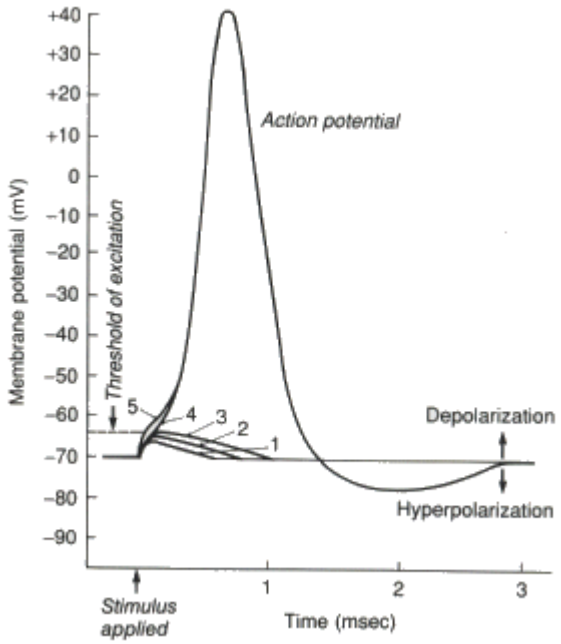

Figure 8 The time course of the action potential can be divided into distinct parts: the rising phase, the peak phase, the falling phase, the undershoot phase, and the refractory period.

Electrical synapse

An electrical synapse, less common than a chemical synapse, is a link between two neurons formed at a gap between the pre- and postsynaptic cells known as a gap junction. At gap junctions, cells approach within about 3.5 nm of each other which is ten times closer than at chemical synapse. Direct electrical coupling between both neurons transmits the signal and therefore it is faster and more reliable than chemical synapses. More specifically, signal transmission across a chemical synapse is delayed at least about 0.5 ms, which is the time required for the neurotransmitter secretion and diffusion.

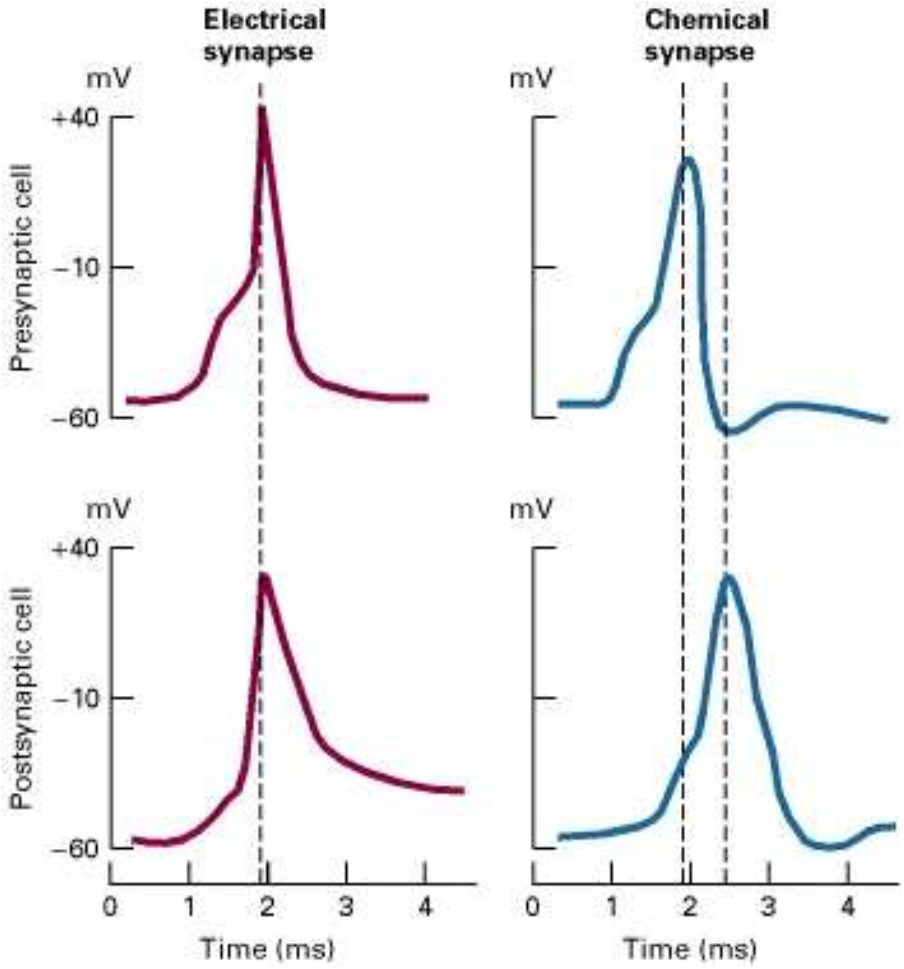

Figure 9 Time course comparison of the chemical and electrical synapse. (http://www.ncbi.nlm.nih.gov/bookshelf/br.fcgi?book=mcb&part=A6187)

Chemical synapse

Chemical synapses are specialized junctions through which neurons signal to each other and also to the other cell types. At a chemical synapses neuron (presynaptic cell) releases neurotransmitter that can be bind to the postsynaptic terminal of the other neuron containing its specific receptor. The 20nm wide gap between pre- and postsynaptic cell is a called the synaptic cleft. The process of signaling can be finished as quickly as in a few tenths of ms. This process begins with a wave of electrochemical excitation called an action potential traveling along the membrane of the presynaptic cell, until it reaches the synapse. The depolarization of the membrane at the synapse makes the channels opened so that they are permeable to calcium ions. Calcium ions flow through the

presynaptic membrane, rapidly increasing the calcium concentration in the interior. The high calcium concentration activates a set of calcium-sensitive proteins attached to vesicles that contain a neurotransmitter chemical. These proteins change shape, causing the membranes of some "docked" vesicles to fuse with the membrane of the presynaptic cell, thereby opening the vesicles and dumping their neurotransmitter contents into the synaptic cleft, the narrow space between the membranes of the pre- and post-synaptic cells. The neurotransmitter diffuses within the cleft. Some of it escapes, but some of it binds to chemical receptor molecules located on the membrane of the postsynaptic cell. The binding of neurotransmitter causes the receptor to be activated.

The resulting change in voltage is called a postsynaptic potential. In general, the result is excitatory, in the case of depolarizing currents, or inhibitory in the case of hyperpolarizing currents. Whether a synapse is excitatory or inhibitory depends on what type(s) of ion channel conduct the postsynaptic current display(s), which in turn is a function of the type of receptors and neurotransmitter employed at the synapse.

Neurotransmitter binding to a receptor and opening it is called the receptors agonist. Therefore receptors agonist produces the action while the antagonist is the term for the substance blocking the action of agonist. When the antagonist competes over binding sites, the antagonist is competitive. As a result only sufficient amount of competitive antagonist can activate the receptor.

Modulation of synaptic transmission

Synaptic transmission can be modulated by e.g. desensitization, when the response is decreased to the same amount of neurotransmitter stimulus, homosynaptic plasticity where the change in the synaptic strength is increased as a result of the history of the activity at a particular synapse and heterosynaptic plasticity, which is the change resulting from the activity of other neurons. This plasticity can alter the number of vesicles or their replenishment rate or the

relationship between calcium and vesicle release and also affect calcium influx directly. In the context of the whole organism, modulation of synaptic transmission lies in the heart of the processes comprising learning and memory.

Volume transmission and extracellular space

Neurons themselves and neurons and glia can communicate by chemical signals that flow through the extracellular space. Volume transmission is mediated by diffusion in the extracellular space and constitutes rather new communication system complementing synaptical transmission and describes the spatial relationships of neurons and glia. Glial cells play an predominantly important role in volume transmission cause affecting ECS compositon.(Sykova and Chvatal, 2000)

The composition of size of extracellular space changes dynamically during neuronal activity, the changes can be even more pronounced in several pathological conditions. Extracellular space occupies a volume franction of between 15 and 30% in normal physiological conditions and can fall to 5% during global ischemia (Sykova and Nicholson, 2008). Intrinsic optical signals can be correlated to changes of volume of extracellular space (Witte, 2001).

Volume changes

In general volume changes are the function of keeping osmolarity inside and outside of the cell on the constant level. Astrocytic swelling can be a side effect of the uptake of Na, Cl, K or glutamate from the extracellular to the intracellular space with the active transporter the Na K 2Cl transporter, NaK adenosine triphosphatase and volume sensitive Cl channels.

Astrocytes and the glial cells in common also occupy most of the brain tissue volume and alterations in the intracellular volume have a great impact not only on the volume but also on the shape of the extracellular space and subsequently it can have impact on the neuronal function and ion balance.

1.5 Detection of Neuronal Activity

1.5.1 Electrophysiology

Neurons are exceptional mainly because of their ability to change electric properties on the membrane. Through these changes the neuronal cell is able to communicate and transfer the information.

Electrophysiology involves measurements of electrical signal, which is represented by voltage changes or currents following movements of the ions inside and outside of the cell. In terms of electrical signal we are able to measure the action potential activity and to record large-scale electric signals as well as the signals emerging from one cell activity. The principal detecting electrodes are most frequently just simple solid conductors such as needle or hollow tubes filled with salt solution. The measurements can be done on the whole organism or just on excised living tissue, cultured or acute or just on dissociated cells.

In the last century electrophysiology was the main technique for the activity registration. Already in 1902 Julius Bernstein advanced the hypothesis about the fact that change in the permeability evokes action potential. His hypothesis was confirmed by Ken Cole and Howard Curtis. Julius Bernstein introduced the Nernst equation for the resting potential across the membrane and this hypothesis has been generalized by David E. Goldman to Goldman equation in 1943.

The first notice about the voltages and currents of the action potential generation was made by Hodgkin and Huxlex in 1952, they described the model to explain the basic ionic mechanisms that stands behind the initiation and propagation of action potentials in the squid giant axon. In 1963 they got the Nobel Prize in Physiology for it. The technique has advanced so far, these days we are able to record even a single channel activity.

Extracellular field potentials are produced by many cells. Its source and compositon is often ambiguous, since the individual signals overlap. With the advances of other imaging techniques such as presented optical signals, voltage sensitive dyes or fluorescence, we can partially overcome the limitation of these classical electrophysiological techniques.

The recording of the electrical activity advanced and these days it can be done in different places of the cell either intracellulary or extracellulary. We are detecting activity of one single neuron or group of neurons.

Intracellular recording of electric activity

Intracellular recording means measuring currents or changing voltage across the membrane of neuron. The voltage accessed with the detection electrode is compared to the volatage of a reference electrode which is in contact with the extracellular fluid. According to the type of electrode we are using, we can distinguish into two types of recordings:

Patch-clamp is technique when the micropipette is attached to the cellular membrane. Patch clamp is used for the activity of one ion channel (cell attached mode). Sharp electrode technique measures the potential inside the cell membrane with minimal effect on the ionic constitution of the intracellular fluid. The pore of the detecting electrode is small and doesn't allow exchange of the intracellular and extracellular fluid.

In general an very briefly, we have two mode in which we can record, these are:

Votage clamp clamps the cell and measures the ion currents across the membrane of neuron. It uses two electrodes and so called feedback circuit to keep the membrane potential set at a certain level to be able to detect ion flux across the membrane. In **current clamp** voltage on the membrane varies,

amplifier record responses to changing currents. How a cell respond to electric current entering a cell.

Extracellular recording of electric activity

Single-unit recording when the electrode is small enough (1um) the electrode usually detect the activity of a single neuron. The signals are smaller than these detected intracellulary (around 1mV). When the electrode is larger (10um), we can record the activity generated by several neurons. This type of recording is called multi-unit recording.

Field potentials are local currents generated by the activity of many cells. The main component of the signal is the most frequently synaptic transmission. We have certain specific methods that reduce confusion over the signal of a large group of cell (pool) and make it equivalent to a single ideal element. Different models can be applied, the closed field, the open field, open closed field.

The model **open field** corresponds to the cell arrangements in the cerebral cortex, the cerebellum or the hippocampus, where the dendrites of the cells are oriented orthogonally. This type of arrangement can be substituted by a single element having a soma and a single dendrite oriented in the same direction as the main axes of dendritic tree. The current field generated between the soma and dendrite spreads through the volume conductor, generating a negative field potential at all points at the somatic side and positive field potential at all points at the somatic side and positive field potential at all points at the dendritic side to zero isopotential surface. When viewed from the distance the activated neuronal system will resemble a dipole. The **closed field** applies in pool of predominantly multipolar cells with radially oriented dendritic trees. Pool is organized in a way somas are in the center whereas most of the dendritic trees are in the periphery.

The **open-closed field** is field in which both kinds of neural elements are in the pool.

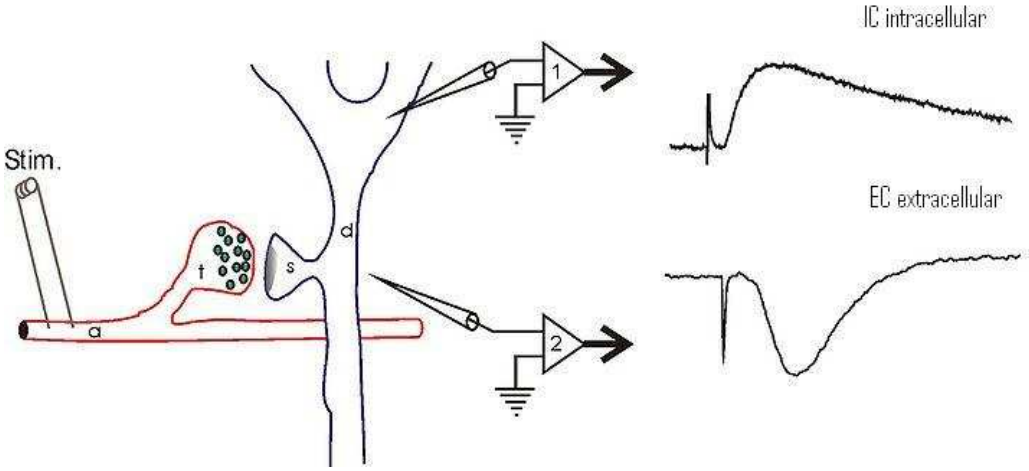

Figure 10 A schematic diagram of presynaptic terminal and postsynaptic neuron. The field potential represents a large population of synapse and neurons. The synapse releases excitatory mediator into the posynaptic cell, it opens ionotropic channels and causes inward movement of the Na+ ions. The nearby electrode detect this as a extracellular negativity

1.6 Optical properties of the nervous tissue

1.6.1 Absorption and reflectance

When we follow the trajectory of the light through a translucent object, we can observe that the light is transmitted and modified by reflection, refraction, absorption and scattering. In the place where one medium changes in the other, the light is bent in a refractive angle on the interface between the media. Some amount of light is reflected back from the surface. The amount lost equals the sum of scattered and absorbed light.

Absorption indicates the conversion of light into another form of energy depending on the constitution of the object, often into fluorescent emission with a corresponding Stokes shift in wavelength, but also in heat. In special cases the light may be converted into chemical energy in photochemical processes. We will deal with the term fluorescence in the following chapter.

Scattering means dispersion of the light at random away from the incident path, often in many different directions. Scattering is dependent on the angle of the light. There may be considerable reflection by the tissue.

All biological tissues are translucent to some degree. Living tissue containing different cells with its infrastructure is not homogenous from the differences in protein concentration to the amount of organelles.

We want to describe changes in the optical properties of the tissue as a whole in connection to possible changes during its activation, these optical signals can be used as an imaging device of this living tissue. Osmotically induced cell volume changes principally influences light scattering cause there are changes in macromolecules in the cytoplasm which directly affects both the refractive index of the cytoplasm and also scattering by the macromolecules and organelles directly. In conclusion multiple elements that are present in the cell involve

scattering as the light penetrates the tissue, reflection at different angles both from cellular membranes and from the interface with intracellular cytoplasmic contents, the refractive index changes between extracellular and intracellular processes (Aitken et al., 1999)

Intrinsic optical signals has the potential to detect changes in the optical properties of the tissue without the need to add any dye or fluorescent markers to the tissue, making advantage of the reflected or transmitted light. It has been concluded that two main processes are responsible for the generation of the signal in slices of the nervous tissue. The first one is caused by scattering of light that change inversely with cell volume and is related to the dilution of the cytoplasm. The other opposite in sign may be due to mitochondrial swelling. (Aitken et al., 1999)

1.6.2 Fluorescence

Fluorescence is a phenomenon when visible light is emitted by a substance that previously in a brief interval (nanoseconds) absorbed light of a different wavelengts.

Fluorescence occurs when a molecule, atom relaxes to its ground state after being excited, more specificaly, the orbital electron of a molecule relaxes to its ground state by emitting a photon of light after excitation. Molecules undergoing these transitions resulting in fluorescence are indicated as fluorescent probes, fluorochromes or just dyes. Fluorochromes attached to a larger molecule such as nucleic acid are called fluorophores. The wavelength absorbed is usually a smaller than that of the emitted light. Some cellular components are naturally fluorescent (called intrinsic or autofluorescent). Some other components can be labelled with a extrinsic fluorophore, a fluorescent dye to became fluorescent and visible for further evaluation. Extrinsic fluorophores are synthetic dyes or modified chemicals that are added to produce fluorescence with specific spectral properties (6).

$$S_0 + h\nu_{ex} \rightarrow S_1$$

$$S_1 \rightarrow S_0 + h\nu_{em} + heat$$

(6)

Fluorescence (emission) hv is a generic term for photon energy,

h = Planck's constant

v = frequency of light

S_0 is the ground state of the fluorophore (fluorescent molecule) and S_1 is its first (electronically) excited state.

Stokes shift (Stokes was british scientist who described the phenomenon of fluorescence in 1852) is the difference between band maxima of the absorption and emission spectra. Stokes fluorescence is the re-emission of longer wavelenghts photons that were previously absorbed by molecule that has absorbed photons of shorter wavelengts. Some fluorescent dyes exhibit small Stokes shift and some, such as fura-2 exhibit large Stokes shift (Miklavc, 2010). The smaller stokes shift the harder it is not to overlap between excitation and emission pass bands (the range of wavelength going through certain wavelenght-selective optic).

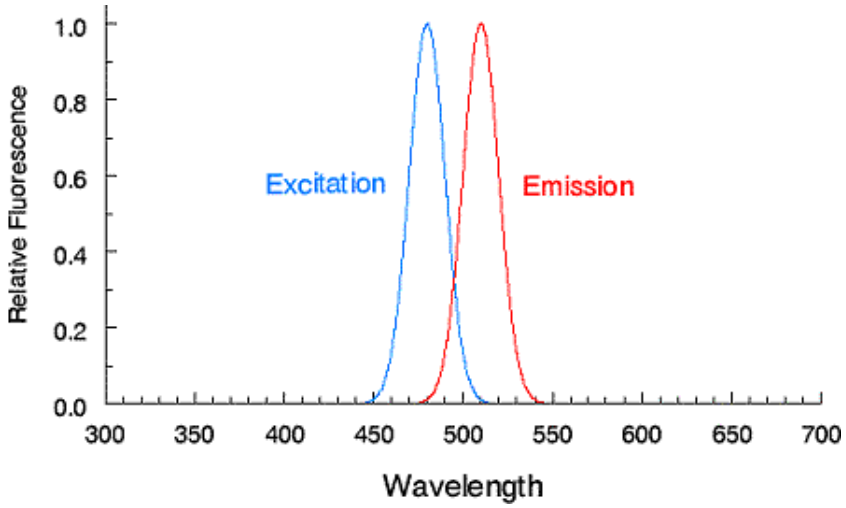

Figure 11 The schema of the fluorescence exitation and emission wavelenght, in this case the excitation wavelenght is at the value of 480nm in the blue range, emission at 510nm in the red range (http://www.fluorescence.com/images/tutorial/smstokes.gif&imgrefurl)

Autofluorescence refers to the fluorescence that arises from compounds present naturally in the tissue (endogenous compounds) (Figure 12). They offer the posibility to detect their changes without loading tissue artificial indicators. These substances are among other the structural proteins such as collagen and elastin, coenzyms for cellular energy metabolism (FAD, NADH) as well as certain amino acids and precursors to heme porphyrins.

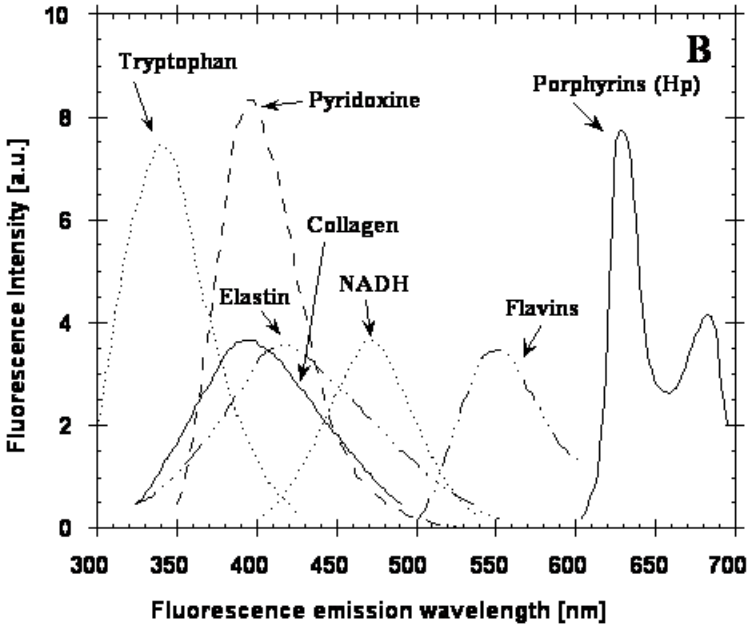

Figure 12 Examples of intrinsic autofluorescent compounds present in the cell with the maximum of thein emission wavelength [nm]

1.6.3 Mitochondrial signal

Cells are the fundamental units of all living organisms. There are about 200 different kinds of specialized cells in the human body. Every cell of the human organism needs energy for its live. The universal carrier of energy in cell is adenosinetriphosphate (ATP), whose main production in the central nervous system is thought to be generated by oxidative metabolism within mitochondria. (Kann and Kovacs, 2007) Thus the integrity of mitochondrial function is

fundamental to cell life. Disturbances of mitochondrial function will lead to the disruption of cell function which can be expressed as a disease or even death (Duchen, 2004). Mitochondria represent very useful information about the cellular metabolism. As it has already been mentioned changes in optical properties of the tissue detect neuronal activity indirectly via mitochondria and its imaging bear important information about the metabolic state of the cell. Mitochondria has own membrane potential, which can be correlated with the mitochondrial energy status and is one of the modalities that helps us while revealing the processes occurring in the neurons.

Very advantageous is for us the fact that FAD and NADP are autofluorescent substances have different concentrations in the cell regarding mitochondrial energy status. If we go into the detail, NAD and FAD are reduced to NADH and FADH. These substances provide further reducing equivalents to the respiratory chain (energy providing process) which consists of series of enzyme systems (complex I.-IV.). During respiratory chain H^+ is transferred outside the inner mitochondrial membrane causing depolarization of the membrane (which is approximately 150mV-180mV negative to cytosol).

In contrast to fluorescent oxidized NADH, FAD autofluorescence decrease when the carrier bins the electron (reduces). During oxidation, the energy is used for the formation of ATP.

Mitochondrial membrane potential provides us with important information regarding energy status of the cell. Mitochondrial membrane not only facilitates the respiratory chain but also plays an important role in cellular signaling. Such negative mitochondrial membrane potential takes up mitochondrial calcium and sets relatively low intramitochondrial Ca^{2+} concentration. If the respiratory chain is inhibited, or if the cytosolic concentration of Ca^{2+} in increase, mitochondrial Ca^{2+} concentration can increase and lead to mitochondrial damage mitochondria and even to start apoptotic cell death. The functional significance of

mitochondrial Ca^{2+} uptake lies in the regulation of mitochondrial metabolism and thus the whole cell.

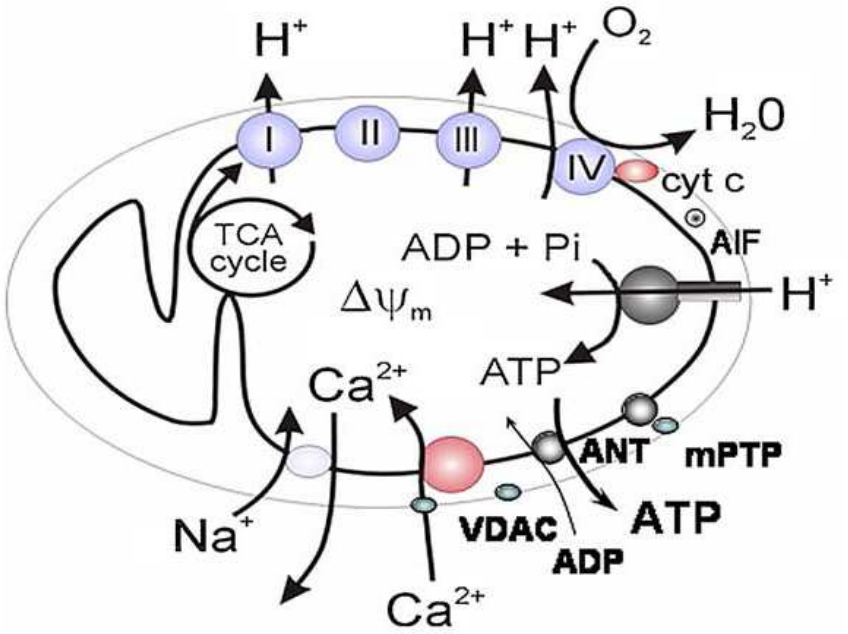

Figure 13 schema mitochondrial transport through the inner membrane

Nicotinamide Adenine Dinucleotide (NADH)

Nicotinamide adenine dinucleotide, abbreviated NAD^+, is a coenzyme found in all living cells. As it has been already mentioned, reduced NADH is fluorescent which makes it directly detectable. The fluorescence of NADH is excited in the UV (peak excitation at about 350 nm) and emits blue fluorescence (with a peak at about 450 nm) (Chance, 1979). Unfortunatelly NADPH has similar optical properties and thus excitation and emission spectra overlaps and thus it is impossible to distinguish these signals. Therefore it is concluded to name the signal as NAD(P)H which means summation of NADH and NADPH fluorescence. It has been shown that NAD(P)H fluorescence provides predominantly a signal of oxidative fosforylation or glycolysis in mitochondria in the nervous tissue. During and after synaptic activity in acute hippocampal slices NAD(P)H fluorescence changes with characteristic biphasic pattern. First phase, a decrease (so called

dip) of the signal, represents oxidation of reduced forms of nucleotide. Second phase, lasting increase (so called overshoot) , starts 4-6s later and represents increased reduction of nucleotides in TCA and glycolysis (Brennan, 2006). It lasts for 120-180 seconds after 10s/20Hz ortodromic stimulation. Confocal microscopy provide tool that is able to indentify the mitochondrial or cytoplasmic origin of the signal. This fact reconciles many traditional views on the brain energy metabolism. (Kasischke et al., 2004; Pellerin and Magistretti, 2004). More precise experiments in vitro are being made to reveal the exact metabolic demand of the tissue in certain areas (Shuttleworth, 2003). In vivo, the experiments are very promising but at the same time very demanding technically because of the cardiorespiratory movements and the other movements of the live tissue. (Mayevsky and Rogatsky, 2007)

Interestingly for us, while dealing with IOS, the changes during hypoxic spreading depression are present during farmacological inhibition of mitochondrial metabolism and membrane potential changes, this indicates that severe mochondrial depolarization or failure of mitochondrial metabolism is not a major source of IOS associated with states such as spreading depression. (Gerich et al., 2006)

FAD

Flavin adenine dinucleotide (FAD) is a redox cofactor involved in important reactions in metabolism. FAD can exist in two different redox states, which differe between by accepting or donating electrons. FAD is fully oxidazed form that can be reduced to FADH or FADH2. So, in contrast to what we detect with NADH, flavoprotein fluorescence decreases when the FADH is oxidized. Thus when compared to the signal of NAD(P)H it overlaps but is inverse. However, FAD signal is strictly mitochondrial in contrast to NAD(P)H where mitochondrial and cytosolic signals overlap.

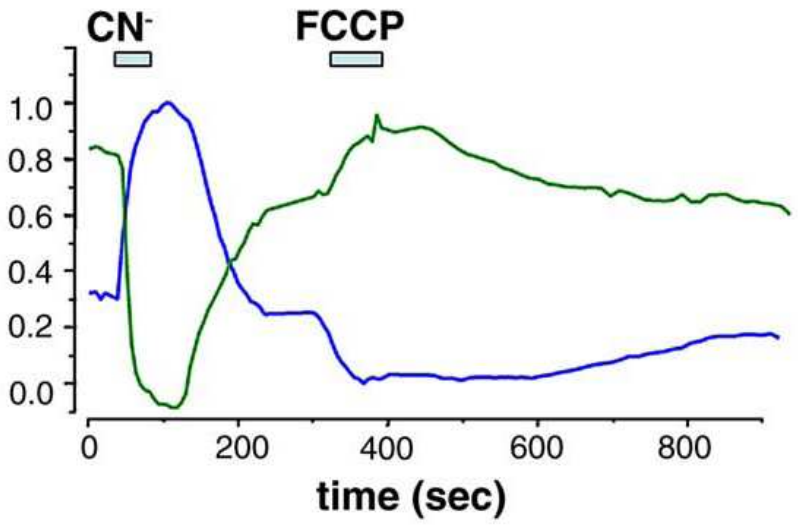

Figure 14 In the picture, you can see emission FAD signal in green and NADH in blue range. When the cellular respiration is inhibitied by CN there is decrease of FAD signal because FADH cannot be oxidazed to FAD. When using uncoupler FCCP which is substance facilitating H transferr through the inner membrane and thus facilitation of mitochondrial respiration, FAD fluorescence is increased. NADH signal is opposite. For this purpose, adipocyte cell line was used.

Mitochondrial swelling

As noted previously, during activity of the neuron there is massive movement of the ions across membranes of the mitochondria which is followed by water movement. Depolarization of the mitochondria thus leads to its prominent volume and morphological changes which can produce optical signalling. Therefore inhibiton of these changes is associated with a decrease in the amplitude of IOS signal and time decay of the stimulation induced IOS response was prolonged. (Buchheim, 2005)

1.7 Biomechanical properties of the nervous tissue

1.7.1 Cellular level

Mechanical properties of the nervous tissue are one of the crucial elements for the assessment of the further fate of light in the nervous tissue.

Biomechanics of very soft tissues which do not bear mechanical loads such as brain haven't been investigated in such detail in the past years mainly because of the lack of methods that would enable more accurate measurement. The first reports in the field of biomechanics described the brain tissue like something less stiff than a gel and less plastic than a paste with adhesion that is enhanced by slight dehydratation and also some first measurements of the stress application on the slices of the nervous tissue were present in the sixties. (Ommaya, 1968) Recently with increasing possibilities of new techniques more studies and also mathematical models dealing with behaviour of neuronal tissue or the whole brain deformation in tension or in compression are appearing (Miller and Chinzei, 2002).

At the cellular level, all CNS cells possess elastic behavior dominating over the viscous behavior. The distinct compartments differ especially due to its unequal distribution of cellular organelles. Using scanning force microscope both neurons and glial cells have been considered as an elastic and glial cells are even more defomable than neighbouring neurons. From biomechanical point of view, Glial cells are a soft, compliant embedding for neurons, which protect them and also serve as a substrate required for neurite growth and facilitates neuronal plasticity (Lu et al. 2006).

In this thesis we would like to define the changing optical properties of the tissue. While applying three dimensional confocal morphometry, it is possible to visualize astrocytes in the brain slices and evaluate the differences in astrocytic swelling in response to the changes in osmolarity. As it was suggested the astrocytes swells and change their shape into a more round one, furthermore the

swelling within the slice is not equally distributed (Chvatal et al., 2007). Morphological observations proved that astrocytic swelling is the most pronounced cellular swelling in the grey matter in a large number of pathological states such as ischemia (Kimelberg, 2005).

Biomechanical aspects are important in the field of neuroscience. It has been proved that mechanical stress can stimulate neurons in the tissue with intriquinq results. It has been suggested that for example mechanical tension can elongate the axons or processes of the neuron (Lamoureux et al., 2009; Lamoureux et al., 2002).

The tissue react also on the over activation and produce substances that can further influence the properties of the tissue and subsequently influence the biomechanical characteristics of the tissue. The utrastructural and immunocytochemical data verified the enrichment of collagen in the neuropil, which possibly originates from fibroblasts, which might contribute to cell and axonal migration and even influence the possible subsequent epileptogenesis. (Veznedaroglu, 2002)

We can conclude that mechanical properties of substrates underlying cells have profound effect on cell structure and function.

AFM

To determine the mechanical properties of regions within hippocampus, mainly as a part of the research dealing with traumatic brain injury (TBI), the AFM was adopted.

AFM is scanning probe microscope with resolution of nanometers, which is 1000 better than optical diffraction limit on it allows opportunities to investigating biophysical properties of the cell in time. The reason why the resolution is so good is the fact AMF is not a optic probe, but mechanical device. Very briefly AFM uses sensor (cantilever) a tip whose end is use to scan the surface of the sample. When the tip is brought close enough to a samples surface, the forces

between the tip and the sample leads to a deflection which is usually measured using a laser light (

Figure 15).

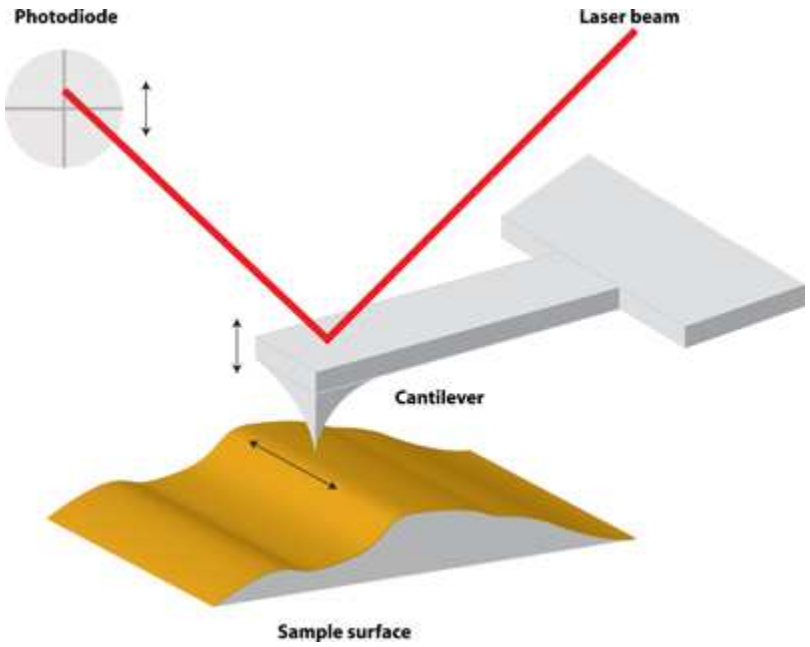

Figure 15 fine tip on the end of a cantilever is used to probe the surface contours. A laser beam is focused in the back of the cantilever reflected onto a photodiode, like this the laser beam gets deflected as well as the cantilever moves. The sharper the cantilever tip the better resolution AMF possess (the vertical resolution below 0,1nm.)

In cell biology AFM is currently used for example in migrating cells to detect the gradient of rigidity in lamelllipodium (Laurent et al., 2005). Measuring the mechanical properties of brain tissue is challenging due to its morphologic heterogeneity, low modulus of elasticity and dependence on its physiological state. (Fountoulakis, 2001, Gefen, 2004) It has been showed that certain regions of hipocampus possess heterogenous mechanical properties. Interestingly for us, AFM was adopted for use on living brain tissue resp. to determine the local mechanical properties of anatomical subregions within the rat hippocampus. The so called depth-dependent elastic modulus has been determined for the following hippocampal regions (Elkin, 2007).

Pyramidal layer of CA1 (CA1P), dendritic region called stratum radiatum (CA1SR), pyramidal cell layer of CA3 (CA3P), stratum radiatum of CA3 (CA3SR) and dentate gyrus (DG) with elastic modulus in the depth of 3um was as follows: 234 ± 15,2 Pa for CA3P, 308 ± 18,4 Pa for CA3SR, 137 ± 9,7 Pa for CA1P, 169 ± 5,2 Pa for CA1SR, a 201 ± 13,3 Pa for DG (Elkin, 2007).

Note that CA3 stratum radiatum is significantly more stiff than all other regions of the hippocampus under consideration including its adjecent CA3 pyramidal cell layer while the CA1 stratum radiatum is not that stiff even compared to CA1 pyramidal cell layer.

The increased stiffness of the CA3 pyramical cell layer and those of CA1 may be explained by differences in the cytoskeleton of pyramidal neurons that differ in each region. Heterogenous distribution of cytoskeletal elements including neurofilaments (Lopez-Picon, 2003) and f-actin (Capani et al., 2001) were found in the hippocampus more in CA3 compared to CA1. F-actin can further influence another physiological parameters such as the conductivity of Ca2+ activated K+ channels and potentially contribute to excitotoxic cell death, which one of the pathophysiological mechanisms for damage following traumatic brain injury. Interestingly, It has been presumed that CA1 region of hippocampus is more succeptible to damage caused by ischemia (Shiino et al., 1998), different biomechanical properties within these region could elucidate some of those phenomenon.

AFM enables to study single receptor properties. Yersin observed AMPA receptor, mediator of the most rapid excitatory neurotransmitter in the mammalian CNS, trafficking with combination of recording of the elastic properties. It has been detected that AMPA receptors are located in nannodomains stiffer than the surrounding cell surface (Yersin et al., 2007)

Another important aspect of mechanical properties is reported in relation with the development, and that there is a increse in stiffness during maturation. (Sparrey, 2009) We can observe such difference macroscopicaly while cutting the

rat's brain. The preparation of the hippocampal slices in very young rats such as 7days is very tricky and demand experience and skill because the tissue is very watery and inconsistent.

All these biomechanical aspect could help us while determining the response of the stimulation and change in the the optical properties with are tightly coupled to the overall biomechanical properties. Knowing more about the biomechanics on microscopical level would prevent us from making early imprecise conclusions.

1.7.2 Cerebrospinal fluid and in vivo measurements

For increasing accuracy of in vivo experiment, it is necessary to think of CNS as a whole and consider all its biomechanical properties. Biomechanics of the central nervous system as a whole embodies its movements, vascularisation and compliance. CNS is surrounded by cerebrospinal fluid (CSF) which protects it, maintains the ionic balance and lowers its weight down to 97%. The pulsative flow of CSF not only maintains homeostasis and ionic levels but it is also a heat conductor maintaining the stable temperature of the tissue.

Compliance of the brain tissue compared to the other structures and is increased because of rich vascularisation and is also different within CNS. Unequal distribution of compliance is a key factor for the dynamics of the cerebrospinal fluid in craniospinal system and the overall movements of the brain. Because of the fact compliance is higher in the cranial portion it makes pulsations of CSF differently distributed.

CSF and its movements and balance are in the scientific interest and many recent papers have changed the previous knowledge and image of CSF. With the emergence of new methods new possibilities of further understanding certain pathologies affecting CSF are opened. (Greitz and Hannerz, 1996, Greitz, 2007)

Movements of the CNS are influenced by respiratory (Sasaki et al., 2003), cardiac pulsations (Schroth and Klose, 1992) and are also dependent on the whole posture (Alperin et al., 2005). It has been proposed that the pulsations of the spinal channel are dependent on the respiratory movements. During inspiration mainly pulsative flow in distal parts of the spinal cord is affected with the overall caudal flow in the spinal channel (Henry-Feugeas et al., 2000;Greitz and Hannerz, 1996;Greitz, 2007).

With such a complicated biological system, the emergence of mathematical modeling appeared. Stepanik, following the previous works dealing with mathematical computation of the system (Kaczmarska, 2009), made up model of

CSF circulation where the different aspect describing compliance of the tissue as a whole, different part of the central nervous system and specific movements (respiratory and cardiac related movements). The model is made up of five compartments, two intracranial and three spinal. This structure enables to map dynamic parameters of the system in spinal cord. This makes possible to simulate both cardiac and respiratory pulsations of the cerebrospinal fluid and describes mechanical properties of the system during physiological and patophysiological states

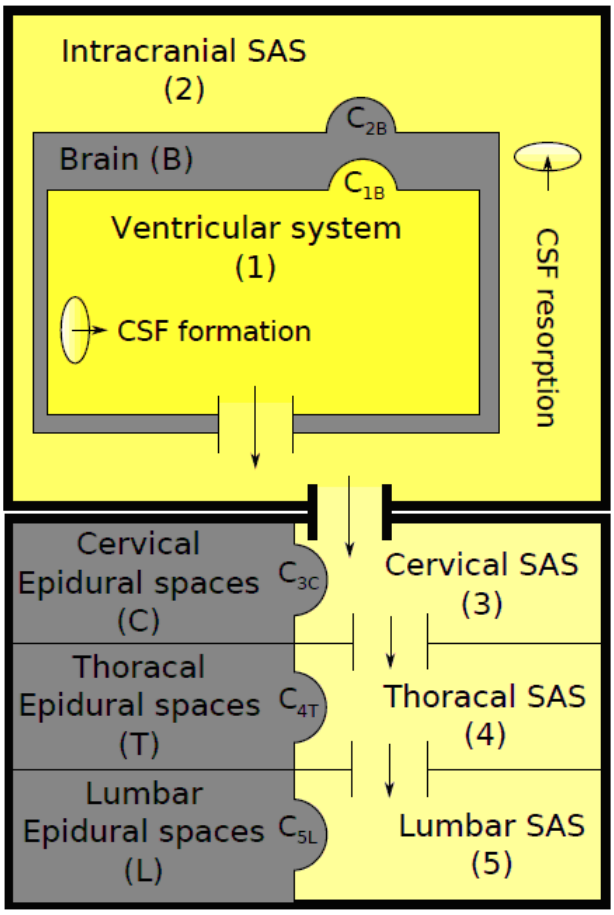

Figure 16 Compartment of the model is described using physical quantity: pressure, volume, resorption and production of CSF. There are flexible borders that have defined compliance. Production of SCF is constant and placed into ventricular system.

The model encompasses also interaction with cardiovascular apparatus, which is the main source of cardiac and respiratory pulsations within the CSF and nervous tissue.

Intracranial subarachnoideal space is connected to SAS of that of spinal channel which is devided into cervical, thoracic and lumbar part. Every compartment is described using the volume and the pressure. The compartments are connected to each other with flow channels with constant resistance and can have elastic septum between each other. This elastic septum is described with nonlinear function of compliance.

Model encompasses interactions with the cardiovascular apparatus that is supposed to be the main mediator of the transfer of both cardiac and respiratory pulsation in CSF. It is especially pronounced in production and resorption of cerebrospinal fluid, autoregulation of blood flow and the others.

Cardiac pulsation is described as a linear pulsation of arterial blood. In the model, these pulsations are transferred into a dividing line in between the set part B and parts 1 and 2

Respiratory pulsations are put into the model from the spinal segments following the literature. More precisely during inspiration, systolic arterial pressure is increased which results in the supply of the blood into cranium and spinal cord. It has been assumed that the influence of respiration will be markedly increased the pressure on spinal extradural space.

In the model approximate values of the compliance has been set. As the time constant of the system of the expected values the dominant value was the heart rate which makes this model exceptional.

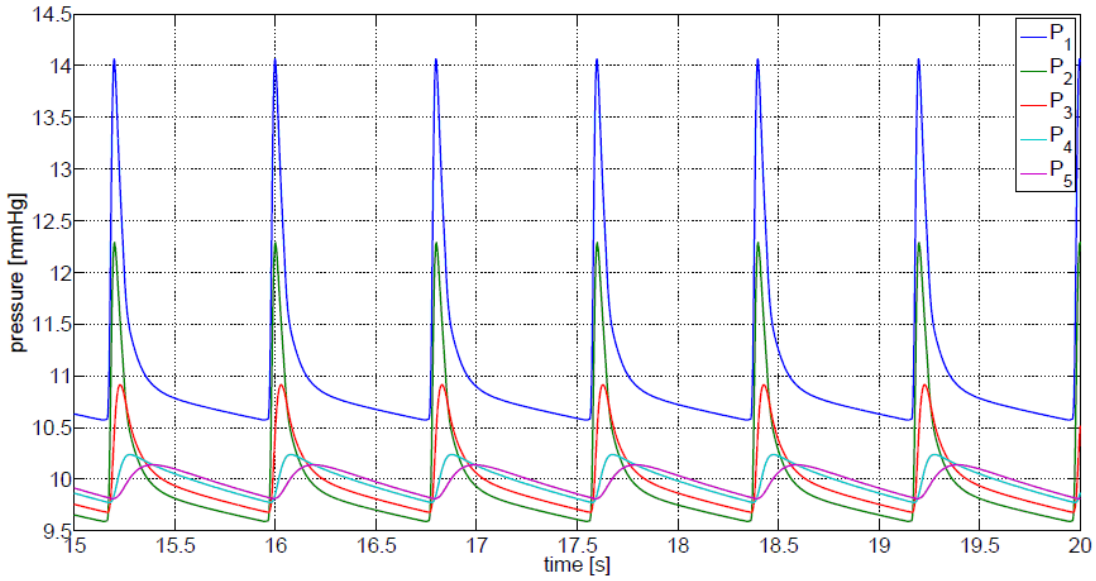

Figure 17 example of Stepanik's model: pressure in the separate departements of the craniospinal system, simulated via presented model. On the picture, you can see 6 heart pulses.

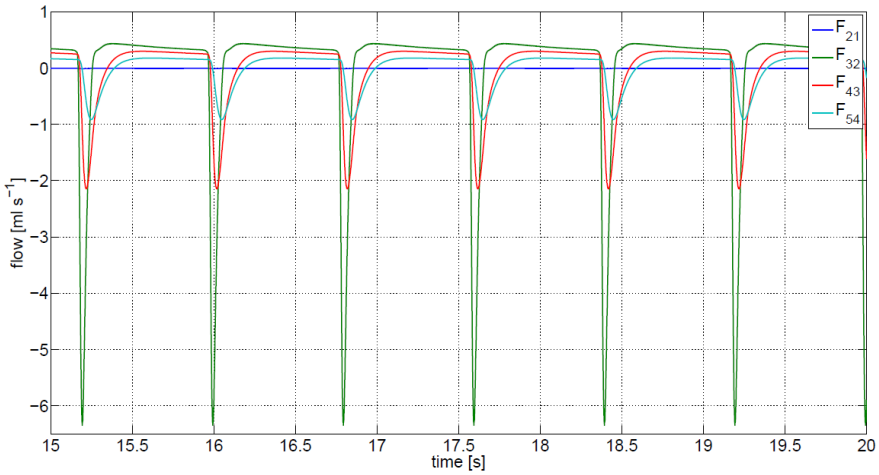

Figure 18 SCF flow in the separate departements of the craniospinal syatem simulated with the model. Caudally the negative values stands for the flow.

In the upper part of the picture, course of the pressure simulated using the model in intracranial SAS and in the lumbar portion, there are normal conditions.

In the lower part of the picture, there is the course of simulated pressures in the same portions with the infusion speed of 0.035 ml s−1. as we can see, the infusion makes the pressure amplitudes more similar in intracranium and in spinal cord .

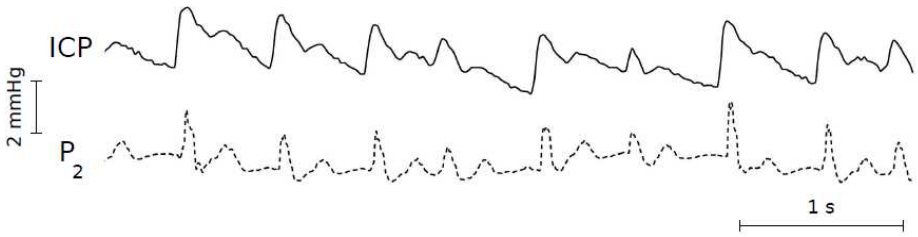

Figure 19 Comparison of the course of intracranial pressure measured and the simulation with the model.

As it has been demonstated in the upper graphs, using this model, we are able to predict the character of CSF, set the basic biomechanical properties of the CNS and predict some movements during in vivo measurements (Stepanik, 2009).

Cranial Part			
C^0_{1B}	$=$	1.500×10^{-4}	ml mmHg^{-1}
C_{1B}	$\approx$	4.500×10^{-6}	ml mmHg^{-1}
R_{12}	$=$	1.600×10^{2}	mmHg s ml^{-1}
C^0_{2B}	$=$	2.000×10^{-1}	ml mmHg^{-1}
C_{2B}	$\approx$	6.000×10^{-3}	ml mmHg^{-1}
R_{23}	$=$	3.000×10^{-1}	mmHg s ml^{-1}
Spinal Part			
C^0_{3C}	$=$	1.125×10^{0}	ml mmHg^{-1}
C_{3C}	$\approx$	1.350×10^{-1}	ml mmHg^{-1}
R_{34}	$=$	4.000×10^{-1}	mmHg s ml^{-1}
C^0_{4T}	$=$	1.500×10^{0}	ml mmHg^{-1}
C_{4T}	$\approx$	1.850×10^{-1}	ml mmHg^{-1}
R_{45}	$=$	3.000×10^{-1}	mmHg s ml^{-1}
C^0_{5L}	$=$	2.250×10^{0}	ml mmHg^{-1}
C_{5L}	$\approx$	2.800×10^{-1}	ml mmHg^{-1}

Figure 20 Brief summary of the resistence and compliance of the different compartments in the system. The values have been set to correspond with the previously measured real values.

1.8 IOS - the Processes underlying optical changes

1.8.1 In vitro signals

In the year 1948 Hill and Keynes, while stimulating the non-myelinated fibres of nerve trunk of the walking leg of the shore crab, noticed the increase in the scattering of white light during the illumination with white light beam from a tungsten lamp (Hill and Keynes, 1949). These changes were thought to represent axonal swelling during the activity of the nerve.

A few years later in 1973 Lipton (Lipton, 1973) made the first more sophisticated recordings of changing optical properties on the cerebral tissue slices using photodiode. He suggested that the conditions such as the lowering bath osmolarity, hypoxia, elevated K^+ concentration and electrical stimulation decreased the reflectance of the illumitated tissue to varying degrees, and these changes were further reported as a result of the changes of the volume of the active tissue. Changing volume of the tissue was considered as the main determinant of the light reflectance changes.

In the studies on the tissue slices we are not restricted the reflected light, but we also detect the light that is transmitted through the tissue. LT is similarly proportional to the osmolality-induced increase or decrease in cell volume and correlated with appropriate changes in extracellular resistance (as the extracellular space increases (MacVicar, 1994, Andrew, 1999) it is in accordance with the swelling of the whole tissue slice, resp. more planar membranes, swollen organelles, reduced reflectance between intra and extracellular spaces, reduce light scatter and consequently elevate the transmitance (Andrew, 2006).

Accordingly the first mechanism of IOS change is connected to an increased light transmittance when ISV (intersticial volume) shrinks and the opposite event when the ISV expands. The magnitude of IOS should correlate with the magnitude of the cell-volume changes. The second mechanism is probably due to the scattering changes of organels and seems to be independent of the cell

volume, and decrease light transmittance in spite of lasting increase in cell swelling.

Mac Vicar and Hochman were one of the first scientist suggesting that intrinsic optical signals as a new imaging method posses great potential because of the fact it is suitable for mapping of a spread of activity in time in brain tissue slices without the need to load the tissue with dyes. They introduced this method and defined conditions and the signal for the further measurements. They made experiments proving that the optical signals associated with synaptically transmitted excitation in hippocampal slices result in increase in light transmittance with the maximum for the longer wavelengts (Macvicar and Hochman, 1991). IOS further posses substantial spatial specificity allowing for example experimental evaluation of the neural mechanisms that mediate the response of different cortical layers to repetitive stimuli.(Kohn et al., 2000) IOS has been applied to the study of epileptic activity in vitro (Holtkamp, 2003)

Spreading depression

Another part in the studies of optical signals encompasses the extensive studies dealing with so called spreading depression. SD that have been first described in cortical tissue some 60 years ago (Leao, 1944), is a wave of depolarization spread consisting of a sharp drop in the DC potential (20mV) spreading in nervous tissue with the velocity around 50 um/sec. Experimentally SD can be elicit as a result of application of glutamate (Obeidat, 2000), elevated potassium (Somjen, 2002),electrical stimulation (Petzold, 2008) or hypoxia (Muller and Somjen, 1999; Obeidat and Andrew, 1998). In the clinic SD is connected to redistribution of blood flow and plays part in pathologies of CNS such as epilepsy, migraine and stroke (Somjen et al., 1992). Light transmittance changes during SD differ from those we can observe during ischemia.(Tao et al. , 2002) For mapping of SD optical signals are very usefull tool. Very prominent change in IOS resp. increase in light transmittance and decrease in light reflectance have been recorded during experiments in conditions with very hight levels of

extracellular potassium, one of the most well known models eliciting SD. Microinjection of KCl 1.2 M evokes a wave of CS that propagates further from the place of application. The changes of IOS in connection with high potassium levels has been confined to astrocytes because their volume changes. (Kimelberg and O'Connor, 1988; Basarsky et al., 1998), which also leads to spread within the region (Pomper et al., 2006). Propagation of wave of depolarization could be with help of IOS done also in developing embryonic CNS which enables to detect with high tempal and spatial resolution of this depolarization wave that is believed to play important role in the development of the CNS (Momose-Sato et al., 2005)

As I have mentioned previously, there are many different processes underlying changes in optical properties of the tissue. In vitro, the direct detention of volume of the tissue or changes in autofluorescence can be detected, all these are the result of many metabolic processes which makes difficult to define the signal. We have to keep up in mind that IOS actually image the consequence of metabolic changes following synaptic transmission or the other processes and it doesn't describe the tissue processes directly, but via changes in their optical properties following metabolic processes (Aitken et al., 1999). It should also be mentioned that the optical signal is slower than the electric one: several seconds are required for evoking it. In hippocampal slices the first detectable change in IOS was at 2-3 s after the stimulation after approximately 20-30 electrical pulse stimuli (Macvicar and Hochman, 1991). It has been mentioned in the previous chapter, the other option for optical imaging is usage of extrinsic markers such as voltage sensitive dyes to facilitate the recording of electrical activity changing in membrane voltage respectively (Miyakawa et al.,2003).

1.8.2 IOS in vivo

In vivo, the situation contrasts with the in vitro activity because the signal includes many more components which predominantly consistent of blood flow, cardiac and respiratory movements.

This has been reported for the first (Fulton, 1928) in patient with arteriovenous malformation that there could be even audible changes in cerebral blood flow when performing some visual tasks. Not only blood flow, but also oxy and deoxyhemoglobin levels and metabolites have distinctive characteristics in terms of absorption or fluorescence. The difference of absorption spectra of oxygenated and non oxygenated hemoglobin is well established diagnostic technique used for revelation of oxygenation of the blood and is also another modality of functional brain mapping via defining the vascularization of the tissue (Vanzetta et al., 2005).

IOS itself comprise more complex information about optical changes in the tissue. IOS responses recorded with the different wave lengths represent different processes coupled to neural activity, wave lengths around 480-590nm is the signal most sensitive to changes of blood volume, 600-660 corresponds to the different oxygenation state of hemoglobin and with the wavelengths higher than 660nm is connected to the different fluid shifts (Malonek, 1996).

For IOS the white light is used has been systematically applied to the research in neurophysiology recently. IOS has several distinct advantages among these there is high spatial resolution 50 um (1mm in fMRI) low cost and the fact that is doesn't require loading dyes into the tissue (Pouratain, 2003). Among disadvantages there is especially the delay of the response which is considerably slower than the single action potential. Furthermore the exact physiological components of IOS at each wavelength are not yet fully understood. In the first 100ms of the activity onset, there is initial dip in the local oxygenation, the opening of sodium, potassium and calcium channels and subsequent change in the cellular volume. 300-500 ms later, there is dilatation of vessels (which can

not be observed in vitro) with increase in blood volume. 0.5-1.5 there is increase in blood flow and higher oxygenation of the tissue which further overwhelms the demand of the tissue, and causes inverted optical signal in the larger blood vessels which is visible even on on fMRI as so called BOLD signal (Vanzetta, 1999).

IOS has been further exploited in the anatomical studies for the revelation of functional architecture predominantly in cortical areas. One of the first reports indicating that it is possible to use IOS in vivo study for the exploration of functional architecture of cortex have been made on primates. (Roe, 2007; Roe, 2008; Grinvald et al., 1991) The stimulation of sensory receptors results in reflectance changes of the activated areas. (Grinvald et al., 1996) The use of IOS was a breakthrough in analyzing cortical information processing in sensory systems (Holthoff et al., 2007).

IOS has been implied and is very advantageous in the field of epileptiform activity of CNS. The first report of in vivo imaging of pharmacologically induced spontaneous epileptiform events has been performed in 1992 (Haglund, 1992).

1.8.3 Human IOS

Following preliminary experiment in primates, IOS become a diagnostic tool even in humans. Patients suitable for intraoperative imagining are those who suffer from such diseases as epilepsy, tumors or vascular malformations or such neocortical pathologies because the skull needs to be open and the light in contact with the tissue, the curvature of the surface of the brain has to me illuminated homogenously which is another source of difficulty.

The fast time course and high special resolution and also in connection with low cost made IOS technique attractive to usage in the human medicine. The IOS was intraoperatively first used by MacVicar in 1990 (macvicar, hochman) for the imaging of stimulation evoked cortical activation. This was followed by Haglund

who imaged both stimulation evoked and cognitively evoked activity (Haglund, 2004).

The fluorescent and techniques using reflectance changes can be also combined with IOS (Gebhart et al., 2007). In general human IOS detection is promising imaging technique in certain conditions, still it is rather complicated this signal to be detected because of the fact the signal refers to many different processes and there is also a large source of noice including predominantly cardiorespiratory movements.

2 Aims of the study

We would like to characterize and define the optical signal in our in vitro conditions with the aim to apply these data in the other experiments such as pharmacological studies and studies mapping the epileptic activity in vitro.

We would like to define the different sources of noise and to use this knowledge in the following experiments.

The last aim of this thesis is the concept of development of device for the clinical practice based on IOS, for the animal in vivo experiments enabling detection of both optical and electrical signals using our specialized software.

3 Experimental Definition of the IOS and its Origin

3.1 Methods

3.1.1 Tissue preparation

For in vitro measurements slices of hippocampal nervous tissue have been used.

For the purpose of our study we have live brain tissue slices and recordings in the submerged recording chamber. Briefly, rat is decapitated under ether anesthesia, the skull is incised, the brain rapidly removed from the scull. For the purpose of the study, transversal slices were used. Before positioning the piece of nervous tissue on the glued surface of the desk in the vibratome, frontal and parietal part of the cortex is removed. The remaining piece of the brain is positioned on the glued surface so that it stands on the parietal part of the brain. The brain is subsequently cut in oxygenated (95%) and cooled ACSF (artificial cerebrospinal fluid) using vibratome (Figure 21); slices of 400μm of thickness are transferred immediately after the preparation to a holding chamber (Figure 22) and after 120 min recovery they can be used and placed into submerged recording chamber. The slices are perfused with oxygenated ACSF to stay alive. In the recording chamber, we have different possibilities to use pharmacological agents to influence function of the nervous tissue. We can incubate the slice in the recovery chamber or add substances into the perfusion during recording. The experiment I am going to mentioned in this work used pharmacological agents added into ACSF.

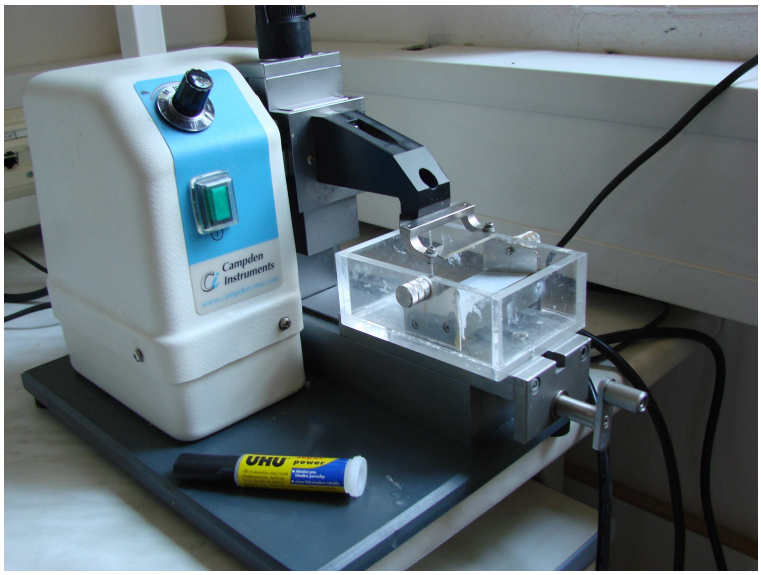

Figure 21, Figure shows vibratome, used for cutting the tissue slices.

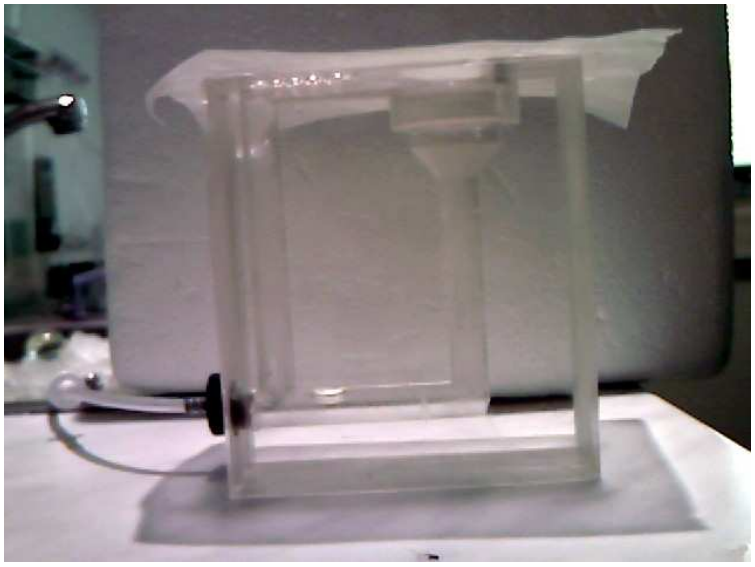

Figure 22, This figure show holding chamber, used for sustaining of the sloves.

Our faster flow of ACSF (6ml/min) without substantial movements of the slice enables better oxygen saturation in the tissue and facilitates the recording of electrophysiological measurements that would be otherwise difficult in this kind of recording chamber (Hajos et al, 2009).

3.1.2 Drugs

TTX

TTX is an especially potent neurotoxin, specifically blocking voltage-gated sodium channels on the surface of nerve membranes. TTX mimics the hydrated sodium cation, enters the mouth of the Na^+-Channel peptide complex, binds to a peptide glutamate side group, among others, and then further tightens it hold when the peptide changes confirmation in the second half of the binding event. Following complex conformational changes, TTX is further electrostatically attached to the opening of the Na+ gate channel. Sodium movement is thus effectively shut down by TTX and in this case the action potential along the nerve membrane ceases completely. The extreme toxicity is expressed with the fact that just single milligram or less of TTX - an amount that can be placed on the head of a pin, is enough to kill an adult.

AVP, CNQX

Competitive glutamate receptors agonists selective NMDA receptor blocker APV (R-2-amino-5-phosphonopentanoate) and further selective AMPA/kainate receptor blocker CNQX (6-cyano 7 nitroquinoxaline-2,3-dione). Competivite agonists means that they can compete over the binging site with the other agonists which further results in that there has to be sufficient concentration of such these so that they fully occupy all the binding sites.

DL-TBOA

Glutamate is the major excitatory transmitter within CNS. Glutamate have to be removed from the synaptic cleft, this arranged by glial transporters. DL-TBOA is a potent blocker of all subtypes of of the excitatory amino acid transporters. Like that transporters limit spillover of synaptically released glutamate to all extrasynaptic glutamate receptors.

Furosemide

Loop diuretic are used in the treatment of congestive heart failure and edema. Furosemide acts by inhibiting the **Na-K-2Cl symporter** not only in **loop of Henle**, but also in the CNS. Within CNS, furosemide is used to decrease ECS. Furosemide can be used in the treatment of epilepsy as a anticonvulsive agent. (Haglund, 1991) Furosemide even in micromolar concentrations is also a noncompetitive subtype-specific blocker of ionotropic GABA-A receptor Recent study indicates that furosemide requires only alpha6 and beta3subunits (Korpi, 1997).

3.1.3 Experimental Setup

Cooled 12-bit CCD-camera (RETIGA2000R) was used for optical imaging of the signals. Images are analyzed using anatomically based regions of interest (ROI), generating a series of 12-bit (averaged across multiple pixels) intensity numbers for plotting, as a function of time. The 12-bit pixel values are linear and proportional to the absolute lightlevel. Difference images were also calculated for each series on a pixel by pixel basis, using a control image as a baseline for each further image in the series

$$\Delta I / I = (\text{Image}_i - \text{Image}_{control}) / \text{Image}_{control} \quad (7)$$

3.1.4 Statistics

For the statistical evaluation the software sigmaStat ane sigmaPlot were used. The data were presented as a mean ± standart error of mean (S.E.M.). To compare two groups T-test or Mann-Whitney test was used. ANOVA or ANOVA on ranks were performed where appropriate e.g. when compared more than 2 groups.

3.2 Noise

While dealing with changing optical properties we have to think of the noise, we inevitably detect as well. Primarily two different sources of the noise can be distinguished; noise in the captured scene and the noise arising from the light detector (CCD camera Retiga 2000R, QImaging). The final quality of the measurement is characterized by **signal-to-noise ratio (SNR)**, the ratio of signal power to the noise power corrupting the signal. **SNR** higher than one indicates more signal than noise.

3.2.1 CCD Noise

In the later digital cameras, the noise performance is limited by the CCD rather than by associated system electronic components. The Charge Coupled Device (CCD) is an electronic component, chip, sensitive to light and work by converting photons into electrons which are then stored in each pixel well (one pixel). Each pixel can hold a fixed maximum number of electrons depending on the specific model of CCD (manufacturer's specification for Retiga 2000R cites linear full wel equal to 40000e-). While integrating or exposing an image, photons striking individual pixels are converted to electrons and stored in each pixel well. The number of electrons stored in each pixel well is proportional to the number of photons that struck that pixel. After an exposure has been completed, the electrons for each pixel are shifted out of the CCD and converted to a number, indicating how dark or light each particular pixel is.

There are several different sources of noise that are appearing during the integration and read out of an image from a CCD. The three primary components of noise in a CCD imaging system are photon noise, dark noise, and read noise.

Photon noise refers to the inherent natural variation of the incident photon flux. Photons collected by a CCD exhibit a Poisson distribution (a discrete probability distribution that expresses the probability of a number of events occurring in a fixed period of time if these events occur with a known average rate and

independently of the time from the last event) and have a square root relationship between signal and noise.

Dark noise arises from statistical variation in the number of electrons thermally generated within the structure of the CCD sensor, which is independent on photon-induced signal, but highly dependent on device's temperature. Dark current is the amount of electrons in the well and in every other part of the signal path, due to the temperature. Dark noise, which also follows a Poisson relationship, is the square root of the number of thermal electrons generated within a given exposure. Cooling of the CCD chip is important. If we cool the chip from room temperature to -25°C, we would reduce dark current by more than 100 times. Manufacturer's specifications for Retiga 2000R cites dark current equal to 0.5e-/pix/s for not-cooled camera. We used for all experiments camera with thermoelectric cooling to 25°C below ambient.

Read noise refers to the uncertainty introduced during the process of quantifying the electronic signal on the CCD. The major component of readout noise arises from the on-chip preamplifier. Technically this noise is defined as the number of electrons introduced in the final signal when reading the device. Each camera possesses different values. Manufacturer's specifications for Retiga 2000R cites read noise equal to 16e-.[1]

---

http://www.qimaging.com
http://www.scribd.com/doc/6715284/CCD-Noise-Sources
http://learn.hamamatsu.com/articles/ccdsnr.html
http://www.photomet.com/resources/learningzone/signaltonoiseratio.php

The following equation is commonly used to calculate CCD camera sensor signal-to-noise ratio (8):

$$SNR = \frac{IQ(e)t}{\sqrt{IQEt + Ndt + Nr^2}} \quad \textbf{(8)}$$

I is the photon flux(photons/pixel/second),
$Q(e)$ represents the CCD quantum efficiency,
t is the integration time (seconds),
Nd is dark current (electrons/pixel/second)
Nr is read noise (electrons).

3.2.2 Image Noise

The noise that originates to the captured scene is the second and more pronounced component that influences noise in result captured image.

The captured scene here is influenced by several independent components and to quantify the noise influencing the captured data several recordings in different measuring conditions were made. We captured 100 frames in 12 bit resolution with 1s period and camera settings; binning 4 and exposure 0.1ms. Using Matlab we evaluated percentage and absolute change of sum of intensity in whole image.

Scenes definitions and possible noise sources:

1. **scene** – empty recording chamber
2. **scene** – recording chamber filled with water
3. **scene** – recording chamber with floating water – flow and pulsation of water, gas bubble
4. **scene** – recording chamber with floating bubbled acsf – flow and pulsation of acsf, gas bubble
5. **scene** – tissue slice without stimulation – slice movement caused by acsf flow

3.2.3 Signal to Noise Ratio

Signal-to-noise ratio (SNR) is a measure that defines how much a signal has been corrupted by noise. It is defined as the ratio of signal power to the noise power corrupting the signal. A ratio higher than 1:1 indicates more signal than noise. SNR equals

$$SNR = \frac{P_S}{P_N} \tag{9}$$

P_S is power of deterministic signal

P_N represents the power of noise

SNR is frequently expressed in decibels as

$$SNR = 10\log_{10}\frac{P_S}{P_N} = 20\log_{10}\frac{A_S}{A_N} \tag{10}$$

A_S resp. A_N is root mean square amplitude of the signal resp. noise and for discrete signal consisting of set of n values $\{x_1, x_2, ...x_n\}$ is given by:

$$x_{RMS} = \sqrt{\frac{x_1^2 + x_2^2 + \cdots x_n^2}{n}} \tag{11}$$

We calculated SNRs for set of images that was captured with 0.5s period in 12bit resolution and whole image was used as region of interest to calculate sum of intensity. Ten second period at the beginning signal before stimulation was used for calculation of the level of noise.

3.3 Results

3.3.1 Detector and Noise

3.3.1.1 Image Noise

Data measured for every different scene described in previous chapter are shown in table 1 and figures (Figure 23, Figure 27) illustrate measured courses.

Scene	**mean[%]** $\overline{X} = \frac{1}{n}\sum_{i=1}^{n} X_i$	**var[%]** $S^2 = \frac{1}{n-1}\sum_{i=1}^{n}(X_i - \overline{X})^2$	**Mean [shades of grey]**	**Var [shades of grey]**
1.	0.0159	0.00011584	0.2575	0.0304
2.	0.056	0.00095494	1.1245	0.03771
3.	0.0572	0.0013	1.1383	0.5190
4.	0.056	0.0014	1.1158	0.5356
5.	0.585	0.0054298	0.8605	0.1175

Table 1: Statistical characteristics of the noise, changes in LT in % recorded in the different conditions with the absence of physiological signal.

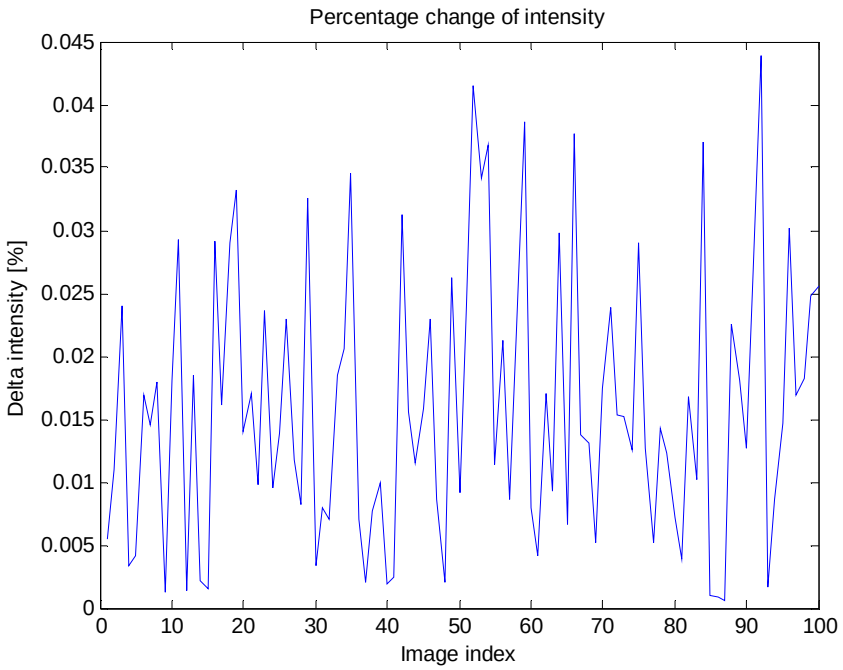

Figure 23 : Scene 1, empty recording chamber, 100frames/s, the mean value of the fluctuations reached 0.0159 % with the variance 0.00011584%

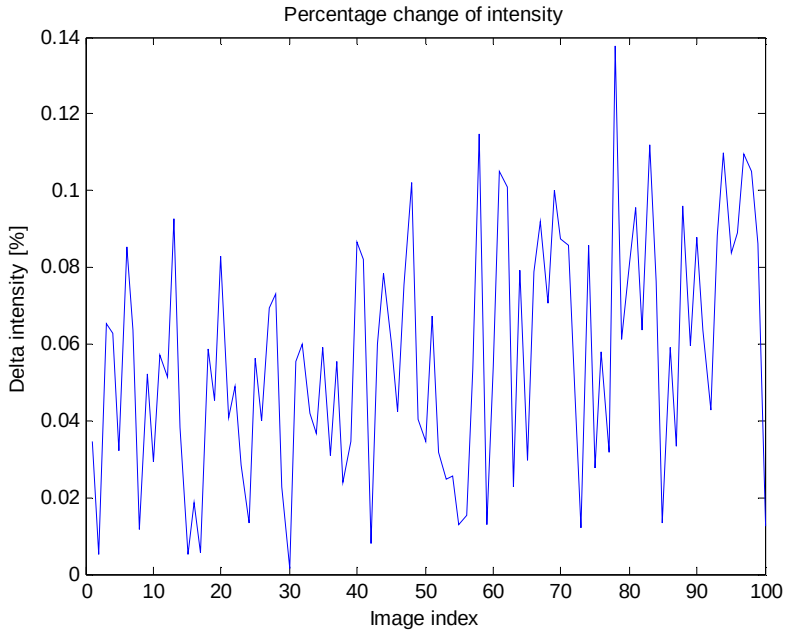

Figure 24 : Scene 2, recording chamber with floating water – flow and pulsation of water, gas bubble,100frames/s, the mean value of the fluctuations reached 0.056% with the variance 0.00095494%

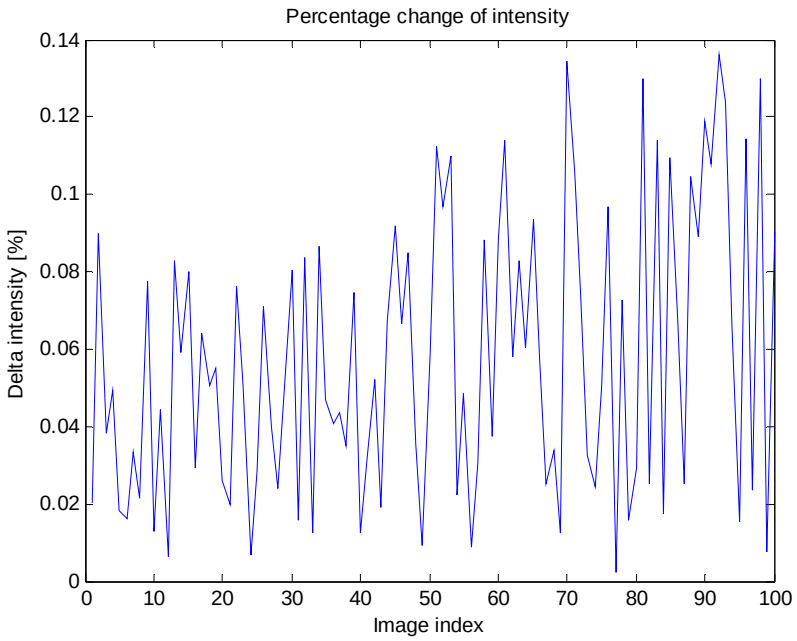

Figure 25 : Scene 3, recording chamber filled with water, 100frames/s, the mean value of the fluctuations reached 0.0572% with the variance 0.0013%

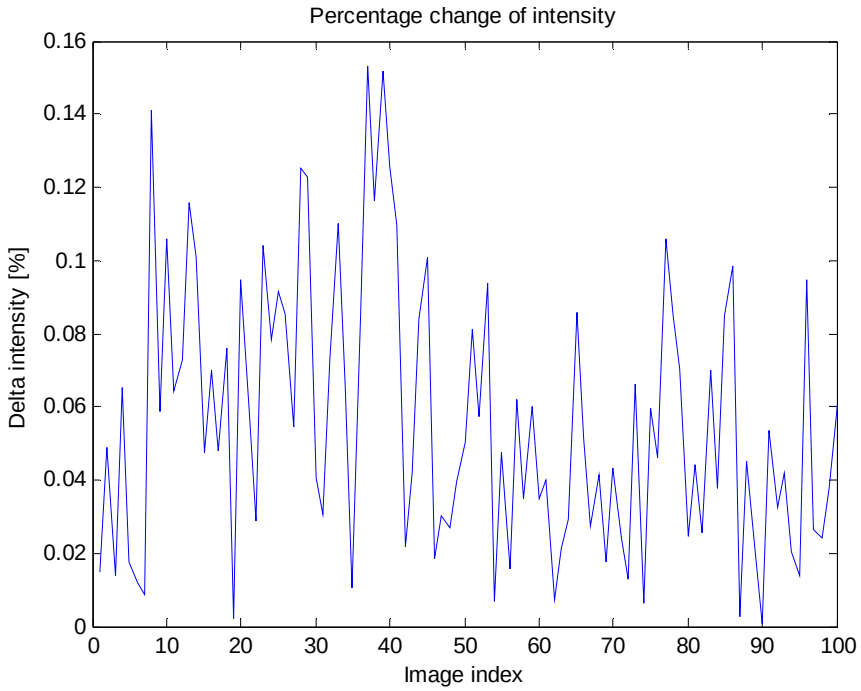

Figure 26: Scene 4– recording chamber with floating bubbled acsf – flow and pulsation of acsf, gas bubble, 100frames/s, the mean value of the fluctuations reached 0.056% with variation 0.0014%

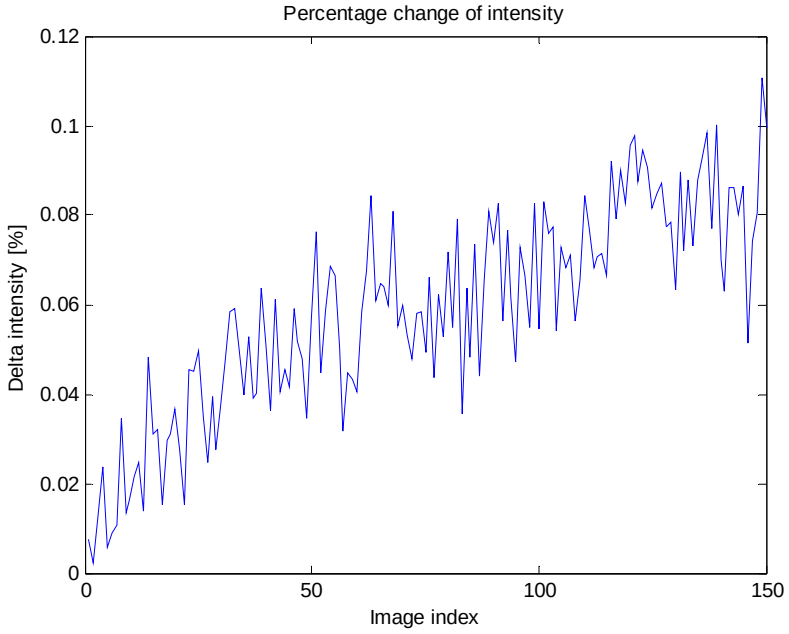

Figure 27 : Scene 5– tissue slice without stimulation – slice movement caused by acsf flow, 100frames/s, the mean value of the fluctuations reached 0.585% with variance 0.0054298%

3.3.1.2 Signal to Noise Ratio

Table 2 summarizes SNRs calculated for set of signals. The average SNR equivalent to 23.7dB indicates that level of actual signal is approximately one digit place higher than level of noise.

Index	SRN [dB]
1	25.0394
2	24.1494
3	18.9537
4	23.5003
5	24.1979
average	**23.1682**

Table 2: Signal to Noise Ratios

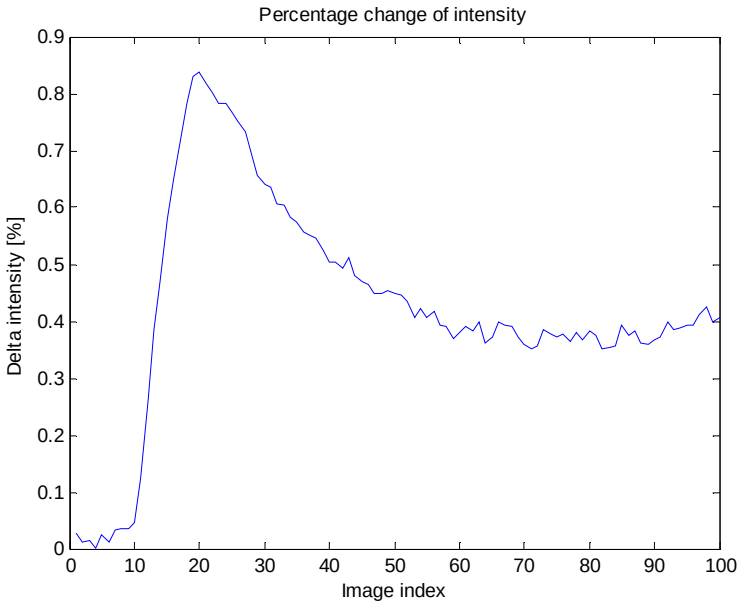

Figure 28 : Example of signal used for calculation of SNR, the x axis stands for the change in the light intensity and the y values are s. the stimulation started 10s after the snapping.

Certain sources of noise can be eliminated. Several sources of the noise that can influence resulting signal can be easily avoided. The figure 7 illustrates further the impact of the surrounding light. The step corresponds to covering of faraday cage that prevents from detecting other light that the one from microscope light source. If we can't afford to have the door closed, we have to at least make the conditions constant.

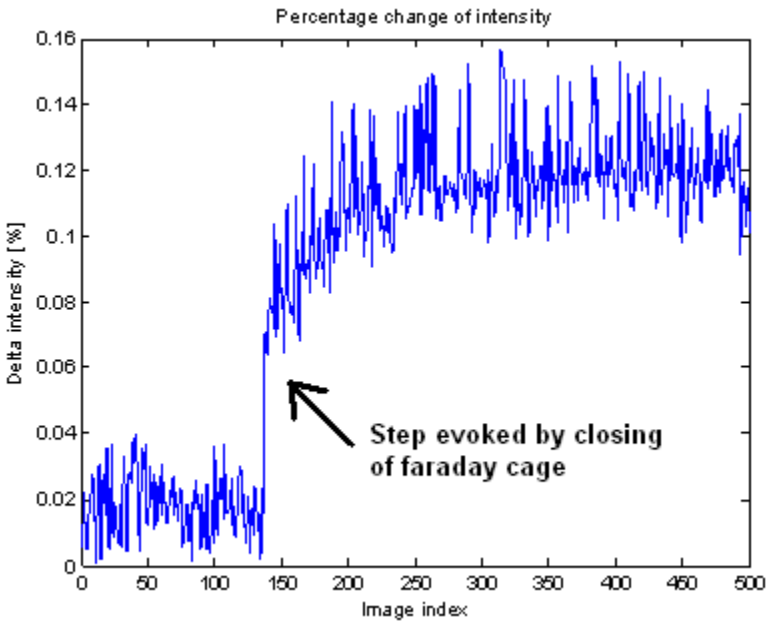

Figure 29 : Step change of the light intensity evoked by closing the faraday cage

The other fact that has to be considered during recording is the transition curve that accompanies every change of intensity of the light source (Figure 30, Figure 31) illustrates those characteristic, measured during increasing resp. decreasing the intensity. The course has got decreasing signal in case the light has been decreased and the opposite course during increase of the signal. This problem can be easily eliminated when we wait sufficient period of time period till we start the detection after the last change of the intensity of the light source. During experiments, we should avoid manual adjustment of the light source and correct the lightening by the the time of the exposition. Or the other radical change is to use more stable light source like LEDdiode.

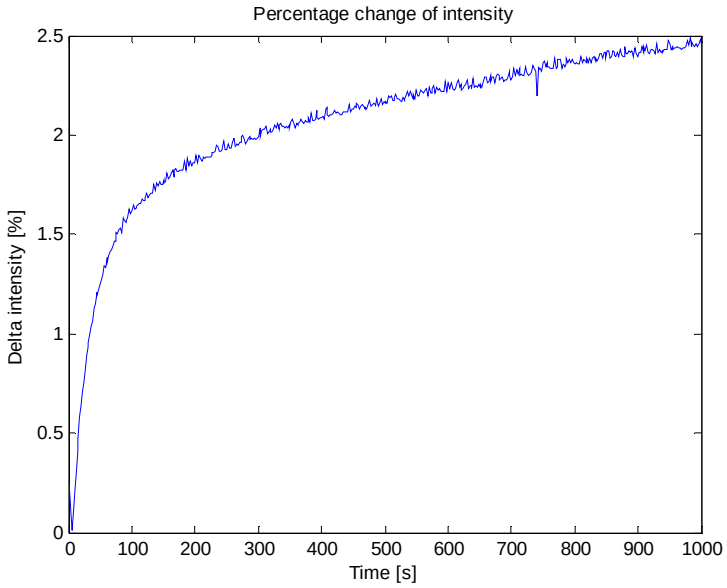

Figure 30

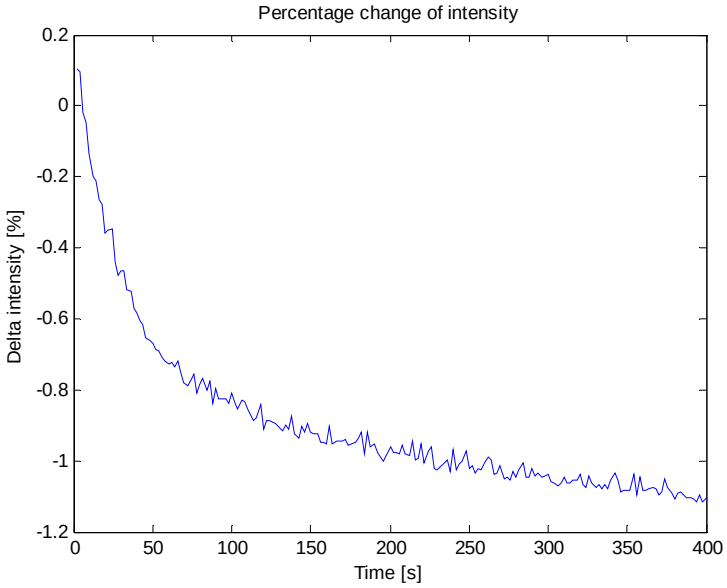

Figure 31

Figure 30 and Figure 31 : Change of the intensity evoked by decreasing the intensity of the light source, Change of intensity evoked by manually increasing of intensity of the light source, x axes stand for time course, the capturing have been done with the pattern frames per 2seconds

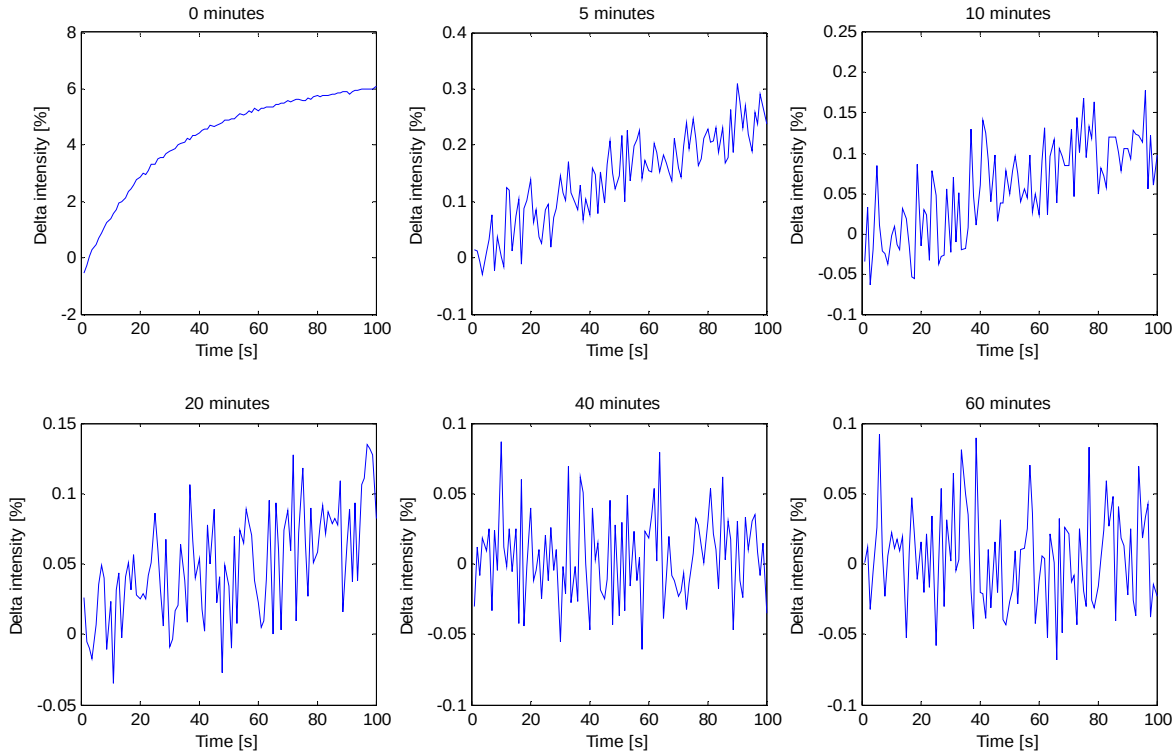

Figure 32 The time course of the 0,5,10,20,40,60 min after the manually set the illumination increase

Ilumination start[min]	Koeficient Linear Regression
0	0.0775
5	0.0026
10	0.0012
20	9.2275e-004
30	4.8190e-004
40	9.1709e-005
60	4.6662e-005

Figure 33. For the further evaluation, koeficient of linear regression has been set to illustrate the slope of the curve.

As we can see some noise components that can be quite easily eliminated, some of them not. Such inevitable components are caused basically by time variance of the captured scene; water or ACSF flow, gas bubble movements, and natural movement of the slice. Several experiments (see results) were made to define the influence of the different components. Noise amplitude caused by those

components is at least one digit place lower than amplitude of actual signal which is sufficient for the detection of the signal.

3.3.2 Experimental definition of IOS, origin of the signal

3.3.2.1 Strenght of IOS signal

Aim: The aim of the first study was to determine the dependency of LT on the neuronal activity of rat hippocampal slices.

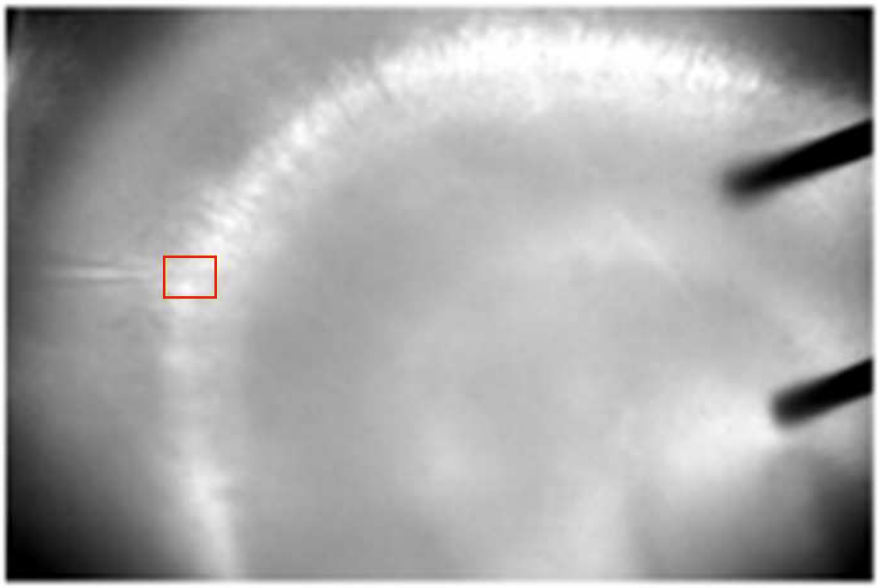

Fig. 34: On the right side, note the stimulating electode placed in DG (dentate gyrus) of hippocampus, on the left, we can see glass registrating electrode in the pyramidal layer of CA3 region of hipocampus. ROI was places in the region where the registration electrod was placed which was in CA3, see the yellow square. Fluorescence microscope image (20/0.5) (Olympus BX51WI)

Methods: We stimulated the slices while increasing the intensity of the stimulation, which was 2T, 3T, 4T. There was at least 5min recovery between every stimulation. Synaptic activation of the tissue was made with bipolar stimulating electrode placed in hillus of the dentate gyrus of hippocampus (Mossy fibers). A 10s stimulus train (20Hz) was delivered.

ROI: pyradimal cell layer (Fig. 34)

Results: The total number of 11 slices has been in the evaluation. The maximum intensity achieved was determined and included into the measurements. The first maximal intensity obtained during 2T stimulation has

been set as 100% value and the other intensities has been counted in percents of this value. There was statistically significant difference between both groups compared to the 2T (P=>0.001). The change in LT in the 3T stimulation was 150.6% compared to 100% for the stimulation 2T with standart error 16.3%. In the stimulation 4T the change in LT was 173.9% with standart error 21.8%.

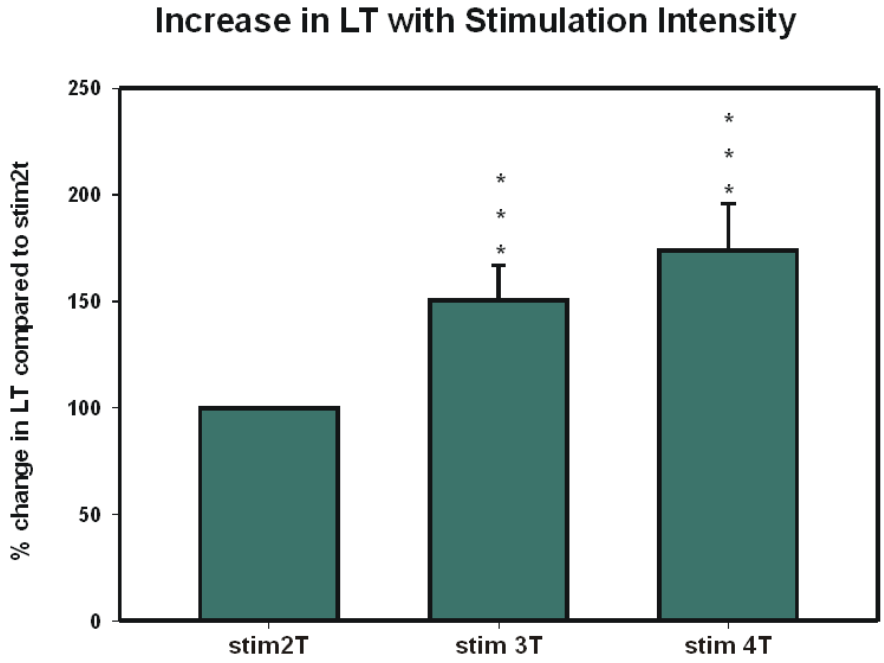

Figure 35 for the statistical comparison, Mann-Whitney test was used. There was statistically significant difference between the 2T and 3T group and 2T and 4T group (P=>0.001). With the following results: the change in LT in the 3T stimulation was 150.6% compared to 100% for the stimulation 2T with SE 16.3%. In the stimulation 4T the change in LT was 173.9% with SE 21.8%.

Conclusion: LT increase is stimulation intensity dependent. The other experiments are essential to estimate the strength of the signal and its neural character.

3.3.2.2 Block of AP

Aim: The further aim was to get to know whether the IOS signal depends on the activity of the tissue and AP spread. To shut down sodium movement by TTX and disable the action potential along the nerve membrane ceases.

Methods: TTX is especially potent neurotoxin, specifically blocking voltage-gated sodium channels on the surface of nerve membranes. The TTX-Na Channel binding site is extremely tight (K_d = 10^{-10} nM). TTX mimics the hydrated sodium cation, enters the mouth of the Na^+-Channel peptide complex, binds to a peptide glutamate side group, among others, and then further tightens it hold when the peptide changes confirmation in the second half of the binding event. Following complex conformational changes, TTX is further electrostatic attached to the opening of the Na+ gate channel. Slice was submerged in ACSF, approximately 15 min of wash in with ACSF containing TTX (1µM). TTX has been washed out. The AP appeared 45min of wash out.

ROI: pyramidal cell layer of CA3 region of hippocampus

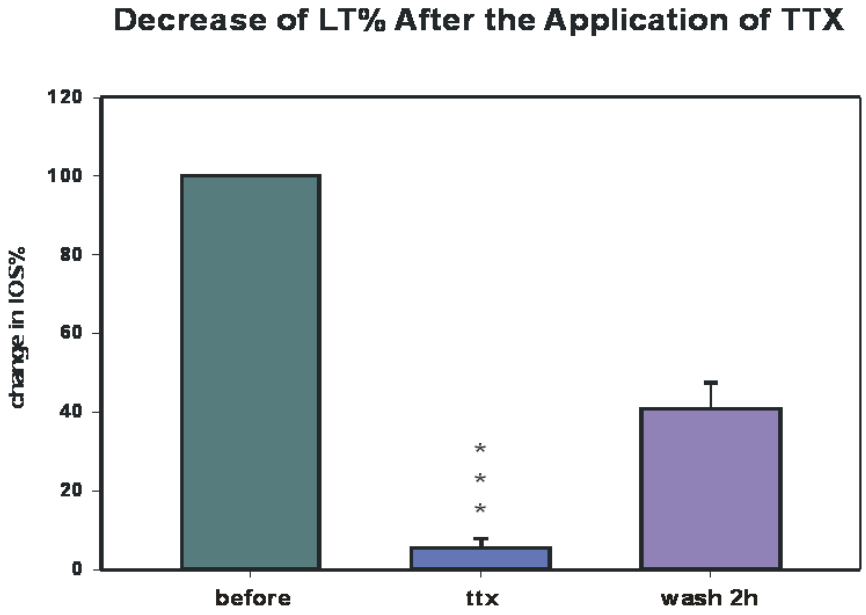

Figure 36 The changes in LT were almost completely abolished by TTX (1uM in ACSF), LT increase was led down to 5.4 ± 2.4% compared to the control measurement, indicating that the synaptic activation was responsible for the changes of LT. For the statistical comparison, Mann-Whitney test was used. There was statistically significant difference between in the group before and after the application of TTX (P=>0.001).

Results: We determined the maximal change in LT in 4 slices with and without the application of TTX. LT has been descreased to 5%.

Conclusions: If we block Na channels (generation of action potential), LT is significantly increased, which points to the fact LT is a consequence of the activity of the nervous tissue and action potential generation.

3.3.2.3 Pharmacology - IOS Glutamatergic Transmission block APV/CNQX

Aim: to determine the dependency of light transmittance on the neuronal activity. We wanted to determine the dependency of LT changes on glutamatergic synaptic activity and further to also reveal the limitations of IOS measurements.

Methods: To distinguish between the synaptic transmission and non-synaptic activity of the nervous tissue, we completely blocked excitatory glutamate receptors using a selective NMDA receptor blocker APV 50uM (R-2-amino-5-phosphonopentanoate) and further AMPA/kainate receptor blocker 10uM CNQX (6-cyano 7 nitroquinoxaline-2,3-dione). Maximal stimulation intensity: supramaximal

ROI: CA3 pyramidal cell layer

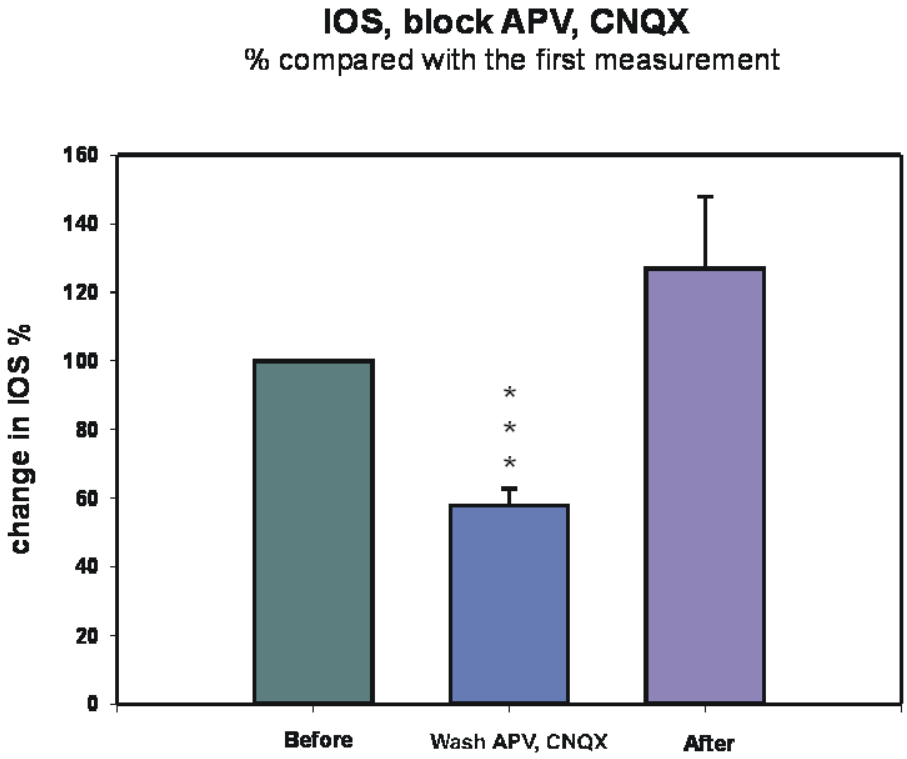

Figure 37 The changes in LT were led down to 57.9 ± 4.9% compared to the control measurement, indicating that the glutamatergic synaptic activation was responsible for the changes of LT. For the statistical comparison, Mann-Whitney test was used. There was statistically significant difference between in the group before and after the application of APV, CNQX (P=>0.001).

Results: In this case LT was also decreased to 57.9% ± 4.9%.The first measurement, slice was submerged in ACSF, 40 min of wash in with ACSF with APV, CNQX in the concentration 50μM (APV) and 10μM (CNQX). After the second measurement, the wash out (40min), the third stimulation was being made.

Conclusion: The LT signal was block to half which proves that the signal is glutamate dependent. The exact dependency of the signal is might be changed reflecting the fact we used glutamate receptor blocker that might compete over the binding site of glutamate and don't bind to all the binding sites.

3.3.2.4 IOS signal arising from glial cells

Aim: to define the glial origin of the signal.

Methods: DL-TBOA in the concentration has been used in the perfusion (ACSF) to block glial glutamate reuptake.In the second set of experiments TBOA has been added into the perfusion in combination with APV, CNQX. Stimulation intensity: supramaximal

ROI: pyramidal cell layer

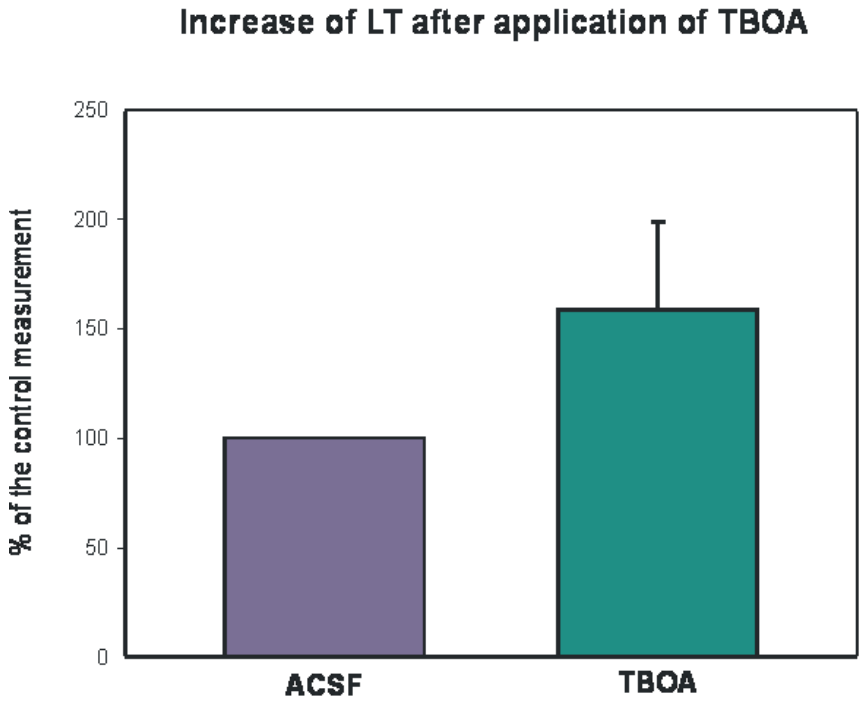

Figure 38, The graf represents percentage of the change of the maximal increase of the IOS during the stimulation. When adding TBOA into the perfusion media the optical signal during stimulation increased up to 159% ± 19.62%

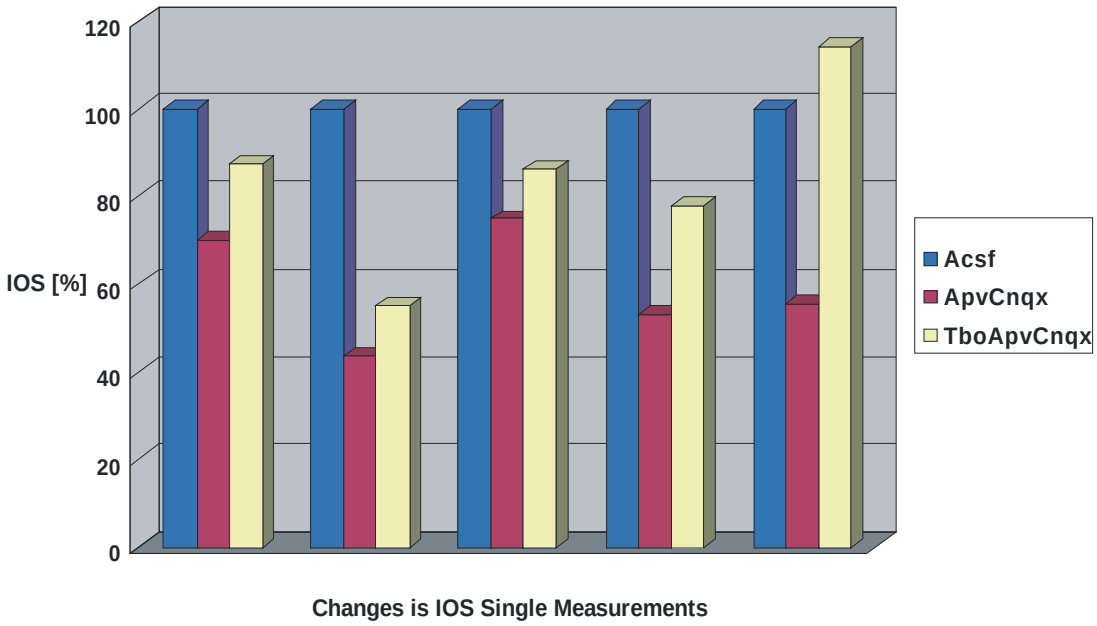

Figure 39 The graf represents percentage of the change of the maximal increase of the IOS during the stimulation. When adding APV, CNQX into the perfusion media the signals were reduced to 60.46% ± 7.2% and when adding TBOA the optical signal during stimulation increased up to 76.74% ± 7.48%

Results: The changes of LT while inhibiting glial glutamate transport using TBOA showed the increase of LT 159% ± 19.62% in 4 slices. When using APV, CNQX into the perfusion media the signals were reduced to 60.46% ± 7.2% and when adding TBOA the optical signal during stimulation increased up to 76.74% ± 7.48% in 4 slices

Conclusion: TBOA application results in the increase of the optical signal. While reducing the signal via APV, CNQX and subsequent application of TBOA into the perfusion media, the signal slight increase.

3.3.2.5 Furosemide- changes in ECS, volume changes

Aims: to define the changes in the ECS, resp. decrease

Methods: Furosemide incubation in concentration of 0,2mM. IOS has been evaluated as the maximal increase of LT during supramaximal stimulation intensity.

ROI: pyramidal cell layer

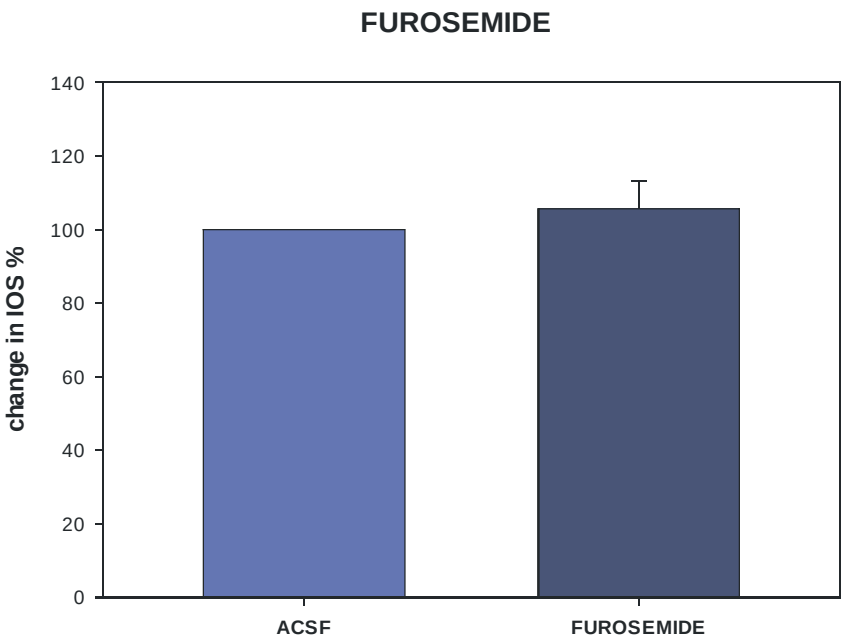

Figure 40 The graf represents percentage of the change of the maximal increase of the IOS during the stimulation. There was insignificant increase after application of FUR (111.88% ± 19.18%)

Results: The change of the LT didn't show significant results after evaluation of 7slices. Although there was increase in the furosemide group 111.88% ± 19.18%.

Conclusion: There was slight increase in LT after application of furosemide into the perfusion media.

3.3.2.6 Mitochondrial origin of the optical signal

Aim: to detect changes in flavin adenine dinucleotide (FAD) autofluorescence in dependence on the stimulation intensity.

Methods: For the purpose of this work live slices 400μm thick of wistar rat were used. The stimulated area was in DG of hippocampus, the activity was registered in the CA3 region of hippocampus, specifically pyramidal cell layer. The first measurement of LT was made during the stimulation 10s/20Hz with

supramaximal stimulation intensity. The snapping started 10s before the stimulation. Fluorescence (FAD) was excited at 490 ± 10 nm. Recordings were made with an epifluorescence illumination system (Olympus) that combines a fast driven excitation filter wheel and a triple band filter, allowing excitation FAD with a delay of 130 ms. FAD fluorescence images (emission 530 ± 10 nm) were recorded at 0.5 Hz using a CCD camera. Changes in FAD fluorescence are presented as changes in $\%\Delta F/F_0$, where F_0 is the averaged fluorescence of a 20 s period before stimulation of the tissue. The first maximal value from the begining of the recording has been evaluated which corresponds to the initial fluorescence increase e.g. oxidation of FADH.

ROI: CA3 pyramidal cell layer

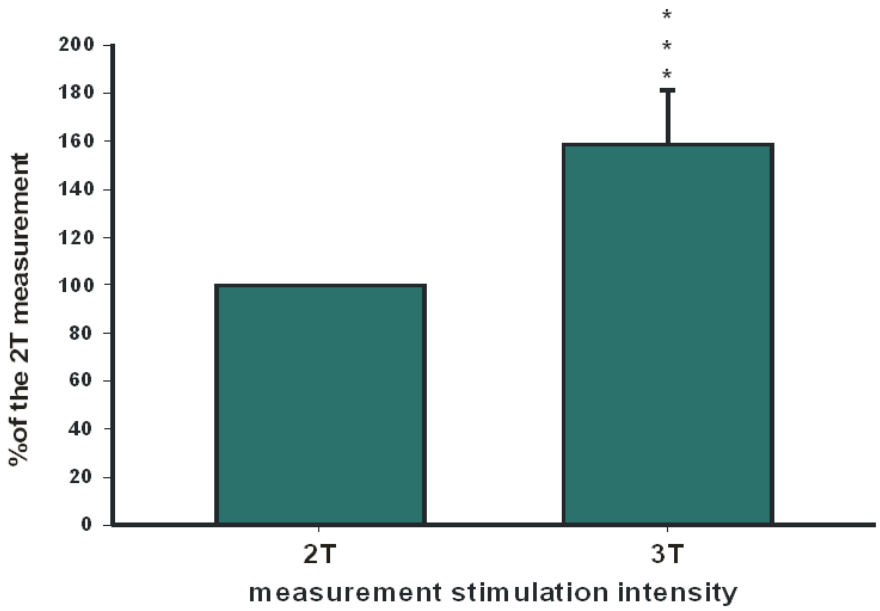

Figure 41 This graf represents the percentage of the maximal change in the intensity during stimulation of the 2T intensity.

Results: There was an increase in the maximal value of FAD fluorescence corresponding with the increase of stimulation intensity (158.544 % ± 59.713%).

Conclusion: with our setup, we are able to detect mitochondrial signal. Increase of FAD fluorescence with stimulation intensity is probably the sign of increase of mitochondrial stimulation.

4 Design of imaging setup

4.1 General description of the system

The knowledge about IOS and changing optical properties allows us to use this method in vivo. For the animal experiments, one of the crucial element for the experiments and detection of optical devices in vivo is the attachment of the optic fibre to the skull of the experimental animal. The animal should bear minimal weight and should be restricted of any movements.

Aim: Our aim is the design the construction of device enabling detection of changes of IOS in vivo. This device should be able to detect FAD, NAD(P)H and hemoglobin in cortical areas of the rat, with the field of view 2-3mm in diameter, possibility to disconnect the device, minimal weight, biocompatibility and the size appropriate to the size.

Methods: Device should be attached to the animal all the time of the experiment and enable easy reattachment. During the experiments, the device should enable the movement of the animal in regard to the bearing weight and also the possibility of attachment. This aim was achieved with optical device including optical fibre bound to the rotating connector with the solid attachement to the skull of the rat which includes the source and detection of the light with CCD camera. Optical connectors should enable easy removal of the optical fibre and protect the fibres against destruction. Optic fibre transmitting the signal from the brain surface is connected through FC connector. The split of the parallel light beam going into the optic fibre is made by beam splitter. Different filters further enable to choose different wave lengths on both sides (light detector, light source). During surgery the device can be attached to the skull into the 4mm wide hole, this fixation probe should stay in the skull the rest of the device could be removed with help of rotatory connector (Figure 42).

Results: The design of the construction is presented in the following figures (Figure 42, Figure 43) The whole device contains the light source, optic fibre, attachment to the skull and CCD camera, which is the detector. The other optical and mechanical components are described in the figures (Figure 42, Figure 43)(Horacek, 2008).

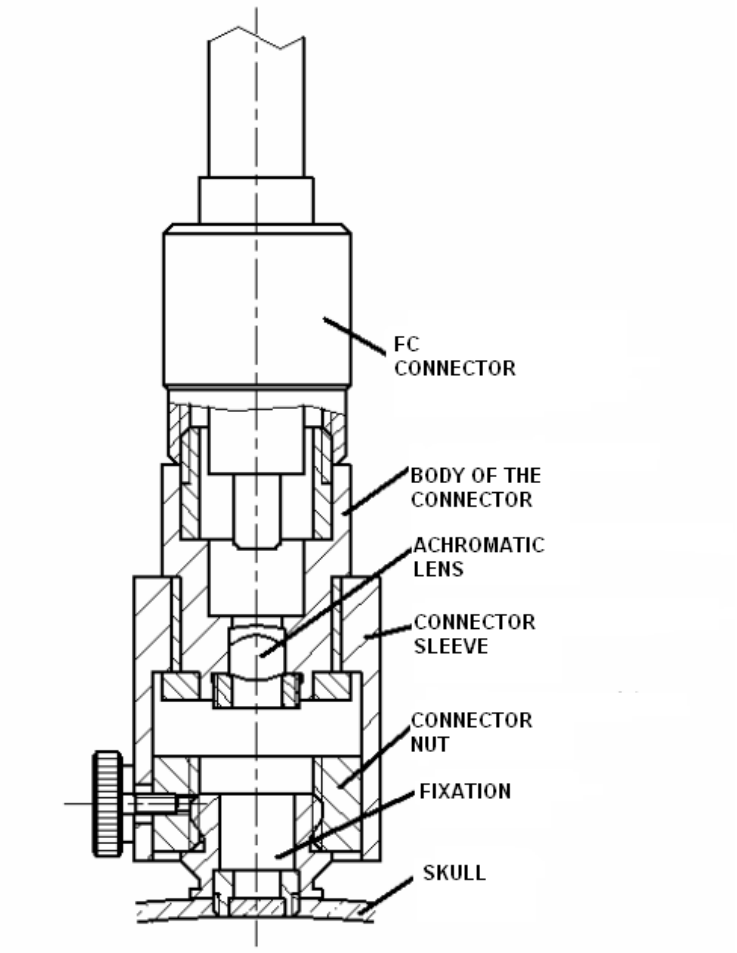

Figure 42 Design of connector of the optical fiber. The connector can be screwed to the attachment in the skull of the experimental animal. Skull has to be opened at the diameter of around 4mm.

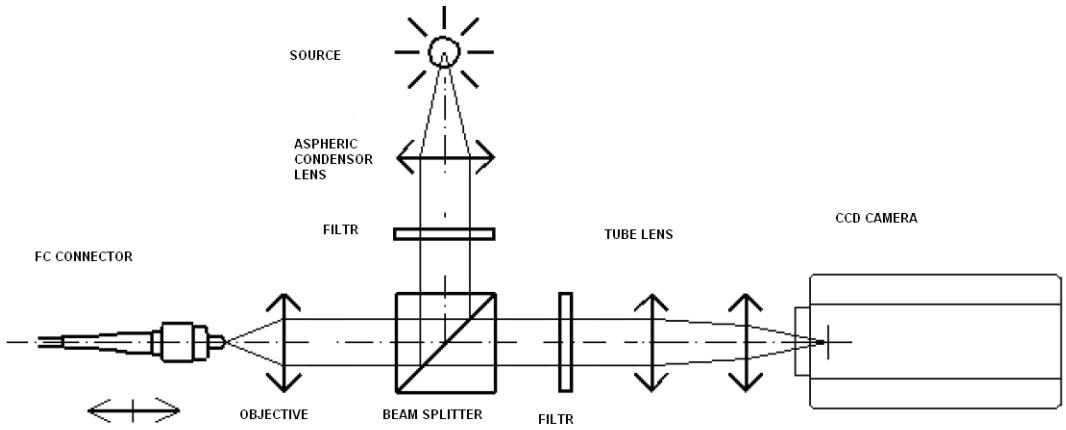

Figure 43. The device is designed to incomporate the light source, optic fibres, attachment to the skull and CCD camera.

4.2 Light source

LED light-emitting diode is a semiconductor light source. LED emit narrow-spectrum light when electrically biased in the forward direction of the P-N junction, electrons are able to recombine with holes within the device while releasing energy in the form of photons (electroluminiscence).

LEDs as a light source present many advantages such as lower energy consumption and longer lifetime. Primarily, we want to take advantage of the possibility to fast switch in between the different light wavelenghts for the fluorescent measurements. Fluorescence techniques require rather high intensity of the light. The progression in the field of fluorescent markers has a perspective to make products that are not that demanding in terms of light intensity and don't display with such excitotoxicity and enables also in vivo measurements. Fast multispectral fluorescence is achieved with help of the fast switching of the wavelenght of the excitation light with synchronous detection of the emitted light by a camera of photomultiplier. The aim of multispectral fluorescence is to get as much information as possible about the processes occuring in the tissue at the same time.

Aim: the aim was to use LED with the aim to make it possible to switch as fast as possible in between two diffent wave lengths.

Methods: We set the light source with 3 LEDs with different wave length of the emitted light. The main problem for the construction of such light source is to direct all three sources into one light beam. We would like to reach this goal with dichroic mirrors.

Results: We have designed the preliminary basic setup containing 4 LED chips of certain wavelength and beam combiners (dichroic mirror) (Figure 45) (Paska, 2008)

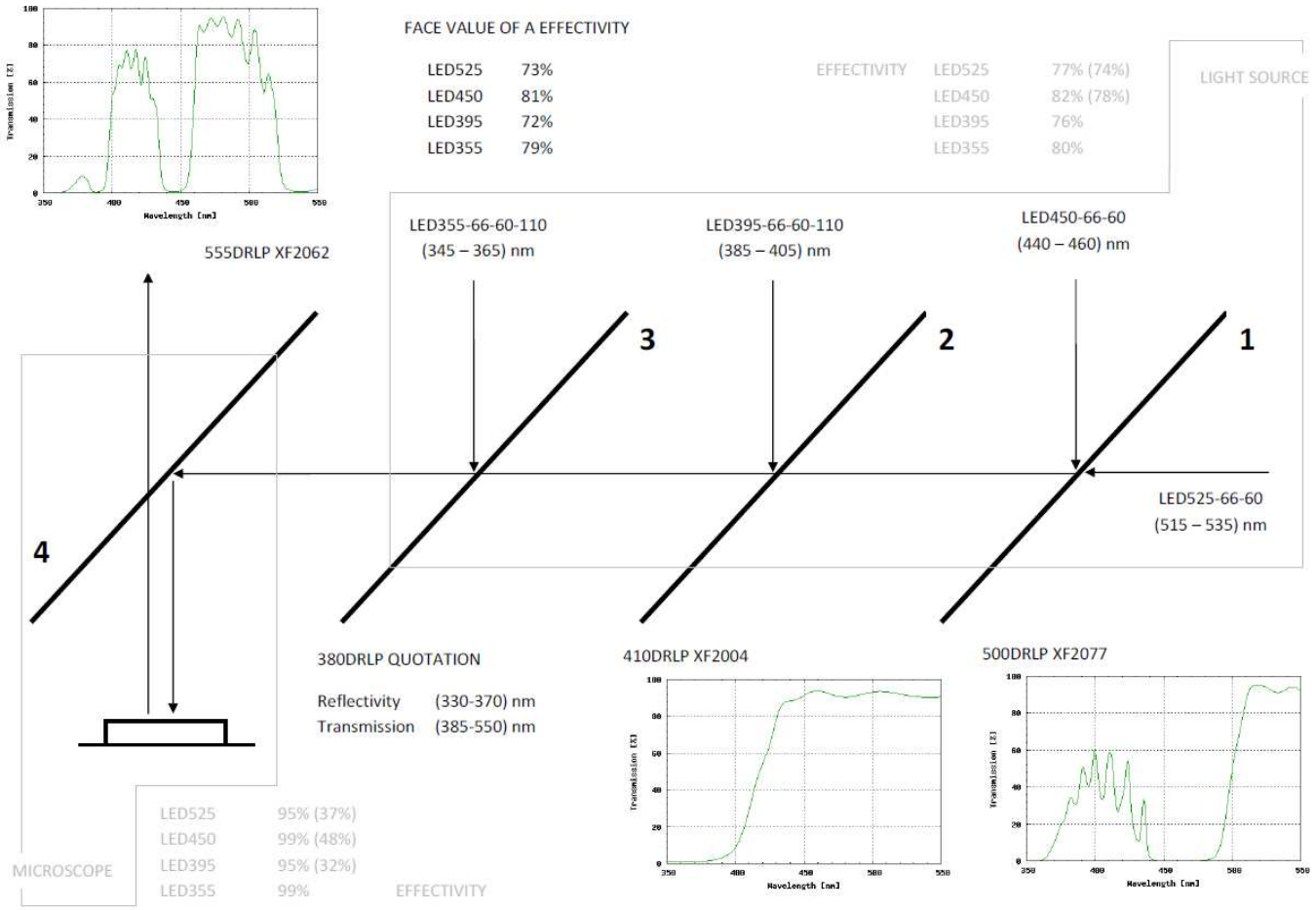

Figure 44 Shema of the LED chips integration and the specific information about beam splitters we have used in our design..

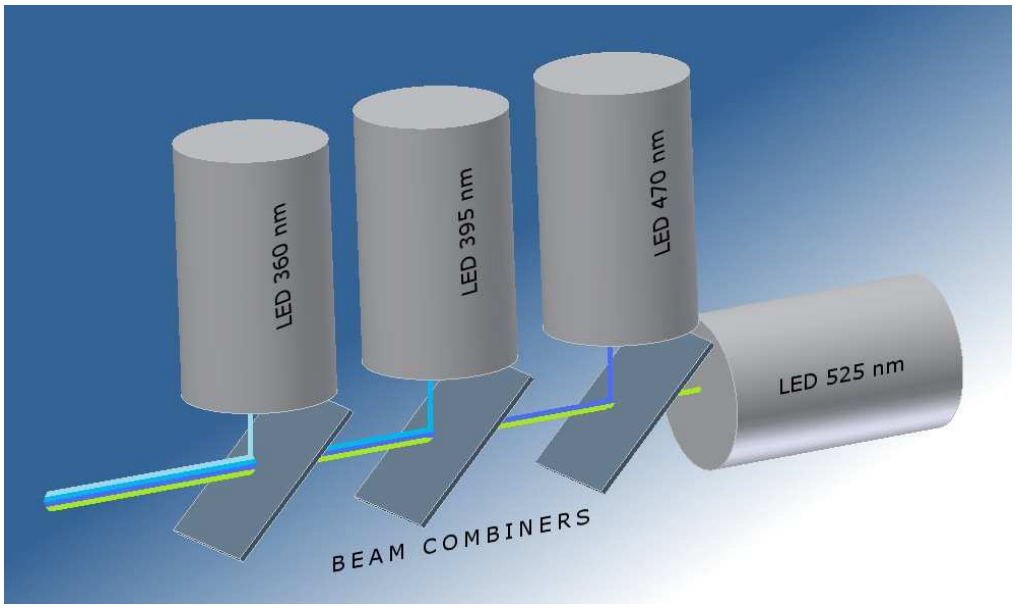

Figure 45 Schematic design of 4 LED chips directing light into one parallel light beam via 3 different dichroic mirrors

4.3 Software, Simultaneous recordings of electrical and optical signal

4.3.1 Software, VisionBrain

Simultaneous detection of both optical and electrical signal is advantagous and provide us with relevant information about ongoing processes within CNS.

Aim: Our aim was to create software enabling redording of both electrical and optical signal, using one environment. Our software should provide us with unified user interface for control of synchronous electrophysiological and video recording. Morover a digital I/O interface should enable control of other equipment like electrical stimulator or light source.

Methods: The software was programmed using Microsoft .NET Framework 3.5 library and C# programming language. The software consists of two acquisition components; electrophysiological data component and video component. The main component of electrophysiological data component is a digitalization card. In VisionBrain system there is the multifunction card M Series developed by National Instruments (NI). These cards communicate and transfer data through the PCI (Peripheral Component Interconnect) bus.

Analog data captured from digitalization card are stored in Brain Vision Data (BVD). The file is divided into several sections; primary header, secondary header and data. The primary header contains main information about the file and the experiment, the secondary header contains necessary card settings for I/O channels, after that follows data stored block-by-block. For storage of data from digital outputs/inputs, synchronization events and other user defined events was designed another file format called Brain Vision Event (BVE). The file structure is similar to previous BVD file format.

The second acquisition component is the video one. It can cooperate with several different camera devices that can be divided into two groups.

Firstly there are standard web cameras and DV cameras. Data captured from those cameras are stored in commonly used AVI file that can be compressed or uncompressed according to user preferences and need. Secondly there are selected high sensitive cameras for microscopy use (Q-Imaging) controlled by manufacturer's camera drivers. Those cameras usually perform in high resolution and enable external triggering, whereby provide possibility of synchronization between image and electrophysiological signals. Images captured from those cameras can be stored in two types of file; in previously mentioned AVI file and in our own binary file called Brain Vision Graphics (BVG). The BVG file consists of three main parts. The first one is the main header which is located at the beginning of every BVG file and contains information common to all images, e.g. header sizes and camera settings. This part is followed by repetitious secondary image header containing period between two images and start time of an image and image own data.

The synchronization between video component and electrophysiological data component consequently between recorded electrical and video data can be realized in two ways. If camera enables external triggering (high sensitive cameras for microscopy use), it is realized through its input and output trigger signals controlled from digital inputs and outputs of data acquisition card. If external triggering is not supported (standard web cameras), the synchronization is realized using LED controlled from data acquisition card that flickers in exactly defined time sequence.

Results: The software has been has been successfully tested using Series PCI-6221 data acquisition card (16bit, 250 kS/s, 16AI, 2 AO and 24 digital I/O lines) with homemade EEG four channel amplifiers for signal preconditioning and several different cameras; standard webcam (for example: Philips SPC900NC, MSI StarCam Racer (Micro-Star International Co., Taiwan), Logitech eFace2050AF and others), industrial cameras UI-2230C and UI-2230M (Imaging

Development Systems, Germany) and high sensitive cooled cameras Retiga 2000R and Retiga 4000R (Q-Imaging, Canada).

5 Discussion

5.1 Methods:

5.1.1 Slice preparation:

Studies that are made with help of brain slices provide a valuable data on the basic features of neurons and synapses. There are two major types of the in vitro placement of the slice that maintains them alive during recordings. The slice of the brain tissue can be either put on the filterpaper with ACSF and be surrounded with humidified gaseous atmosphere (interface type of the chamber) or the slice can be surrounded just with ACSF. Both types have its advantages and disadvantages and differ from the situation in the intact brain, especially in relation to the rhytmic synchronous neuronal events as reflected in EEG. In vitro placement of the tissue allows us the other relevant information and make possible to change the conditions and apply pharmacologic agents. By altering the ionic composition of the superfusion media or by the addition of pharmacological agents it has been possible to capture naturalistic network activity even in such brain slice preparations. This has been particularly successful in interface-type chamber where sharp wave ripples (peculiar hippocampal activity connected to the memory consolidation) has been investigated. (Maier et al., 2003)

For the maintenance of the live rat slices and subsequent optical and electrical recording the submerged type of chamber has been used in our experiments. Submerged type of chamber brings some specific advantages in the physiological studies slightly similar to conditions in real life compared to so called interface chamber where the slice lies on the ACSF and is rather surrounded by gaseous atmosphere. Submerged type of chamber further enables optical imaging of the slice because it allows the usage of water immersion microscopy. The submerged type of the chamber offers equally important experimental advantages including faster exchange of pharmacological agents, visually guided patch-clamp

recordings and the advanced imaging techniques including our research with IOS.

Experiments with tissue slices represents promarily conditions where the different structures and even distinct cells are nicely seen, avoiding certain sources of noice, but only with the disadvantage that oxygen supply and connectivity is changed in a simplified manner(Davies, Kirov, and Andrew, 2007). Slices of the tissue can be further modified in many more ways compared to the situation in vivo. The slices are cut, so like this we are loosing connections to the other structure, but not only the connectivity but also the surface of the slice is corrupted. Different conditions such as higher temperature during preparation have impact on the slice at the level of synapses. In ice cold preparations reversible cytoskeletal changes can apprear and the inhibition of ATPas occurs. Slices prepared at room temperature can suffer from metabolic stress and can lose some synapses, but via warmer preparation, we can avoid the excessive spine loss occurring at colder temperatures due to Na+, Na+ ATPase inhibition. (Bourne et al., 2007)

We have to also keep in mind that there is also an unequal distribution of vulnerable regions within hippocampus with increased vulnerability to hypoxia-ischemia in CA1 than in CA3 region both in vivo and in vitro (Kreisman, Soliman, and Gozal, 2000).

One of the most prominent disadvantages of the submerged type of chamber is the insufficient oxygen supply. Furthermore the oxygen is transferred into the tissue via diffusion which might not be adequate and doesn't respect the demand of the tissue compared to the situation in vivo where the instantaneous demand is covered via increased blood flow. (Turner et al. 390-98)

The way to increase the diffusion is the temperature increase or the speed of the bubbled ACSF (Hajos et al., 2009). In our setup, the speed of the flow is approximately 5.5 ml/min which makes possible better electrophysiological measurements, diffusion of pharmacological agents.

5.1.2 Light source and optical detection

The unwanted part of every signal is the noise. While recording intrinsic optical signals, as well as any other signal, we have to consider every possible noise source and try to avoid them or define them if possible and include them in the final conclusions.

Certain sources of the noise can be easily eliminated. Our results confirm the impact of the surrounding light on the final optical signal detected. As an example I can present the step in detected light intensity corresponding to shutting of doors of recording room. The conditions such as surrounding light should be stay constant at all times.

Other source of noise is in the intensity of the light source. There is a transition curve that accompanies change of the intensity of the light source. The results illustrate those characteristic measured during increasing resp. decreasing the intensity. This problem can be easily eliminated if we switch on the light source and start the measurement sufficient time period after the last time of the detection or intensity change. The settling of the intensity appears within 40 minutes. This fact makes uneasy mainly electrophysiological measurements and we tend to have the slice illuminated for minimal time possible because of the toxicity of the light. This finding is very important for us and for further measurements because we can easily confuse this source of noise and the movement of the slice. To get rid of such complication, LED diode as a light source has been proposed.

5.2 Results in vitro experiments, the origin of the optical signals:

The present experiments we are demonstrating that the optical methods are useful in the studies of processes in the CNS applying tissue slices. A series of experiments have been performed to demonstrate that we can detect changing optical properties of the nervous tissue in connection to its specific activity with a slight delay from electrical signal in range of 0.5s. (Grinvald, 1981)

5.2.1 Stimulation intensity

Imaging of optical signals revealed the fact neuronal activity can be detected via changes in transmittance of the light through the tissue by causing swelling of the cells. Evaluating these changes provide advantageous method for imaging neuronal activity (Grinvald, 1986). When applying different stimulation intensity, we can conclude that increasing intensity of stimulation causes subsequent increase in the optical signal. The more neuronal connections we activate the bigger the changes are. This is in accordance with the previous studies where increase in LT and cellular swelling were graded with increasing frequences of stimulatin in optic nerve (MacVicar, 2002). The cellular swelling occurs as a consequence of ionic flow during action potential. The crucial for these changes is Na-K-2Cl cotransport. In cell tissue culture, high extracellular potassium causes astrocytic swelling as a consequence of KCl uptake and water movements (Walz, 1984).

5.2.2 TTX

We used TTX to distinguish from the non-neural origin of the signal. TTX block voltage-gated sodium channels on the surface of the neuronal membrane with very tight binding site. Sodium movement is like that effectively shut down and the action potential along the nerve membrane is not spread anywhere. The results showed that the signal was reduced to app. 5% of the previous value, so

the signal wasn't blocked entirely. We assume that TTX didn't fill all the binding sites and that some Na/K channels were activated. The other explanation for this event could be the fact that the electrical pulse itself influences the cellular volume. MacVicar also suggested that TTX block electrically induced LT changes but not high K indused IOS increase, for these changes Na-K-2Cl cotransport is responsible (Walz, 1984), for the remaining LT change Na-K-2Cl can be responsible. This signal was reduced sufficiently to neglect these and we could focus on the exact mechanism and the possible pharmacological reduction of IOS.

5.2.3 APV/CNQX

To distinguish between the synaptic transmission and non-synaptic activity of the nervous tissue, we blocked glutamate receptors using a selective NMDA receptor blocker APV (R-2-amino-5-phosphonopentanoate) and further AMPA/kainate receptor blocker CNQX (6-cyano 7 nitroquinoxaline-2,3-dione). In this case the IOS signal during stimulation was blocked to the half values of the previous signal. This indicates that the signal is mainly of synaptic origin. The other questions remain unrevealed such as if all Glu binding sites were occupied with APV, CNQX since these substances can compete over the binging site. Anyhow, it has been proved that the signal is strongly glutamate dependent. It goes in accordance with MacVicar who blocked the LT with kynurenic acid which is noncompetive glutamate receptor antagonist and confirms that postsynaptic activation is necessary for the generation of LT (MacVicar, 1991). MacVicar has managed to block the change in LT with was probably because of the fact they use noncompetitive glutamate receptor antagonist. Interestingly glutamate antagonist were not able to block anoxic depolarization (increase in LT due to lack of oxygen) (Jarvis, 2001)

5.2.4 TBOA

Physiological interactions between astrocytes and neurons are coupled and there is no rigorous generalization of both cell type and their role in IOS generation.
Removal of neurotransmitter out of the extracellular coordingated by many signalling pathways is necessary for the normal functioning of neural structures. (Agulhon, 2008) In principle, some of the slow optical signals may come from glia, rather than neurons. Previous studies showed that uptake of K into astrocytes was probably responsible for the cellular swelling and high K (MacVicar, 2002, Ransom,1985). That's why we were interested in the evaluation of glial contribution to the IOS signal. In the previous experiment, we concluded that the LT signal is strongly dependent on the synaptic glutamatergic transmittion in hippocampus. Glial cells are responsible for the removal of Glu from the synaptic cleft. In our set of experiments we examined two conditions. Firstly we added blocker of glial glutamate transport blocker TBOA to prevent reuptake of Glu and this increased the IOS to 159% ± 19.62%. This indicates that the accumulation of glutamate in the synaptic cleft due to lack of Glu glial cleaning leads to a slight increase of the signal. Therefore we concomitantly blocked Glu receptors using APV and CNQX in the next set of the experiments. This reduced the optical signal during stimulation down to 76.74% ± 7.48%. We assume that this occurred as a result of increase in extracellular glutamate, so the IOS increased independly of the fact glutamatergic transmission was abolished.
It has been suggested that after ischemic injury, extracellular glutamate concentration rises and during cerebral ischemia actually reaches levels capable of inducing neuronal death. Using glu-transport blockers such as TBOA indicated that this significant rise in glu occurs as a consequence of reduces uptake and increased vesicular and nonvesicular release of glutamate.(Jabaudon et al., 1999) On the contrary acute disruption of the activity of glutamate transporters

results in the accumulation of extracellular glutamate which can further lead to cellular death.(Jabaudon et al., 2000)

5.2.5 Furosemide

The aim of this furosemide incubation was to determine the dependency of ECS decrease on the IOS. ECS is important for the volume transmission, cellular signals and also changing resistance of the extracellular space. Furosemide thanks to increasing extracellular space through action on Na-K-2Cl cotransporter results in descrese of the excitability of the nervous tissues and has been used as a anticonvulsant drug in humans (Haglund, 2005). Our main hypothesis consisted in the fact that the stimulation increases light transmittance of the tissue will be further suppresed with the application of furosemide. Indeed, the high K induced IOS ware depressed by furosemide and bumetanide, antagonists for Na-K-2Cl cotransporter (MacVicar, 2002). The results were surprising compared to what we expected. The perfusion with furosemide result in increased signal although in the study of Holthof lead to the decreas in LT in rat neocortical slices (Holthof, 1996).

To better understand mechanism of furosemide action ion-selective electrode should be used. Underlying changes in K+ and volume of ECS can clarify processes responsible for IOS changes. Unfortunatelly, during the experiments we did not have an opportunity to use ion selective electrodes. . Nevertheless, we might suppose that the cellular swelling was in our case predominant component of the optical changes and mismatch the changes caused by decrease of extracellular space.

Furosemide has dose dependent effect on GABA A receptor in micromolar concentrations and thus in our case when 0.2 mM concentration was used we should assume that this might suppress GABA inhibition. Korpi et al. applied furosemide (5uM) has show selective antagonism at GABA A receptors. Morover, there is also a different expression of GABA receptors in the hippocampus during

development, which might have played role in our experiments as well because we have used animals in age group 20-30 days which is rather larger age group which could explain the differences in the furosemide effect on the tissue. In future experiments we will use bumetanide which lacks GABA A activity.

5.3 Hardware and software

In addition to the experimental aims, the other part of the study was to design software and devices enabling recording and evaluation of IOS in combination with the electrophysiological signals. These signals are usually recorded using two different environments, one for optical data and second one for electrical data. In our case, we designed software enabling just one environment which in principle facilitates usage and detection of both signals. One environment accomplishes our aim of the highly accurate synchronous recordings of both electrical and optical signal.

A software component of the setup is presented by the VisionBrain program. The software was designed using C# programming language and Microsoft .NET framework 3.5. because of its object orientation, wide range of class libraries and easy portability among different computers running Microsoft Windows operating systems.

To make this detection system available in terms of cost the hardware components National Instruments multifunction lowcost card M Series were used for recordings of electrophysiological data. QImaging Retiga 2000R camera was used for recording video data because of its high resolution (12bit images with max resolution 1600 x 1200 pixels, 16bit a/c convertor) and low noise (chapter 3.3.1). The synchronization is realized using camera's trigger output and input signals that are connected to the card's digital outputs and inputs. The quality of the measured data (12bit images with max resolution 1600 x 1200 pixels, 16bit a/c convertor) enabled by used hardware is sufficient for our purposes, but can be increased using higher models of digitalization card or camera. Also just minimal requirements are requested for PC's computational resources; this

includes 1GB RAM, dual core processor and sufficient capacity to store the captured data. This all makes the system available especially in terms of cost.

To enable utility of the software for other types of experiments, where synchronization of electrical and optical data is required (e.g. long term video-eeg monitoring), it is enables communication with another types of camera such as standard web cameras. When compared to the other systems and the other imaging methods, our system is user friendly and rather inexpensive.

6 Conclusions

Intrinsic optical signal are one of the possible modalities in the imaging of the activity of nervous tissue.

We characterized the genereation of changing optical properties with set of experiments with the tissue slices to prove that the signal is of neuronal origin and we were able to detect and influence pharmacologicaly ion channels, synapses, glial reuptake and mitochondrial fluorescence signal. We defined and revealed the different sources of noise and showed up one of the biggest sources of noise which was the noise of the own light source.

We designed the experimental setup for in vivo experiments where we would use these obtained data in the whole animal the attachment of the optic fibre and LED diode light source.

Specialized software VisionBrain for in vivo detection enabling detection of both optical and electrical signals using our specialized software has been developed.

Abbreviations

AVI - audio video interleave

CCD-camera

CNQX - (6-cyano-7-nitroquinoxaline-2,3-dione) is a competitive AMPA/kainate receptor antagonist

CNS - central nervous system

CSF- cerebrospinal fluid

DL-TBOA - DL-threo-b-Benzyloxyaspartic acid, competitive, non-transportable blocker of excitatory amino acid transporters

EAAT - excitatory amino acid transporters

EEG - electroencephalogram

FAD - flavin adenine dinucleotide

FADH2 - flavin adenine dinucleotide hydroquinone form

fi - fimbria

fMRI - functional magnetic resonance

FURO - furosemide

fx - fornix

GD - gyrus dentatus

HC - hippocampus HC

IOS - intrinsic optical signals

LED - light emitting diode

LT - light transmittance

MEG - magnetic encefalogram

MS - medial septum

NAD - nicotinamide adenin dinucleotide

NADP - Nicotinamide adenine dinucleotide phosphate

NIRS- near-infrared refractory spectoscopy

NKCC - Na-K-Cl cotransporter

OT - optic tomografy

PET - possitron emisson tomography

PNS - peripheral nervous system

ROI - region of interest

SNR - signal to noise ratio

TBI - traumatic brain injury

TCA - tricarboxylic acid cycle

TTX - tetrodotoxin

7 References

1. N. J. Abbott, L. Ronnback, and E. Hansson. Astrocyte-endothelial interactions at the blood-brain barrier. *Nat.Rev.Neurosci.* 7 (1):41-53, 2006.

2. L. F. Agnati, G. Leo, A. Zanardi, S. Genedani, A. Rivera, K. Fuxe, and D. Guidolin. Volume transmission and wiring transmission from cellular to molecular networks: history and perspectives. *Acta Physiol (Oxf)* 187 (1-2):329-344, 2006.

3. C. Agulhon, J. Petravicz, A. B. McMullen, E. J. Sweger, S. K. Minton, S. R. Taves, K. B. Casper, T. A. Fiacco, and K. D. McCarthy. What is the role of astrocyte calcium in neurophysiology? *Neuron* 59 (6):932-946, 2008.

4. P. G. Aitken, D. Fayuk, G. G. Somjen, and D. A. Turner. Use of intrinsic optical signals to monitor physiological changes in brain tissue slices. *Methods* 18 (2):91-103, 1999.

5. N. Alperin, S. H. Lee, A. Sivaramakrishnan, and S. G. Hushek. Quantifying the effect of posture on intracranial physiology in humans by MRI flow studies. *J.Magn Reson.Imaging* 22 (5):591-596, 2005.

6. T. Amedee, A. Robert, and J. A. Coles. Potassium homeostasis and glial energy metabolism. *Glia* 21 (1):46-55, 1997.

7. N. C. Andreasen. Brain imaging: applications in psychiatry. *Science* 239 (4846):1381-1388, 1988.

8. R. D. Andrew, C. R. Jarvis, and A. S. Obeidat. Potential sources of intrinsic optical signals imaged in live brain slices. *Methods* 18 (2):185-96, 179, 1999.

9. C. M. Armstrong. The Na/K pump, Cl ion, and osmotic stabilization of cells. *Proc.Natl.Acad.Sci.U.S.A* 100 (10):6257-6262, 2003.

10. O. J. Arthurs, T. Donovan, D. J. Spiegelhalter, J. D. Pickard, and S. J. Boniface. Intracortically distributed neurovascular coupling relationships within and between human somatosensory cortices. *Cereb.Cortex* 17 (3):661-668, 2007.

11. J. Badaut, F. Lasbennes, P. J. Magistretti, and L. Regli. Aquaporins in brain: distribution, physiology, and pathophysiology. *J.Cereb.Blood Flow Metab* 22 (4):367-378, 2002.

12. S. Bahar, M. Suh, M. Zhao, and T. H. Schwartz. Intrinsic optical signal imaging of neocortical seizures: the 'epileptic dip'. *Neuroreport* 17 (5):499-503, 2006.

13. T. G. Banke and C. J. McBain. GABAergic input onto CA3 hippocampal interneurons remains shunting throughout development. *J.Neurosci.* 26 (45):11720-11725, 2006.

14. T. A. Basarsky, S. N. Duffy, R. D. Andrew, and B. A. Macvicar. Imaging spreading depression and associated intracellular calcium waves in brain slices. *J.Neurosci.* 18 (18):7189-7199, 1998.

15. T. A. Basarsky, D. Feighan, and B. A. Macvicar. Glutamate release through volume-activated channels during spreading depression. *J.Neurosci.* 19 (15):6439-6445, 1999.

16. J. Berwick, I. M. Devonshire, A. J. Martindale, D. Johnston, Y. Zheng, A. J. Kennerley, P. G. Overton, and J. E. Mayhew. Cocaine administration produces a protracted decoupling of neural and haemodynamic responses to intense sensory stimuli. *Neuroscience* 132 (2):361-374, 2005.

17. T. V. Bliss and T. Lomo. Long-lasting potentiation of synaptic transmission in the dentate area of the anaesthetized rabbit following stimulation of the perforant path. *J.Physiol* 232 (2):331-356, 1973.

18. T. Bonhoeffer. Optical imaging of intrinsic signals as a tool to visualize the functional architecture of adult and developing visual cortex. *Arzneimittelforschung.* 45 (3A):351-356, 1995.

19. J. N. Bourne, S. A. Kirov, K. E. Sorra, and K. M. Harris. Warmer preparation of hippocampal slices prevents synapse proliferation that might obscure LTP-related structural plasticity. *Neuropharmacology* 52 (1):55-59, 2007.

20. M. Brennan, J. A. Connor, and C. W. Shuttleworth. NAD(P)H fluorescence transients after synaptic activity in brain slices: predominant role of mitochondrial function. *J.Cereb.Blood Flow Metab* 26 (11):1389-1406, 2006.

21. K. Buchheim, O. Wessel, H. Siegmund, S. Schuchmann, and H. Meierkord. Processes and components participating in the generation of intrinsic optical signal changes in vitro. *Eur.J.Neurosci.* 22 (1):125-132, 2005.

22. G. Calamita, D. Ferri, P. Gena, G. E. Liquori, A. Cavalier, D. Thomas, and M. Svelto. The inner mitochondrial membrane has aquaporin-8 water

channels and is highly permeable to water. *J.Biol.Chem.* 280 (17):17149-17153, 2005.

23. F. Cannestra, N. Pouratian, S. Y. Bookheimer, N. A. Martin, D. P. Beckerand, and A. W. Toga. Temporal spatial differences observed by functional MRI and human intraoperative optical imaging. *Cereb.Cortex* 11 (8):773-782, 2001.

24. Chance, B. Schoener, R. Oshino, F. Itshak, and Y. Nakase. Oxidation-reduction ratio studies of mitochondria in freeze-trapped samples. NADH and flavoprotein fluorescence signals. *J.Biol.Chem.* 254 (11):4764-4771, 1979.

25. S. R. Chebabo, M. A. Hester, J. Jing, P. G. Aitken, and G. G. Somjen. Interstitial space, electrical resistance and ion concentrations during hypotonia of rat hippocampal slices. *J.Physiol* 487 (Pt 3):685-697, 1995.

26. L. M. Chen, G. H. Turner, R. M. Friedman, N. Zhang, J. C. Gore, A. W. Roe, and M. J. Avison. High-resolution maps of real and illusory tactile activation in primary somatosensory cortex in individual monkeys with functional magnetic resonance imaging and optical imaging. *J.Neurosci.* 27 (34):9181-9191, 2007.

27. L. M. Chen, R. M. Friedman, and A. W. Roe. Optical imaging of nociception in primary somatosensory cortex of non-human primates. *Sheng Li Xue.Bao.* 60 (5):664-668, 2008.

28. Chvatal, M. Anderova, and F. Kirchhoff. Three-dimensional confocal morphometry - a new approach for studying dynamic changes in cell morphology in brain slices. *J.Anat.* 210 (6):671-683, 2007.

29. L. B. Cohen and B. M. Salzberg. Optical measurement of membrane potential. *Rev.Physiol Biochem.Pharmacol.* 83:35-88, 1978.

30. M. D. Croning and G. G. Haddad. Comparison of brain slice chamber designs for investigations of oxygen deprivation in vitro. *J.Neurosci.Methods* 81 (1-2):103-111, 1998.

31. T. Da and A. S. Verkman. Aquaporin-4 gene disruption in mice protects against impaired retinal function and cell death after ischemia. *Invest Ophthalmol.Vis.Sci.* 45 (12):4477-4483, 2004.

32. M. Darby, J. B. Kuzmiski, W. Panenka, D. Feighan, and B. A. Macvicar. ATP released from astrocytes during swelling activates chloride channels. *J.Neurophysiol.* 89 (4):1870-1877, 2003.

33. M. L. Davies, S. A. Kirov, and R. D. Andrew. Whole isolated neocortical and hippocampal preparations and their use in imaging studies. *J.Neurosci.Methods* 166 (2):203-216, 2007.

34. M. R. Duchen. Roles of mitochondria in health and disease. *Diabetes* 53 Suppl 1:S96-102, 2004.

35. T. Durduran, C. Zhou, B. L. Edlow, G. Yu, R. Choe, M. N. Kim, B. L. Cucchiara, M. E. Putt, Q. Shah, S. E. Kasner, J. H. Greenberg, A. G. Yodh, and J. A. Detre. Transcranial optical monitoring of cerebrovascular hemodynamics in acute stroke patients. *Opt.Express* 17 (5):3884-3902, 2009.

36. B. S. Elkin, E. U. Azeloglu, K. D. Costa, and B. Morrison, III. Mechanical heterogeneity of the rat hippocampus measured by atomic force microscope indentation. *J.Neurotrauma* 24 (5):812-822, 2007.

37. D. Fayuk, P. G. Aitken, G. G. Somjen, and D. A. Turner. Two different mechanisms underlie reversible, intrinsic optical signals in rat hippocampal slices. *J.Neurophysiol.* 87 (4):1924-1937, 2002.

38. J. C. Fiala, S. A. Kirov, M. D. Feinberg, L. J. Petrak, P. George, C. A. Goddard, and K. M. Harris. Timing of neuronal and glial ultrastructure disruption during brain slice preparation and recovery in vitro. *J.Comp Neurol.* 465 (1):90-103, 2003.

39. M. Frontczak-Baniewicz and M. Walski. Glial scar instability after brain injury. *J.Physiol Pharmacol.* 57 Suppl 4:97-102, 2006.

40. B. H. Gahwiler. Nerve cells in organotypic cultures. *JAMA* 245 (18):1858-1859, 1981.

41. S. C. Gebhart, R. C. Thompson, and A. Mahadevan-Jansen. Liquid-crystal tunable filter spectral imaging for brain tumor demarcation. *Appl.Opt.* 46 (10):1896-1910, 2007.

42. F. J. Gerich, S. Hepp, I. Probst, and M. Muller. Mitochondrial inhibition prior to oxygen-withdrawal facilitates the occurrence of hypoxia-induced spreading depression in rat hippocampal slices. *J.Neurophysiol.* 96 (1):492-504, 2006.

43. G. R. Gordon, H. B. Choi, R. L. Rungta, G. C. Ellis-Davies, and B. A. Macvicar. Brain metabolism dictates the polarity of astrocyte control over arterioles. *Nature* 456 (7223):745-749, 2008.

44. D. Greitz and J. Hannerz. A proposed model of cerebrospinal fluid circulation: observations with radionuclide cisternography. *AJNR Am.J.Neuroradiol.* 17 (3):431-438, 1996.

45. D. Greitz. Radiological assessment of hydrocephalus: new theories and implications for therapy. *Neurosurg.Rev.* 27 (3):145-165, 2004.

46. Grinvald, A. Manker, and M. Segal. Visualization of the spread of electrical activity in rat hippocampal slices by voltage-sensitive optical probes. *J.Physiol* 333:269-291, 1982.

47. Grinvald, E. Lieke, R. D. Frostig, C. D. Gilbert, and T. N. Wiesel. Functional architecture of cortex revealed by optical imaging of intrinsic signals. *Nature* 324 (6095):361-364, 1986.

48. Grinvald, R. D. Frostig, R. M. Siegel, and E. Bartfeld. High-resolution optical imaging of functional brain architecture in the awake monkey. *Proc.Natl.Acad.Sci.U.S.A* 88 (24):11559-11563, 1991.

49. N. Gueler, M. Kukley, and D. Dietrich. TBOA-sensitive uptake limits glutamate penetration into brain slices to a few micrometers. *Neurosci.Lett.* 419 (3):269-272, 2007.

50. E. Gunnarson, M. Zelenina, and A. Aperia. Regulation of brain aquaporins. *Neuroscience* 129 (4):947-955, 2004.

51. E. Gunnarson, Y. Song, J. M. Kowalewski, H. Brismar, M. Brines, A. Cerami, U. Andersson, M. Zelenina, and A. Aperia. Erythropoietin modulation of astrocyte water permeability as a component of neuroprotection. *Proc.Natl.Acad.Sci.U.S.A* 106 (5):1602-1607, 2009.

52. K. U. Gutschmidt, K. Stenkamp, K. Buchheim, U. Heinemann, and H. Meierkord. Anticonvulsant actions of furosemide in vitro. *Neuroscience* 91 (4):1471-1481, 1999.

53. M. M. Haglund and D. W. Hochman. Optical imaging of epileptiform activity in human neocortex. *Epilepsia* 45 Suppl 4:43-47, 2004.

54. M. M. Haglund and D. W. Hochman. Furosemide and mannitol suppression of epileptic activity in the human brain. *J.Neurophysiol.* 94 (2):907-918, 2005.

55. M. M. Haglund and D. W. Hochman. Imaging of intrinsic optical signals in primate cortex during epileptiform activity. *Epilepsia* 48 Suppl 4:65-74, 2007.

56. N. Hajos, T. J. Ellender, R. Zemankovics, E. O. Mann, R. Exley, S. J. Cragg, T. F. Freund, and O. Paulsen. Maintaining network activity in submerged hippocampal slices: importance of oxygen supply. *Eur.J.Neurosci.* 29 (2):319-327, 2009.

57. P. Halestrap. Calcium, mitochondria and reperfusion injury: a pore way to die. *Biochem.Soc.Trans.* 34 (Pt 2):232-237, 2006.

58. P. Halestrap. Mitochondrial calcium in health and disease. *Biochim.Biophys.Acta* 1787 (11):1289-1290, 2009.

59. M. Haller, S. L. Mironov, and D. W. Richter. Intrinsic optical signals in respiratory brain stem regions of mice: neurotransmitters, neuromodulators, and metabolic stress. *J.Neurophysiol.* 86 (1):412-421, 2001.

60. E. Hansson and L. Ronnback. Glial-neuronal signaling and astroglial swelling in physiology and pathology. *Adv.Exp.Med.Biol.* 559:313-323, 2004.

61. S. R. Heidemann, S. Kaech, R. E. Buxbaum, and A. Matus. Direct observations of the mechanical behaviors of the cytoskeleton in living fibroblasts. *J.Cell Biol.* 145 (1):109-122, 1999.

62. F. Helmchen and W. Denk. New developments in multiphoton microscopy. *Curr.Opin.Neurobiol.* 12 (5):593-601, 2002.

63. F. Helmchen. Miniaturization of fluorescence microscopes using fibre optics. *Exp.Physiol* 87 (6):737-745, 2002.

64. M. C. Henry-Feugeas, I. Idy-Peretti, O. Baledent, A. Poncelet-Didon, G. Zannoli, J. Bittoun, and E. Schouman-Claeys. Origin of subarachnoid cerebrospinal fluid pulsations: a phase-contrast MR analysis. *Magn Reson.Imaging* 18 (4):387-395, 2000.

65. D. K. Hill and R. D. Keynes. Opacity changes in stimulated nerve. *J.Physiol* 108 (3):278-281, 1949.

66. E. M. Hillman. Optical brain imaging in vivo: techniques and applications from animal to man. *J.Biomed.Opt.* 12 (5):051402, 2007.

67. D. W. Hochman and P. A. Schwartzkroin. Chloride-cotransport blockade desynchronizes neuronal discharge in the "epileptic" hippocampal slice. *J.Neurophysiol.* 83 (1):406-417, 2000.

68. K. Holthoff and O. W. Witte. Intrinsic optical signals in rat neocortical slices measured with near-infrared dark-field microscopy reveal changes in extracellular space. *J.Neurosci.* 16 (8):2740-2749, 1996.

69. K. Holthoff, E. Sagnak, and O. W. Witte. Functional mapping of cortical areas with optical imaging. *Neuroimage.* 37 (2):440-448, 2007.

70. M. Horáček. Návrh zařízení pro autofluorescenční analýzu mozkové kůry potkana, *diplomová práce ČVUT FS*, Praha 2008

71. Huchzermeyer, K. Albus, H. J. Gabriel, J. Otahal, N. Taubenberger, U. Heinemann, R. Kovacs, and O. Kann. Gamma oscillations and spontaneous network activity in the hippocampus are highly sensitive to decreases in pO2 and concomitant changes in mitochondrial redox state. *J.Neurosci.* 28 (5):1153-1162, 2008.

72. Jabaudon, K. Shimamoto, Y. Yasuda-Kamatani, M. Scanziani, B. H. Gahwiler, and U. Gerber. Inhibition of uptake unmasks rapid extracellular turnover of glutamate of nonvesicular origin. *Proc.Natl.Acad.Sci.U.S.A* 96 (15):8733-8738, 1999.

73. Jabaudon, M. Scanziani, B. H. Gahwiler, and U. Gerber. Acute decrease in net glutamate uptake during energy deprivation. *Proc.Natl.Acad.Sci.U.S.A* 97 (10):5610-5615, 2000.

74. R. Jarvis, T. R. Anderson, and R. D. Andrew. Anoxic depolarization mediates acute damage independent of glutamate in neocortical brain slices. *Cereb.Cortex* 11 (3):249-259, 2001.

75. L. J. Johnson, W. Chung, D. F. Hanley, and N. V. Thakor. Optical scatter imaging detects mitochondrial swelling in living tissue slices. *Neuroimage.* 17 (3):1649-1657, 2002.

76. Kaasik, D. Safiulina, A. Zharkovsky, and V. Veksler. Regulation of mitochondrial matrix volume. *Am.J.Physiol Cell Physiol* 292 (1):C157-C163, 2007.

77. A. Kaczmarská. Hydrodynamika mozkomíšního moku v páteřním kanále, *disertační práce FTVS UK*, Praha 2009

78. O. Kann and R. Kovacs. Mitochondria and neuronal activity. *Am.J.Physiol Cell Physiol* 292 (2):C641-C657, 2007.

79. K. A. Kasischke, H. D. Vishwasrao, P. J. Fisher, W. R. Zipfel, and W. W. Webb. Neural activity triggers neuronal oxidative metabolism followed by astrocytic glycolysis. *Science* 305 (5680):99-103, 2004.

80. P. M. Kaskan, H. D. Lu, B. C. Dillenburger, A. W. Roe, and J. H. Kaas. Intrinsic-signal optical imaging reveals cryptic ocular dominance columns in primary visual cortex of New World owl monkeys. *Front Neurosci.* 1 (1):67-75, 2007.

81. H. Kettenmann. Physiology of glial cells. *Adv.Neurol.* 79:565-571, 1999.

82. S. S. Kety. Circulation and metabolism of the human brain in health and disease. *Am.J.Med.* 8 (2):205-217, 1950.

83. H. K. Kimelberg and M. V. Frangakis. Furosemide- and bumetanide-sensitive ion transport and volume control in primary astrocyte cultures from rat brain. *Brain Res.* 361 (1-2):125-134, 1985.

84. H. K. Kimelberg, C. L. Bowman, and H. Hirata. Anion transport in astrocytes. *Ann.N.Y.Acad.Sci.* 481:334-353, 1986.

85. H. K. Kimelberg and E. O'Connor. Swelling of astrocytes causes membrane potential depolarization. *Glia* 1 (3):219-224, 1988.

86. H. K. Kimelberg, B. A. Macvicar, and H. Sontheimer. Anion channels in astrocytes: biophysics, pharmacology, and function. *Glia* 54 (7):747-757, 2006.

87. H. K. Kimelberg. Supportive or information-processing functions of the mature protoplasmic astrocyte in the mammalian CNS? A critical appraisal. *Neuron Glia Biol.* 3:181-189, 2007.

88. R. C. Koehler, D. Gebremedhin, and D. R. Harder. Role of astrocytes in cerebrovascular regulation. *J.Appl.Physiol* 100 (1):307-317, 2006.

89. P. Kofuji and E. A. Newman. Potassium buffering in the central nervous system. *Neuroscience* 129 (4):1045-1056, 2004.

90. Kohn, C. Metz, M. Quibrera, M. A. Tommerdahl, and B. L. Whitsel. Functional neocortical microcircuitry demonstrated with intrinsic signal optical imaging in vitro. *Neuroscience* 95 (1):51-62, 2000.

91. R. Korpi and H. Luddens. Furosemide interactions with brain GABAA receptors. *Br.J.Pharmacol.* 120 (5):741-748, 1997.

92. N. R. Kreisman, S. Soliman, and D. Gozal. Regional differences in hypoxic depolarization and swelling in hippocampal slices. *J.Neurophysiol.* 83 (2):1031-1038, 2000.

93. M. Kurec, G. Kuncova, and T. Branyik. Yeast vitality determination based on intracellular NAD(P)H fluorescence measurement during aerobic-anaerobic transition. *Folia Microbiol.(Praha)* 54 (1):25-29, 2009.

94. P. Lamoureux, G. Ruthel, R. E. Buxbaum, and S. R. Heidemann. Mechanical tension can specify axonal fate in hippocampal neurons. *J.Cell Biol.* 159 (3):499-508, 2002.

95. P. Lamoureux, S. R. Heidemann, N. R. Martzke, and K. E. Miller. Growth and elongation within and along the axon. *Dev.Neurobiol.* , 2009.

96. V. M. Laurent, S. Kasas, A. Yersin, T. E. Schaffer, S. Catsicas, G. Dietler, A. B. Verkhovsky, and J. J. Meister. Gradient of rigidity in the lamellipodia of migrating cells revealed by atomic force microscopy. *Biophys.J.* 89 (1):667-675, 2005.

97. M. Lauritzen and L. Gold. Brain function and neurophysiological correlates of signals used in functional neuroimaging. *J.Neurosci.* 23 (10):3972-3980, 2003.

98. T. S. Lee, T. Eid, S. Mane, J. H. Kim, D. D. Spencer, O. P. Ottersen, and N. C. de Lanerolle. Aquaporin-4 is increased in the sclerotic hippocampus in human temporal lobe epilepsy. *Acta Neuropathol.* 108 (6):493-502, 2004.

99. J. L. LeMaistre and C. M. Anderson. Custom astrocyte-mediated vasomotor responses to neuronal energy demand. *Genome Biol.* 10 (2):209, 2009.

100. P. Lipton. Effects of membrane depolarization on light scattering by cerebral cortical slices. *J.Physiol* 231 (2):365-383, 1973.

101. Y. B. Lu, K. Franze, G. Seifert, C. Steinhauser, F. Kirchhoff, H. Wolburg, J. Guck, P. Janmey, E. Q. Wei, J. Kas, and A. Reichenbach. Viscoelastic properties of individual glial cells and neurons in the CNS. *Proc.Natl.Acad.Sci.U.S.A* 103 (47):17759-17764, 2006.

102. J. J. Luszczki, K. M. Sawicka, J. Kozinska, K. K. Borowicz, and S. J. Czuczwar. Furosemide potentiates the anticonvulsant action of valproate in the mouse maximal electroshock seizure model. *Epilepsy Res.* 76 (1):66-72, 2007.

103. N. Macaulay, S. Hamann, and T. Zeuthen. Water transport in the brain: role of cotransporters. *Neuroscience* 129 (4):1031-1044, 2004.

104. M. Mackowiak, A. Chocyk, K. Markowicz-Kula, and K. Wedzony. Neurogenesis in the adult brain. *Pol.J.Pharmacol.* 56 (6):673-687, 2004.

105. A. Macvicar and D. Hochman. Imaging of synaptically evoked intrinsic optical signals in hippocampal slices. *J.Neurosci.* 11 (5):1458-1469, 1991.

106. A. Macvicar, D. Feighan, A. Brown, and B. Ransom. Intrinsic optical signals in the rat optic nerve: role for K(+) uptake via NKCC1 and swelling of astrocytes. *Glia* 37 (2):114-123, 2002.

107. N. Maier, V. Nimmrich, and A. Draguhn. Cellular and network mechanisms underlying spontaneous sharp wave-ripple complexes in mouse hippocampal slices. *J.Physiol* 550 (Pt 3):873-887, 2003.

108. Mayevsky and G. G. Rogatsky. Mitochondrial function in vivo evaluated by NADH fluorescence: from animal models to human studies. *Am.J.Physiol Cell Physiol* 292 (2):C615-C640, 2007.

109. J. McBain. New directions in synaptic and network plasticity--a move away from NMDA receptor mediated plasticity. *J.Physiol* 586 (6):1473-1474, 2008.

110. P. Miklavc, M. Frick, O. H. Wittekindt, T. Haller, and P. Dietl. Fusion-activated Ca(2+) entry: an "active zone" of elevated Ca(2+) during the postfusion stage of lamellar body exocytosis in rat type II pneumocytes. *PLoS.One.* 5 (6):e10982, 2010.

111. K. Miller and K. Chinzei. Mechanical properties of brain tissue in tension. *J.Biomech.* 35 (4):483-490, 2002.

112. M. A. Mintun, A. G. Vlassenko, M. M. Rundle, and M. E. Raichle. Increased lactate/pyruvate ratio augments blood flow in physiologically activated human brain. *Proc.Natl.Acad.Sci.U.S.A* 101 (2):659-664, 2004.

113. M. miry-Moghaddam, A. Williamson, M. Palomba, T. Eid, N. C. de Lanerolle, E. A. Nagelhus, M. E. Adams, S. C. Froehner, P. Agre, and O. P. Ottersen. Delayed K+ clearance associated with aquaporin-4 mislocalization: phenotypic defects in brains of alpha-syntrophin-null mice. *Proc.Natl.Acad.Sci.U.S.A* 100 (23):13615-13620, 2003.

114. N. Miyakawa, I. Yazawa, S. Sasaki, Y. Momose-Sato, and K. Sato. Optical analysis of acute spontaneous epileptiform discharges in the in vivo rat cerebral cortex. *Neuroimage.* 18 (3):622-632, 2003.

115. Y. Momose-Sato, Y. Honda, H. Sasaki, and K. Sato. Optical imaging of large-scale correlated wave activity in the developing rat CNS. *J.Neurophysiol.* 94 (2):1606-1622, 2005.

116. M. Muller and G. G. Somjen. Intrinsic optical signals in rat hippocampal slices during hypoxia-induced spreading depression-like depolarization. *J.Neurophysiol.* 82 (4):1818-1831, 1999.

117. J. Neal, M. Takahashi, M. Silva, G. Tiao, C. A. Walsh, and V. L. Sheen. Insights into the gyrification of developing ferret brain by magnetic resonance imaging. *J.Anat.* 210 (1):66-77, 2007.

118. O. Nesic, J. Lee, Z. Ye, G. C. Unabia, D. Rafati, C. E. Hulsebosch, and J. R. Perez-Polo. Acute and chronic changes in aquaporin 4 expression after spinal cord injury. *Neuroscience* 143 (3):779-792, 2006.

119. S. Obeidat and R. D. Andrew. Spreading depression determines acute cellular damage in the hippocampal slice during oxygen/glucose deprivation. *Eur.J.Neurosci.* 10 (11):3451-3461, 1998.

120. S. Ogawa, T. M. Lee, A. R. Kay, and D. W. Tank. Brain magnetic resonance imaging with contrast dependent on blood oxygenation. *Proc.Natl.Acad.Sci.U.S.A* 87 (24):9868-9872, 1990.

121. J. E. Olson and N. R. Kreisman. Volume regulation of the hippocampus. *Adv.Exp.Med.Biol.* 559:331-338, 2004.

122. K. Ommaya. Mechanical properties of tissues of the nervous system. *J.Biomech.* 1 (2):127-138, 1968.

123. V.Paska. Vývoj zdroje světla na bázi LEDdiod pro použití ve fluorescenční mikroskopii, *diplomová práce ČVUT FS*, Praha 2008

124. L. Pellerin and P. J. Magistretti. Neuroscience. Let there be (NADH) light. *Science* 305 (5680):50-52, 2004.

125. Perea, M. Navarrete, and A. Araque. Tripartite synapses: astrocytes process and control synaptic information. *Trends Neurosci.* 32 (8):421-431, 2009.

126. C. Petzold, S. Haack, Halbach O. von Bohlen Und, J. Priller, T. N. Lehmann, U. Heinemann, U. Dirnagl, and J. P. Dreier. Nitric oxide modulates spreading depolarization threshold in the human and rodent cortex. *Stroke* 39 (4):1292-1299, 2008.

127. R. Piet, L. Vargova, E. Sykova, D. A. Poulain, and S. H. Oliet. Physiological contribution of the astrocytic environment of neurons to intersynaptic crosstalk. *Proc.Natl.Acad.Sci.U.S.A* 101 (7):2151-2155, 2004.

128. J. K. Pomper, S. Haack, G. C. Petzold, K. Buchheim, S. Gabriel, U. Hoffmann, and U. Heinemann. Repetitive spreading depression-like events result in cell damage in juvenile hippocampal slice cultures maintained in normoxia. *J.Neurophysiol.* 95 (1):355-368, 2006.

129. N. Pouratian, A. F. Cannestra, N. A. Martin, and A. W. Toga. Intraoperative optical intrinsic signal imaging: a clinical tool for functional brain mapping. *Neurosurg.Focus.* 13 (4):e1, 2002.

130. N. Pouratian, S. A. Sheth, N. A. Martin, and A. W. Toga. Shedding light on brain mapping: advances in human optical imaging. *Trends Neurosci.* 26 (5):277-282, 2003.

131. Rafiq, Q. Z. Gong, B. G. Lyeth, R. J. DeLorenzo, and D. A. Coulter. Induction of prolonged electrographic seizures in vitro has a defined threshold and is all or none: implications for diagnosis of status epilepticus. *Epilepsia* 44 (8):1034-1041, 2003.

132. R. Ransom, C. L. Yamate, and B. W. Connors. Activity-dependent shrinkage of extracellular space in rat optic nerve: a developmental study. *J.Neurosci.* 5 (2):532-535, 1985.

133. W. C. Risher, R. D. Andrew, and S. A. Kirov. Real-time passive volume responses of astrocytes to acute osmotic and ischemic stress in cortical slices and in vivo revealed by two-photon microscopy. *Glia* 57 (2):207-221, 2009.

134. W. Roe. Long-term optical imaging of intrinsic signals in anesthetized and awake monkeys. *Appl.Opt.* 46 (10):1872-1880, 2007.

135. W. Roe and L. M. Chen. High-resolution fMRI maps of cortical activation in nonhuman primates: correlation with intrinsic signal optical images. *ILAR.J.* 49 (1):116-123, 2008.

136. L. Rovati, G. Salvatori, L. Bulf, and S. Fonda. Optical and electrical recording of neural activity evoked by graded contrast visual stimulus. *Biomed.Eng Online.* 6:28, 2007.

137. S. Sasaki, K. Sato, K. Shinomiya, and Y. Momose-Sato. Postnatal changes in intrinsic optical responses to peripheral nerve stimulation in the in vivo rat spinal cord. *Neuroimage.* 20 (4):2126-2134, 2003.

138. U. Schridde, M. Khubchandani, J. E. Motelow, B. G. Sanganahalli, F. Hyder, and H. Blumenfeld. Negative BOLD with large increases in neuronal activity. *Cereb.Cortex* 18 (8):1814-1827, 2008.

139. Schroth and U. Klose. Cerebrospinal fluid flow. II. Physiology of respiration-related pulsations. *Neuroradiology* 35 (1):10-15, 1992.

140. G. Schroth and U. Klose. Cerebrospinal fluid flow. I. Physiology of cardiac-related pulsation. *Neuroradiology* 35 (1):1-9, 1992.

141. S. Sekine, M. Miura, and T. Chihara. Organelles in developing neurons: essential regulators of neuronal morphogenesis and function. *Int.J.Dev.Biol.* 53 (1):19-27, 2009.

142. Shen, R. Sood, J. Weaver, G. S. Timmins, A. Schnell, M. Miyake, J. P. Kao, G. M. Rosen, and K. J. Liu. Direct visualization of mouse brain oxygen distribution by electron paramagnetic resonance imaging: application to focal cerebral ischemia. *J.Cereb.Blood Flow Metab* 29 (10):1695-1703, 2009.

143. Shiino, M. Matsuda, J. Handa, and B. Chance. Poor recovery of mitochondrial redox state in CA1 after transient forebrain ischemia in gerbils. *Stroke* 29 (11):2421-2424, 1998.

144. Shimamoto, R. Sakai, K. Takaoka, N. Yumoto, T. Nakajima, S. G. Amara, and Y. Shigeri. Characterization of novel L-threo-beta-benzyloxyaspartate derivatives, potent blockers of the glutamate transporters. *Mol.Pharmacol.* 65 (4):1008-1015, 2004.

145. W. Shuttleworth, A. M. Brennan, and J. A. Connor. NAD(P)H fluorescence imaging of postsynaptic neuronal activation in murine hippocampal slices. *J.Neurosci.* 23 (8):3196-3208, 2003.

146. M. C. Skala, K. M. Riching, A. Gendron-Fitzpatrick, J. Eickhoff, K. W. Eliceiri, J. G. White, and N. Ramanujam. In vivo multiphoton microscopy of NADH and FAD redox states, fluorescence lifetimes, and cellular morphology in precancerous epithelia. *Proc.Natl.Acad.Sci.U.S.A* 104 (49):19494-19499, 2007.

147. H. Slovin, A. Arieli, R. Hildesheim, and A. Grinvald. Long-term voltage-sensitive dye imaging reveals cortical dynamics in behaving monkeys. *J.Neurophysiol.* 88 (6):3421-3438, 2002.

148. G. G. Somjen, P. G. Aitken, G. L. Czeh, O. Herreras, J. Jing, and J. N. Young. Mechanism of spreading depression: a review of recent findings and a hypothesis. *Can.J.Physiol Pharmacol.* 70 Suppl:S248-S254, 1992.

149. J. Sparrey, G. T. Manley, and T. M. Keaveny. Effects of white, grey, and pia mater properties on tissue level stresses and strains in the compressed spinal cord. *J.Neurotrauma* 26 (4):585-595, 2009.

150. Z. Štěpáník. Simulace transportu mozkomíšního moku, *disertační práce FTVS UK*, Praha 2009

151. M. Suh, S. Bahar, A. D. Mehta, and T. H. Schwartz. Temporal dependence in uncoupling of blood volume and oxygenation during interictal epileptiform events in rat neocortex. *J.Neurosci.* 25 (1):68-77, 2005.

152. M. Suh, S. Bahar, A. D. Mehta, and T. H. Schwartz. Blood volume and hemoglobin oxygenation response following electrical stimulation of human cortex. *Neuroimage.* 31 (1):66-75, 2006.

153. Sykova and A. Chvatal. Glial cells and volume transmission in the CNS. *Neurochem.Int.* 36 (4-5):397-409, 2000.

154. Sykova and C. Nicholson. Diffusion in brain extracellular space. *Physiol Rev.* 88 (4):1277-1340, 2008.

155. M. J. Tait, S. Saadoun, B. A. Bell, and M. C. Papadopoulos. Water movements in the brain: role of aquaporins. *Trends Neurosci.* 31 (1):37-43, 2008.

156. Tao, D. Masri, S. Hrabetova, and C. Nicholson. Light scattering in rat neocortical slices differs during spreading depression and ischemia. *Brain Res.* 952 (2):290-300, 2002.

157. Treves, A. Tashiro, M. E. Witter, and E. I. Moser. What is the mammalian dentate gyrus good for? *Neuroscience* 154 (4):1155-1172, 2008.

158. A. Turner, K. A. Foster, F. Galeffi, and G. G. Somjen. Differences in O2 availability resolve the apparent discrepancies in metabolic intrinsic optical signals in vivo and in vitro. *Trends Neurosci.* 30 (8):390-398, 2007.

159. Vanzetta and A. Grinvald. Increased cortical oxidative metabolism due to sensory stimulation: implications for functional brain imaging. *Science* 286 (5444):1555-1558, 1999.

160. Vanzetta, R. Hildesheim, and A. Grinvald. Compartment-resolved imaging of activity-dependent dynamics of cortical blood volume and oximetry. *J.Neurosci.* 25 (9):2233-2244, 2005.

161. varez-Buylla, D. G. Herrera, and H. Wichterle. The subventricular zone: source of neuronal precursors for brain repair. *Prog.Brain Res.* 127:1-11, 2000.

162. S. Verkman. More than just water channels: unexpected cellular roles of aquaporins. *J.Cell Sci.* 118 (Pt 15):3225-3232, 2005.

163. Veznedaroglu, E. J. Van Bockstaele, and M. J. O'Connor. Extravascular collagen in the human epileptic brain: a potential substrate for aberrant cell migration in cases of temporal lobe epilepsy. *J.Neurosurg.* 97 (5):1125-1130, 2002.

164. W. Walz and E. C. Hinks. Carrier-mediated KCl accumulation accompanied by water movements is involved in the control of physiological K+ levels by astrocytes. *Brain Res.* 343 (1):44-51, 1985.

165. O. W. Witte, H. Niermann, and K. Holthoff. Cell swelling and ion redistribution assessed with intrinsic optical signals. *An.Acad.Bras.Cienc.* 73 (3):337-350, 2001.

166. Yersin, H. Hirling, S. Kasas, C. Roduit, K. Kulangara, G. Dietler, F. Lafont, S. Catsicas, and P. Steiner. Elastic properties of the cell surface and trafficking of single AMPA receptors in living hippocampal neurons. *Biophys.J.* 92 (12):4482-4489, 2007.